UNIVERSITÀ
DEGLI STUDI
FIRENZE

DOTTORATO DI RICERCA IN
Gestione Sostenibile delle Risorse Agrarie, Forestali e Alimentari

CICLO XXIX

Coordinatore Prof. LEONARDO CASINI

The effect of flexible vegetation on flow in drainage channels. Field surveys and modelling for roughness coefficients estimation

Settore Scientifico Disciplinare AGR/08

Dottorando
Dott. Errico Alessandro

Tutor
Prof. Preti Federico

Coordinatore
Prof. Casini Leonardo

Anni 2013/2016

INDEX

Abstract

The management of vegetation in drainage channels represents one of the main issues for land reclamation authorities during spring and summer seasons. In fact, the presence of high concentrations of nutrients combined with a constant presence of water enhances the growth of aquatic and hygrophile vegetation within the riverbed and banks. On the one hand, the presence of vegetation within the flow section can significantly increase the bed roughness reducing the discharge capacity, therefore rising the risk of flood. On the other hand, drainage channels constitute a fundamental habitat within the agricultural environment, which needs to be preserved as important habitats for a number of animal and vegetal species, some of which endangered. Following a precautionary approach, channel managers use to remove the entire vegetation cover from the banks and from the bottom of the channel, to maximize the discharge capacity of the drainage network. Considering the proximity to the Massaciuccoli Natural Park, and the importance of the entire reclamation site for bird migration, fish and amphibia reproduction, a more accurate evaluation of the effective need of the vegetation removal is called for. For these reason, a fieldbased estimation of vegetation effects on flow conveyance was carried out, in order to estimate the bed roughness in presence/absence of vegetation for different vegetation covers. The objective of the work is to assess the effect of common reed vegetation, typically growing in drainage channels, on flow rating curves (i.e. in terms of reduction in discharge capacity, water level rise, roughness coefficients) and on velocity distribution in a given monitoring cross-section. The survey location is a straight stretch of length 300 m, located at the end of the Bresciani drainage channel in the Versilia-Massaciuccoli reclamation area. To estimate the equivalent roughness coefficients for different discharges and different management scenarios a control of all the hydraulic variables was set up. Four different discharges were pumped into the channel in order to determine the rating curve for a reference section in presence/absence of vegetation. Topography, hydraulic and vegetation parameters were monitored along the study reach. The three vegetated scenario were chosen taking into account traditional management techniques and a possible less-impactful measure for the channel ecosystem. The tested scenarios were 1) full vegetation; 2) half vegetation (just on one bank); 3) total removal, as traditionally practiced. First step was the field survey of the experimental channel stretch, conducted by a total station. Then, vegetation measures were conducted. A number of vegetation parameters (stem diameters, density, height, position within the channel) were measured, in order to collect the data required by hydraulic models from literature. Thus, for each section the distribution of the natural vegetation parameters along the wetted perimeter was available for modelling. To simulate a flood in the study reach, four portable dewatering pumps carried by agricultural tractors were adopted. Each pump had a maximum discharge of 300-400 l/s. Measures were planned as follows. First, the channel was flooded for four hours to saturate the soil of the banks. For each vegetated scenario, four discharges were pumped, activating in sequence the four portable pumps. The transition time between one discharge and the next was monitored at the staff gages, taking

one hour on average. Velocity measures were carried out when the water level was stable at the three gaged sections. The operations were repeated three times, one for each vegetated scenario, for a total number of twelve velocity measures. The section located in the middle of the study reach was equipped with a mobile bridge for velocity measures. The flow velocities were measured by means of a USGS type AA current meter at seven verticals, every 15 cm of depth from the surface for discharge estimation. The stability of the water levels and slope were controlled during the velocity measures for each discharge. The rating curves for each vegetation scenario were traced. The analysis of the rating curves shows how reed affects the flow within the channel, rising the water levels. Differently, the removal of the vegetation on one bank and within the channel significantly increases the discharge capacity of the section. As expected, the lowest levels are found for the non vegetated scenario. The slight difference between the two different management techniques points out the feasibility of a decrease in terms of impact on the channel ecosystem. The release of a natural strip on one side of the channel resulted to be sustainable also from an hydraulic point of view. In order to give a numerical information to Land reclamation managers, we determined the equivalent roughness coefficients for each layout. Results showed how Manning's roughness coefficients varied from 0.08-0.06 for the vegetated scenario, to 0.02 for the cleared scenario. An average roughness oh 0.03 for the half vegetated scenario suggested the sustainability of less impactful management practices. A methodology to directly measure the equivalent roughness coefficient in vegetated channels was presented. The vegetation observed within the channel was mainly composed by partially submerged common reed (Phragmites australis), which appeared to decrease its flow resistance for increasing flow velocities, reshaping the leafs. A model validation was carried for three different resistance models: James (2004), Nepf (2012) and Yang (2009). The input data was represented by the vegetation parameters collected before the hydraulic measurements. Models were run using average values of vegetation density and dividing the section is subareas with different characteristics. This research brings additional knowledge for practitioners, given that commonly used hydraulic modeling often does not consider variations along the cross section. The results of this work will be useful for water service managers to take decisions about the management of vegetation along the drainage systems of the area, and will be the base for upcoming research planned for the next months.

Introduction

Vegetation dynamics in natural rivers and vegetated channels represent a fundamental aspect of environmental hydraulics. The number of studies about the role of vegetation in flood risk management increased in the last years, thanks to a growing attention of academy and public authorities for the protection of riverine ecosystems and the species that are connected to them. The recent research followed different pathways, from fluid mechanics to plant physiology, passing through forestry ad river ecology.

If on one hand hydraulic modelling have reached a high level of accuracy, thanks to new technologies available for terrain surveying and numerical computation, on the other hand there are still large knowledge gaps in environmental hydraulics. One of the most challenging issues concerning the hydraulic modelling of natural bed channels and rivers is represented by the effects of the hydrodynamic interaction of the natural elements within the flow. These effects are particularly important for predicting flood hazards, as normally required in river engineering and land-use planning.

Operational methods for predicting the effects of in-stream and floodplain vegetation on floods and for assessing optimal river vegetation management strategies are still missing. A few models have been proposed for modelling flow-vegetation interaction in open channels, but these are restricted to academic studies and experiments with limited applicability in operational river management context.

The traditional practice in river management is to account for vegetation as an additional resistance factor, contributing to reduce river discharge capacity. Consequently, riparian vegetation management have been traditionally carried out with a precautionary approach, thus being applied with the leading principle of reducing as much as possible the flood hazards. This traditional management approach clashes with the larger attention more recently paid to the positive effects of vegetation on ecology, geomorphology and global environmental value of a river.

This research study has been planned for enhancing the current knowledge about vegetation flow interaction, with the aim to identify possible management strategies that could balance the traditional flood hazard mitigation strategies with ecological perspective of the river ecosystems. The specific objectives were:

- assessing the hydraulic resistance of a vegetated channel in different management conditions with experiments conducted in a real drainage channel;

- assessing the impact of the vegetation on flood hazard;

- testing the compatibility of innovative vegetation management strategies, having lower environmental impact, with the acceptable flood hazard;

- evaluating the accuracy of existing models in the estimation of roughness coefficients;

The first chapter is a short review of the state of the art on hydraulic vegetation resistance modelling, with a focus on the most recent literature, to highlight the key knowledge gaps about the effects of the riparian and aquatic vegetation on river hydraulics. The second chapter presents the case study and the experimental setup that was implemented on a real channel located in Northern Tuscany, Italy. The third chapter presents the results of the field experiments and the estimation of the roughness coefficients. In the fourth chapter, the field data are exploited for evaluating and comparing the accuracies of three models recently proposed for predicting the roughness coefficient in vegetated channels. The fifth chapter is a summary of the results, with a discussion about the applicability of this research for enhancing vegetated channel management.

1. STATE OF THE ART

Since more than half a century scientists tried to understand flow-vegetation interaction, with the aim to describe the flow resistance in vegetated streams and channels. The number of different theories that were proposed during all these years demonstrates how complex can be this topic. As a matter of fact, riverine ecosystems are characterized by enormous variability in terms of morphology, dimensions, vegetation, discharge, which leads to a great difficulty in standardizing procedures, comparing or simply generalizing results retrieved from specific case studies. A partial solution of this problem was solved using flumes with standard, artificial vegetated elements, but again the research had to deal with the difficulties that have to be faced to extend the results from the laboratory scale to the field scale. Despite this, in literature it is possible to find a number resistance models, able to predict the flow resistance of vegetation with specific characteristics. In this chapter, a review of the state of the art concerning models most recently published is presented.

Vegetation resistance models are drawn from the consideration that flow resistance induced by vegetation is the result of the dynamic interaction of the vegetation within the flow and therefore needs to be modelled with an approach different from that generally adopted for describing the flow resistance induced by granular sediments (e.g. Raupach 1992, Huthoff 2012). Aberle & Järvelä (2013) stated that "*energy losses due to granular sediments result from viscous drag on the bed surface and form drag due to small-scale roughness elements such as grains of the bed material. Energy losses due to vegetation elements, on the other hand, are associated with viscous and pressure drag whose proportions depend on plant mechanical properties, topology, age, seasonality, foliage, volumetric and areal vegetation porosities, vegetation density, and patchiness (e.g. Kouwen and Unny 1973, Järvelä 2002a, Righetti 2008, Yang and Choi 2009, Nikora 2010, Folkard 2011, Shucksmith et al. 2011). Flow in vegetated areas has generally been separated in nonsubmerged (i.e. emergent) and submerged conditions as the flow field changes considerably when the flow depth exceeds the height of vegetation (Nepf and Vivoni 2000, Ghisalberti and Nepf 2004, Sukhodolov and Sukhodolova 2010, Nepf 2012a, 2012b). Taking this flow division into account, various approaches have been proposed for the estimation of flow resistance by subdividing the flow field into layers representing unobstructed surface flow and flow through vegetation (e.g. Huthoff et al. 2007, Yang and Choi 2010, Konings et al. 2012).*" In this chapter, the traditional approach and the state of the art of modelling the riparian and in-stream vegetation resistance are presented.

1.1 The traditional approach to vegetation resistance

The most common hydraulic models are characterized using bulked roughness coefficients for flow resistance estimation. As a matter of fact, the most common practice in river modelling is to apply standard roughness coefficients (i.e. Manning's n or Gauckler-Strickler k) obtained by tables attached to the hydraulic manuals. Roughness tables present a number of possible cases concerning the grain size of sediment, the regularity of the channel, the presence of vegetation, and so on, without implying quantitative estimation of any parameter of the effective roughness components. One of the most known tables were developed by Chow (1959).

Type of Channel and Description	Minimum	Normal	Maximum
A. *Natural Streams*			
1. **Main Channels**			
a. Clean, straight, full, no rifts or deep pools	0.025	0.030	0.033
b. Same as above, but more stones and weeds	0.030	0.035	0.040
c. Clean, winding, some pools and shoals	0.033	0.040	0.045
d. Same as above, but some weeds and stones	0.035	0.045	0.050
e. Same as above, lower stages, more ineffective slopes and sections	0.040	0.048	0.055
f. Same as "d" but more stones	0.045	0.050	0.060
g. Sluggish reaches, weedy. deep pools	0.050	0.070	0.080
h. Very weedy reaches, deep pools, or floodways with heavy stands of timber and brush	0.070	0.100	0.150
2. **Flood Plains**			
a. Pasture no brush			
1. Short grass	0.025	0.030	0.035
2. High grass	0.030	0.035	0.050
b. Cultivated areas			
1. No crop	0.020	0.030	0.040
2. Mature row crops	0.025	0.035	0.045
3. Mature field crops	0.030	0.040	0.050
c. Brush			
1. Scattered brush, heavy weeds	0.035	0.050	0.070
2. Light brush and trees, in winter	0.035	0.050	0.060
3. Light brush and trees, in summer	0.040	0.060	0.080
4. Medium to dense brush, in winter	0.045	0.070	0.110
5. Medium to dense brush, in summer	0.070	0.100	0.160
d. Trees			
1. Cleared land with tree stumps, no sprouts	0.030	0.040	0.050
2. Same as above, but heavy sprouts	0.050	0.060	0.080
3. Heavy stand of timber, few down trees, little undergrowth, flow below branches	0.080	0.100	0.120
4. Same as above, but with flow into branches	0.100	0.120	0.160
5. Dense willows, summer, straight	0.110	0.150	0.200
3. **Mountain Streams, no vegetation in channel, banks usually steep, with trees and brush on banks submerged**			
a. Bottom: gravels, cobbles, and few boulders	0.030	0.040	0.050
b. Bottom: cobbles with large boulders	0.040	0.050	0.070

Table 1.1. Roughness coefficients from the HEC RAS User's Manual (USACE).

In table 1.1 an example of roughness reference tables is provided. When choosing the roughness coefficients, an objective description of the study reach is hard to realize through this method. Although a description of different natural scenarios is provided, the choice of the right roughness coefficients remains strongly debatable, also about the range of variability between minimum and maximum values. Consequently, the riparian vegetation management results unlikely to be based on hydraulic modelling. In fact, a precise reference to parameters of the vegetation cover is not considered, making the quantification of a partial cut impossible to determine. Therefore, a great matter comes out from practitioners: how can we decide the best vegetation management practices for hydraulic risk, if we are not able to quantify the role of vegetation during a flood?

Since the beginning of hydraulic modelling, several authors tried to give an answer to this question. For instance, Cowan (1956) proposed an estimation of the global roughness, factoring the Manning's n in six sub-parameters.

$$n = (n_0 + n_1 + n_2 + n_3 + n_4)m \qquad (1.1)$$

n_0	Smooth alluvial boundary		0.020
	Rock-cut boundary		0.025
Boundary materials	Fine gravel		0.024
	Coarse gravel boundary		0.028
n_1	Smooth: best attainable for the given materials;		0.000
Degree of channel cross-sectional irregularity	slightly eroded banks		0.005
	Moderate: Comparable with dredged channel in fair to poor condition; some minor bank slumping and erosion		0.010
	Severe: Extensive bank slumps and moderate bank erosion; jagged irregular rock-cut materials		0.020
n_2	Gradual: Changes in size and shape are gradual		0.000
Variation in channel cross-section shape and area	Occasional alternation: Large and small sections alternate occasionally or shape changes to cause occasional shifting of flow from side to side		0.005
	Frequent alternation: Large & small sections alternate or shape changes cause frequent shifting of flow from side to side		0.010 to 0.015
n_3	Determination of n_3 is based on the presence and characteristics of obstructions such as debris, slumps, stumps, exposed roots, boulders and fallen and lodged logs. Conditions considered in other steps must not be reevaluated (double counted) in this determination. In judging the relative effect of obstructions, consider the extent to which the obstructions occupy or reduce average water area; the shape (sharp or smooth) and position and spacing of the obstructions.	Negligible	0.00
			0.010
		Minor to	0.015
Relative effect of obstructions			0.020
		Appreciable to	0.030
			0.040
		Severe to	0.060
n_4	Low: Dense but flexible grasses where flow depth is 2-3 x the height of vegetation or supple tree seedlings (willow, poplar)		0.005
	where flow depth is 3-4 x vegetation height	to	0.010
	Medium: Turf grasses in flow 1-2 times vegetation height; stemmy grasses where flow is 2-3 x vegetation height; moderately dense brush on		0.010
	banks where R_h>0.7 m	to	0.025
Vegetation	High: Turf grasses in flow of same height; foliage-free willow or poplar, 8-10 years old and intergrown with brush on channel banks		0.025
	where R_h>0.7m; bushy willows, 1 year old, R_h>0.7m	to	0.050
	Very High: Turf grasses in flow half as deep; bushy willows (1 year old) with weeds on banks; some vegetation on the bed; trees with		0.050
	weeds and brush in full foliage where R_h>5m	to	0.100
m			
	Minor: Sinuosity index = 1.0 to1.2		1.00
Degree of Meandering	Appreciable: Sinuosity index = 1.2 to 1.5		1.15
	Severe: Sinuosity index >1.5		1.30

Table 1.2. Reference table for the Cowan (1956) roughness estimation. The vegetation description is just qualitative.

The Cowan approach proposed a fractioning of the global resistance in six components (Table 1.2), one of which was represented by the vegetation. Despite the method tried to separate the effect of vegetation from the others, the quantitative estimation of the vegetation effect was not available yet. Therefore, despite the method permitted to have a more accurate estimation, the values were still affected by the personal choice of the practitioner, and therefore debatable.

An improvement of the comparative method was proposed by Archement & Schneider (1989), who realized a volume entitled “Guide for Selecting Manning’s Roughness Coefficient for Natural Channels and Flood Plains”, published by United States Geological Survey and adopted by the Federal Highway Administration. The guide is composed by a series of photographs of natural vegetated streams, joined with a short description of the vegetation which help the practitioner to choose the most suitable scenario

and therefore the corresponding roughness coefficient. Although this method is an improvement of the roughness tables approach, since the designer finds more easily a reference situation to compare to his specific case, there are still limits in describing the real dynamics of riparian vegetation. As an example, seasonal variations are not taken into account, as well as the resistance variations with different flow levels.

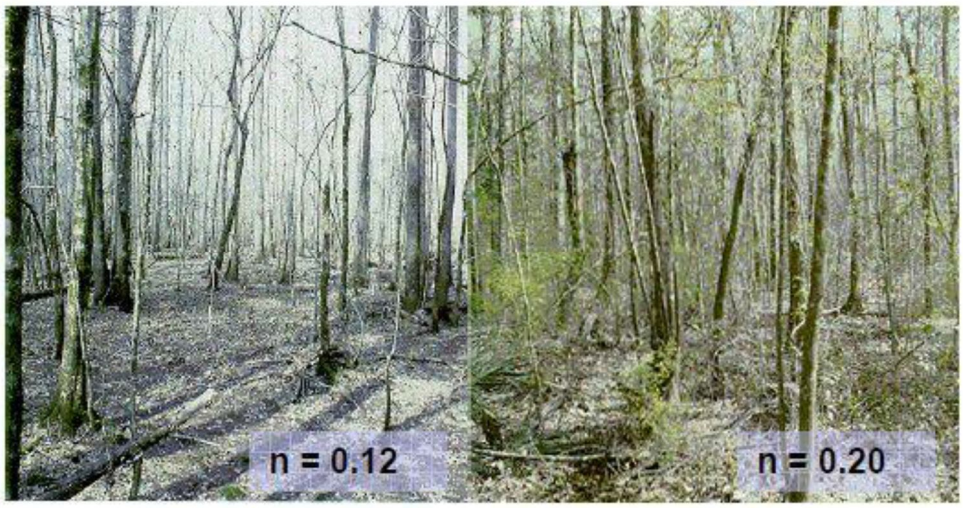

Figure 1.1. Example of reference pictures, from Archement & Schneider (1989).

1.2 Modelling the vegetation

Despite practitioners are still finding difficulties in modelling vegetated streams, academy started debating many years ago about possible approaches to vegetation resistance. The studies about riparian and aquatic vegetation resistance are related to the development of models able to predict the velocity distribution across the channel section, or to determine the drag force or equivalent roughness of plants. To obtain this, a quantification of the vegetation flow resistance became necessary. After the proposal of a wide number of theories, the vegetation resistance has been divided in different families, according to the characteristics of the stems, the submergence ratio and the spatial scale at which it is considered. In particular, significant differences in the modeling approach were proposed for rigid/flexible stems, and for submerged/emergent vegetation. Moreover, different theories were developed according to the different scale of study: the blade scale, the patch scale and the reach scale.

The earliest studies of vegetation hydrodynamics focused on the characterization of flow resistance of aquatic, herbaceous flexible vegetation (e.g. Ree 1949). The first attempts of modelling have focused on characterizing flow resistance in channels with uniform distributions of vegetation, emphasizing the drag contributed at the stem and leaf scale (e.g. Kouwen & Unny 1973). In the same period, the first resistance models for rigid, emergent vegetation were proposed (i.e. Petryk & Bosmaijan, 1975). More recently, research tried to describe also the more complex behavior of flexible woody plants, such as shrubs and

young trees (Järvelä, 2002a, 2002b). Nowadays, the most advanced researches on the three typologies of riparian and in-stream vegetation are represented by Nepf (2012) for flexible, grass vegetation, Baptist et al. (2007) for the rigid leafless stems, and Aberle & Järvelä (2013) for the flexible leafy shrubs. In the next section, the three theories are presented.

In section 1.2.1, an overview on the theories developed for rigid, cylindrical elements is presented. Such approach was one of the first attempts of modeling the hydraulic resistance of floodplain forests. Despite its high level of approximation, its application is still feasible when studying the effect of rigid trees with a base crown height higher than the water level. In section 1.2.2 an evolution of the first approach is presented. describing the more recent models for branched and leafy flexible vegetation elements. These further studies shown how the rigid cylinders are not able to describe the complex turbulences which occur within a shrub or a tree crown. Starting from this consideration, a few authors proposed innovative theories to estimate the global resistance of a tree crown, moreover introducing the possible application of remote sensing techniques for the floodplain roughness spatialization. In section 1.2.3 the most important theories about the estimation of resistance of submerged grass are presented. In this case, attention must be paid to the estimation of bending height of the different grass species subjected to the flow drag. The topic still remains an open question for a number of species all over the world.

1.2.1 Flow resistance through rigid, emergent vegetation

When the vegetation is higher than the water depth, the entire vertical flow profile is influenced by the presence of leafs and stems. More in detail, the flow resistance through emergent, rigid stems is related to the drag forces that occur within the canopy. To better understand this dynamic, several studies tried to describe the flow within arrays of cylinders with different layouts and diameters (Petryk & Bosmajian, 1975; Pasche & Rouvé, 1985; Baptist et al, 2007). In such conditions, the flow velocity distribution is often assumed to be uniform for the whole water depth (i.e. Ricardo et al., 2016). In fact the soil roughness, compared to the high resistance induced by the presence of the stems and leaves, results to be some orders of magnitude lower, and therefore considered negligible. The scale at which the flow is studied in this cases has been defined by Luhar & Nepf (2013) "the patch scale".

Baptist et al. (2007) presented an upgrade of the Petryk & Bosmaijan (1975) theory, which is now the reference for modelling the flow through rigid, emergent stems. The balance of horizontal momentum in uniform steady flow conditions through an array of staggered rigid cylinders dictates that total shear stress is equal to the sum of the bed shear stress and the equivalent shear stress due to the cylinders drag, according to the linear superposition principle (Petryk and Bosmajian 1975, Raupach 1992, Yen 2002):

$$\tau = \tau_b + \tau_v \qquad (1.2)$$

where τ denotes the total fluid shear stress assuming the hydraulic radius equal to the water depth h:

$$\tau_b = \rho_0 g h i \qquad (1.3)$$

τ_b denotes the bed shear stress:

$$\tau_b = \rho_0 g \frac{u^2}{C_b^2} \qquad (1.4)$$

and τ_v is the vegetation resistance force per unit horizontal area:

$$\tau_v = \frac{1}{2} \rho_0 C_D m \, D h u^2 \qquad (1.5)$$

The uniform flow velocity through emergent vegetation follows from the momentum balance and is given by:

$$u_{cb} = \sqrt{\frac{hi}{1/C_b^2 + (C_D m D h)/(2g)}} \qquad (1.6)$$

Once they determined the average flow velocity, Baptist et al. (2007) proposed to determine the Chezy coefficient as follows:

The discharge per unit width is given by

$$q = hu_{cb} \qquad (1.7)$$

Then, given the Chezy formula:

$$q = hC\sqrt{hi} \qquad (1.8)$$

And inverting it to obtain C:

$$C = \frac{q}{h\sqrt{hi}} \qquad (1.9)$$

It is possible to express C as follows:

$$C = \sqrt{\frac{1}{1/C_b^2 + (C_D m D h)/(2g)}} \qquad (1.10)$$

Moreover, assuming negligible the bed resistance compared to the vegetation resistance, the resistance coefficient can be reduced to:

$$C_k = \sqrt{\frac{2g}{C_D m D h}} \qquad (1.11)$$

Similarly, Nepf (2012) proposed the modelling of flow through a patch of just-submerged vegetation basing on the frontal area per volume. At the patch scale, the vegetation drag can be characterized by an average parameter, the frontal area per unit volume, *a* (e.g. Luhar et al., 2008). When the vegetation has a blade-like morphology, the frontal area per unit volume is $a = nb$, where *n* is the number of blades per unit bed area, and *b* is the blade width as before. The solid volume fraction occupied by the vegetation is therefore $\phi = at$, where *t* is blade thickness. When the vegetation has the shape of a cylinder, the frontal area is obtained as $a = nd$, where *d* is the average stem diameter, while the solid volume fraction occupied by vegetation becomes $\phi = ad\pi/4$.

The average flow velocity through dense patches of emergent vegetation has been described by Luhar & Nepf (2013), as a function of the frontal area per unit volume, as follows:

$$u = \sqrt{\frac{2gi}{C_D a}} \qquad (1.12)$$

Where C_D is the drag coefficient. This law resulted to be effective for describing the flow through a patch that fills the channel width, so not considering lateral frictions between cross-section areas with different velocities. Therefore, it is reliable to apply such a model in the case of a grass-reed cover of the entire channel section, as it could happen in the case of absence of management in channels with constant, low water depths.

Substituting u in Eq. (1.12), the Manning's n for just-submerged or emergent vegetation is:

$$n = \frac{h^{\frac{2}{3}} i^{\frac{1}{2}}}{\left(\frac{2gi}{C_D a}\right)^{\frac{1}{2}}} \qquad (1.13)$$

Symplifying:

$$n = \left(\frac{C_D a}{2}\right)^{\frac{1}{2}} \frac{h^{\frac{2}{3}}}{g^{\frac{1}{2}}} \qquad (1.14)$$

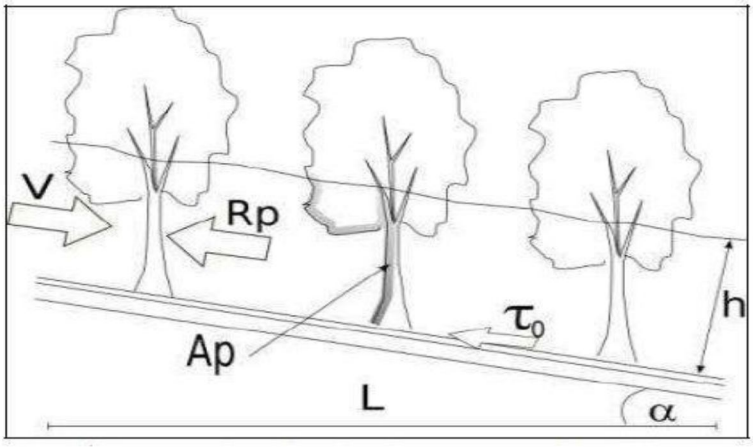

Figura 1.2. Flow resistance through rigid, emergent vegetation (Petryk & Bosmaijan, 1975). τ_0 represents the bed shear stress, further τ_b.

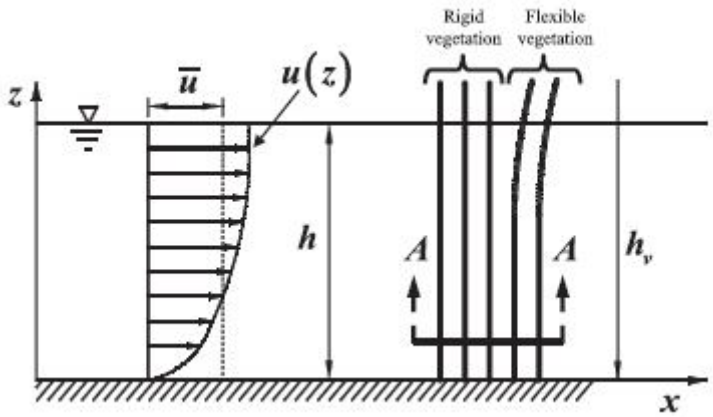

Figure 1.3. Flow velocity distribution through a patch of emergent vegetation (Vargas-Luna et al, 2014).

By means of an important experimental setup, using three different vegetation types (rods, reed *(Phragmites australis)* and bulrush *(Typha capensis)* stems), the authors pointed out that stem's resistance coefficient *(F)* depends on the diameter, density and drag coefficient of the stems considering also that but that stem diameter is a relatively insensitive parameter. The authors purposed as Chezy coefficient:

$$C = \sqrt{\frac{(1 - m\pi D^2}{mDh_v C_D}(2g)}$$

These approaches are not so far to each other. The only difference is given by the different way to express the vegetation density, for which Nepf used the frontal area per volume *a*, while Baptist et al. (2007) preferred the parameter *mD*, which is just the explicit form to express *a*. Among others, Yang & Choi (2010) proposed an analogue formula, proposing a drag coefficient equal to 1.13, instead o the classic Cd=1 used for cylinders. These approaches are substantially identical, as they suppose a constant vertical distribution of the flow through the stems, assumed to be comparable to an array of staggered, rigid cylinders.

These models have a strong theoretical base in modelling flow through rigid stems, since the parameters were derived directly from laboratory measurements on cylinder arrays. As recently observed by other authors (i.e. Aberle & Järvelä, 2013) the natural vegetation rarely presents the features of a rigid cylinder. Even assuming a perfect rigidity of the stems, natural trees present branches (leafy or not according to the season) which have been demonstrated to have even a stronger effect in terms of drag force. Therefore, this approach can be used just in the case of regularly-shaped vegetative elements without branches and leaves.

In the study case of this thesis, the vegetation was composed by emergent reed (*Phragmites australis*). This plant is characterized by the presence of leaves along the whole stem but, in case of high stem density, the leaves in the lower half of the stem die and fall because of the shading of the upstanding canopy. Thus, in such conditions, the flow field through the basal part of emergent reed can be successfully described by these models.

1.2.2 Flow through complex emergent elements: considering branches and leaves

Most of research on vegetative flow resistance was developed on the study of flow around rigid cylindrical elements. The drag coefficient used for vegetation was therefore supposed to be equal to the cylinder drag coefficient, Cd=1. Järvelä (2004) proposed an alternative estimation of Cd, considering

bushes and trees with a more complex structure. For these types of vegetation, the cylinder is not accurate in describing the interaction between vegetative elements and flow (Aberle & Järvelä, 2013).

1.2.2.1 Leafless rigid branched elements

According to the latest studies (i.e. Aberle & Järvelä, 2013) the cylinder approximation resulted to be not effective in describing flow-vegetation interactions, especially when the water depth exceeds the crown base height. A first attempt of going deeper in the question was to take into account the branches, schematizing the plant as a branched element composed by leafless, rigid cylinders. As a matter of fact, branches can contribute more to the total area and volume of floodplain vegetation than the main stem (e.g. Järvelä, 2002b, Wilson *et al.* 2006) and hence the characterization of the characteristic frontal area *Ac* based on the stem diameter cannot be considered adequate for branched leafless trees and shrubs. Several studies demonstrated how the frontal area of a leafless plant does not necessarily increase linearly with the height, as it happens for a cylinder. Moreover, the flow dynamics through an array of branches rarely results comparable to a single equivalent cylindrical element with the same A_c. Since a more accurate description of the branched plant can improve the detail in describing the frontal area interacting with the flow, detailed measurements of the geometrical structure of trees can be used to determine the characteristic area as a function of water depth providing important information for the emergent flow situation.

As observed by Aberle & Järvelä (2013) "*The determination of the global drag coefficients, characteristic areas as well as the relevant approach velocities are hampered by the complex plant shapes, the plants perviousness, and the lack of approaches to adequately determine the influence of wake flow characteristics. Bearing in mind that the drag coefficient is directly linked with the characteristic area and the approach velocity, the wide range of drag coefficients reported in the scientific literature for complex shaped vegetation elements can, besides the influence of tree morphology, also be attributed to the different definitions used for the quantification of these two parameters*". Consequently, most of the parameter values are case-specific and may not be used elsewhere. Basing on this considerations and on his and other previous research, for leafless shrubs and trees Järvelä (2004) stated that a Cd=1.5 is valid for most practical cases for leafless shrubs, which is analogous to the typically made assumption of *Cd* = 1.0 for cylinders.

It is then reasonable to propose as a modelling solution for the flow resistance of branched elements the aforementioned formulae for rigid cylinders, applying instead of the classic drag coefficient C_D=1 the experimental average coefficient C_D=1.5, taking into account also the branches in the determination of the characteristic frontal area. Things are getting more complicated when we consider that a) the branches often present a flexible behavior, different according to specie-specific features and b) the leaves can play

am important role in terms of flow resistance. In the next paragraph, the Leaf Area Index (Järvelä, 2004) approach is presented.

1.2.2.2 Flexible leafy and branched elements (shrubs and tree crowns)

Compared with a non-flexible body, the drag force exerted on trees and bushes can no longer be considered to be proportional to the squared velocity when the flow attack is large enough to deform them (Aberle & Järvelä, 2013).

The deformation of riparian vegetation at the plant scale depends on the flexibility of the stem, branches, and leaves. Hence, for a description of streamlining and associated drag reduction, plant material characteristics such as plant material density ρp, modulus of elasticity E, second moment of area I , flexural rigidity EI, and a number of others must be known (Nikora 2010). Kouwen and Li (1980) were among the first to derive an approach to relate flexural rigidity per unit area (mEI) to deflected plant height. Successively, Fathi-Maghadam and Kouwen (1997) and Kouwen and Fahti-Moghadam (2000) derived a functional relationship between the drag coefficient, flow condition, shape, and flow-induced deformation of a tree. More recently, Chen *et al*. (2011) and Kubrak *et al*. (2012) introduced models to simulate the mechanical behavior of simplified vegetation elements exposed to flow. The model of Chen *et al*. (2011) was used by Stone *et al*. (2011) to investigate the bending behavior of woody riparian vegetation as a function of hydraulic conditions. The latter study revealed a high degree of variability in E between and within vegetation types (willows, cottonwood, and salt cedars). The difference between flexible and rigid plants has been expressed in the literature in a more general way in terms of the Vogel exponent b describing the deviation of the drag force - mean velocity relationship from the quadratic law (de Langre 2008):

$$F_D \sim u_m^{2+b} \qquad (1.15)$$

A value of $b = -1.0$ was suggested for isolated flexible leafy trees in various wind-tunnel investigations (e.g. Cullen 2005, de Langre 2008), indicating a linear relationship between F_D and um and hence implying that $C_D A_c \sim u_m^{-1}$. Similar results were reported in studies carried out in water flows (Fathi-Maghadam and Kouwen 1997, Armanini *et al*. 2005, Wilson *et al*. 2010). However, an a priori assumption of a linear model (i.e. $b = -1.0$) for natural plants is not justified as b depends on the flexural rigidity of the plants (Vogel 1994, de Langre 2008, Dittrich *et al*. 2012). In general, reported values of b for natural vegetation typically range between −0.2 and −1.2 (de Langre *et al*. 2012). In the next paragraphs, a formulation that takes into account the reconfiguration of plants is presented, as the vegetative drag coefficient is corrected by a factor that takes into account flow velocity and the intrinsic characteristics of leaves and stems."

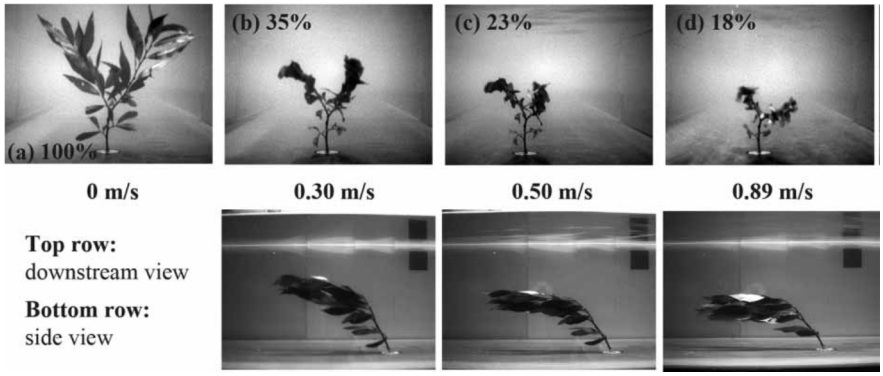

Figure 1.4. Stem and leaves reconfiguration with flow. Percentages are referred to the proportion of the frontal area in respect to the no-flow situation (data from Schoneboom, 2011).

Starting from the already presented assumption that the total shear stress can be considered as the sum of the bed shear stress and the vegetation drag force, Aberle & Järvelä (2013) proposed an alternative approach to estimate the effect of this second factor taking into account the effect of branches and leafs. Assuming that for floodplain vegetation the plants volume is commonly some order of magnitude smaller than the water volume, and that the vegetation basal area per bed unit area is negligible, they assume that the total friction factor can be split as follows:

$$f = f' + f'' \qquad (1.16)$$

where $f = 8gSh/u_m^2$ denotes the Darcy–Weisbach friction factor, $f' = 8\tau_b/(\rho u_m^2)$ the friction factor related to the substrate surface and $f'' = 4m\langle C_D\rangle\langle Ac\rangle\langle u_c^2\rangle/u_m^2$ the friction factor due to form drag.

The determination of C_D resulted to be a challenging issue, since a branched leafy or leafless element cannot be compared to any other standard form. First studies have shown that the pattern and distribution of trees and bushes do not have a significant effect on the friction factor, i.e. *Cd* should be practically constant for a given *Re* range (Fathi-Moghadam, 1996; Järvelä, 2002a). What resulted to make the difference is the presence/absence of branches leafs.

Several studies have shown that foliage contributes significantly to plants total drag (Vogel 1994, Järvelä 2002a, James *et al*. 2008, Wilson *et al*. 2008, 2010, Västilä *et al*. 2011, Dittrich *et al*. 2012), as leaves may account for a large portion of the frontal area of riparian plants (up to 78% according to Armanini *et al*. 2005) or of the total mass (up to 70% according to the review of de Langre 2008). Studies with foliated artificial and natural specimens at different scales (twigs and full-scale trees) showed that the contribution of foliage drag *Ffol* to the specimens' total drag *Ftot* depends on flow velocity and involves significant natural variability (Armanini *et al*. 2005, Wilson *et al*. 2008, Dittrich *et al*. 2012, Västilä and Järvelä 2012). According to the observations of Aberle & Järvelä (2013), the leaves contribute more significantly to total drag at low velocities and their contribution gradually decreases with increasing velocity because of the reduction of frontal area due to reconfiguration. More in detail, Dittrich *et al*. (2012) associated the reduction of the leaves contribution with the different streamlining mechanisms of leaves and wooden

plant parts. They supposed that, when the leaves at a certain velocity reach the maximum streamlining, the drag associated with wooden parts dominant but that the contribution of the leaves to total drag remains constant (approximately 25%). Similar trends were found also by other authors, Västilä and Järvelä (2012), showing the need to distinguish foliated and defoliated conditions.

Quoting the review by Aberle & Järvelä (2013): "The recent studies of Schoneboom (2011), Jalonen *et al*. (2012) and Västilä *et al*. (2012) are a strong indicator that the one-sided leaf area A_L, a commonly used growth property in agricultural and forestry research, represents a suitable reference measure for the characteristic area of foliated vegetation at both plant and reach scale. In fact, the data of Schoneboom (2011) and Jalonen *et al*. (2013) from laboratory investigations with artificial poplars arranged in staggered patterns with identical spacing but different stages of foliation suggest that, dividing the spatially averaged drag force $\langle F_D \rangle$ by the spatially averaged one-sided leaf area $\langle A_L \rangle$, which corresponds to the division of the drag force by the momentum absorbing area (Fathi-Maghadam and Kouwen 1997), the corresponding $\langle F_D \rangle / \langle A_L \rangle - u_m$ data collapse almost on a single line. As observed by Aberle&Järvelä (2013), the advantage of the one-sided leaf area is that it can be upscaled easily to the reach scale by means of the leaf area index (LAI)."

As the same authors pointed out, the essential physical properties to be considered in formulating a resistance equation are density of vegetation and its ability to reconfigure in a flow. Fathi-Maghadam and Kouwen (1997) postulated that for emergent conditions, the vegetation density is always a dominant parameter regardless of tree species or foliage shape and distribution. The combined effect of vegetation density and foliage on flow resistance can be described by the LAI, which is conventionally defined as the one-sided leaf area per ground area assuming that the leaves are flat with negligible thickness (Aberle & Järvelä, 2013). Järvelä (2004) suggested characterizing flexible leafy woody vegetation based on three parameters: (1) LAI; (2) a species specific drag coefficient $Cd\chi$; and (3) a vegetation parameter χ which is unique for a particular species. Järvelä (2004) proposed to determine f'' for such vegetation in just submerged conditions (i.e. where the flow depth is equal to deflected plant height) as:

$$f'' = 4C_{dx} LAI \left(\frac{U}{U_x}\right)^x \qquad (1.17)$$

where $u\chi$ is used to guarantee dimensional homogeneity of the relationship and is equal to the lowest velocity used in determining χ. The vegetation density is considered implicitly in LAI. In order to apply the equation for flow situations where the flow depth is smaller than the deflected plant height, this formulation may be modified by taking into account the vertical structure of the plants and hence the vertical distribution of momentum absorbing area. Until specific data sets become available from hydraulic engineering studies, it may be assumed that the one sided leaf area is vertically uniformly distributed over the height of vegetation and thus LAI may be scaled by the ratio of the water depth h and deflected plant height H (e.g. Järvelä 2004):

$$f'' = 4C_{dx}LAI\left(\frac{U}{U_x}\right)^x \frac{h}{H} \qquad (1.18)$$

To determine the equivalent Manning's *n*, as the global roughness coefficient for a vegetated section, the conversion has to be conducted as follows. Note the relation between the Darcy-Weisbach friction factor *f* and the Manning's roughness coefficient *n*:

$$n = R^{\frac{1}{6}}\sqrt{\frac{f}{8g}} \qquad (1.19)$$

Combining eq. (1.18) with eq. (1.19), and assuming that the bed shear stress is negligible:

$$n = R^{\frac{1}{6}}\sqrt{\frac{4C_{dx}LAI\left(\frac{U}{U_x}\right)^x \frac{h}{H}}{8g}} \qquad (1.20)$$

From which, simplifying:

$$n = \sqrt{\frac{C_{dx}LAI\left(\frac{U}{U_x}\right)^x \frac{h}{H}}{2g}}\, R^{\frac{1}{6}} \qquad (1.21)$$

If a specific (non-linear) vertical distribution of LAI is known, Järvelä's equation can be easily adjusted modifying the *h/H* factor with the corresponding relation. According to Aberle & Järvelä (2013), this approach may currently be seen as the most suitable approach for the determination of flow resistance of leafy floodplain vegetation for practical applications.

1.2.3 Flexible submerged aquatic vegetation

The aquatic herbaceous vegetation was the first typology that has been studied, since for artificial channels is the most frequent to find. In projecting a drainage channel or similar hydraulic structure, the designer has to take into account the development of at least a grass cover on the whole wetted perimeter. Therefore, it has been a necessity since the beginning of hydraulic design to understand the role of such vegetation with different flow conditions. For conciseness, we will treat just the latest and most advanced theories for modeling the flexible vegetation resistance in submerged and emergent conditions. In particular, we will discuss the theory of Heidi Nepf and her colleagues. An interesting conceptualization that she introduced was the distinction of modelling at three different scales: the blade scale, the patch scale and the reach scale.

At the blade scale, modeling is focused on the description of turbulences around the single resistance element, and the energy losses that are occurring because of those. For our study, the blade scale is even

too much detailed, since this work focuses more on the macro-effects of vegetation during a flood. More related to the present research is the patch scale, which considers the flow through an homogeneous porous medium composed by a patch of submerged or emergent vegetation. The dynamics at the patch scale are particularly relevant when a whole part of the flow section is occupied by vegetation, and this occurs especially in the conditions of just-submergence or emergence of vegetation. The most common theories about this situation are presented in the section treating flow in emergent conditions through rigid stems. A focus on the dynamics occurring at the patch scale in case of submerged vegetation is introduced in this section. Last, the reach scale approach was developed to conceptualize the case of partial obstruction of the stream cross-section by means of dense vegetation patches, alternated with undisturbed flow areas, among which the flow velocity is several orders of magnitude different.

1.2.3.1 Submerged meadows of flexible vegetation

The meadow geometry is defined by the size of the single blades and stems, and by their density per unit bed area. As already presented for the flow through emergent vegetation, the most important parameter are the number of stems per square meter and the frontal area per volume a, which can be determined as $a = d/\Delta S^2$, where d is the average diameter or width of the single elements and S is the average spacing. As it happens for shrubs, also herbaceous vegetation can present a non-homogeneous distribution of a along the plant height. For simplicity, for short vegetation as grass, this assumption is acceptable.

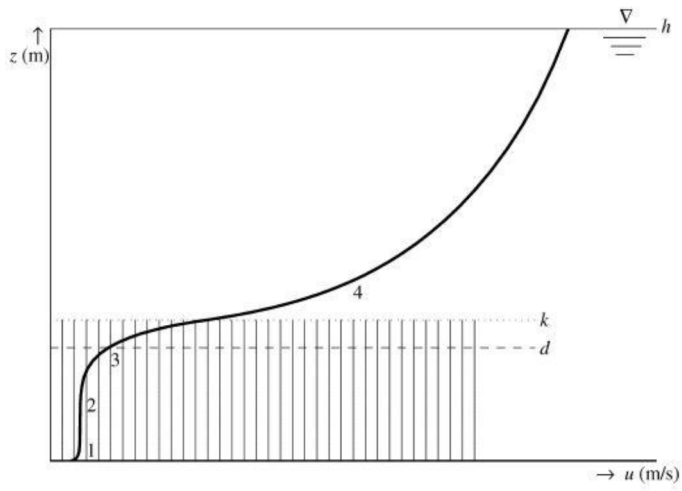

Figure 1.5 a. Velocity profile through a submerged canopy of high density divided in four different layers (Baptist et al., 2007).

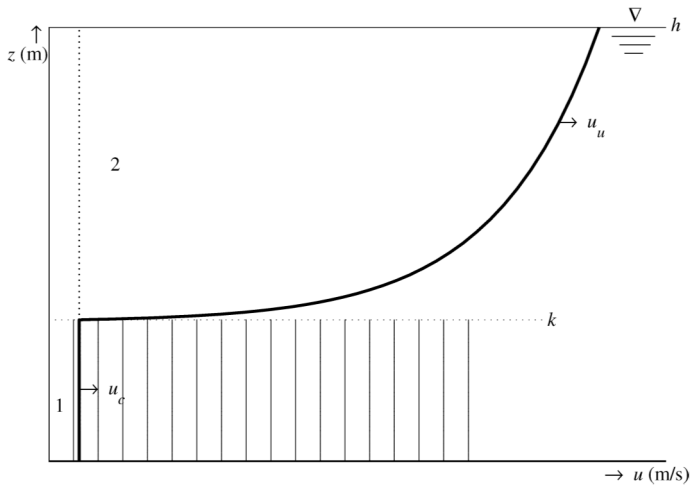

Figure 1.5b. Velocity distribution at a lower degrees of approximation (Baptist *et al*, 2007).

In Fig. 1.5a the flow velocity is split in four different zones. In zone 1 the bed shear stress is dominant. In zone 2, an almost vertically constant velocity is found, influenced by the resistance of stems and leafs. In this part of the profile, flow resistance is well described by the law already presented for the flow through emergent vegetation (eq. 1.14). In zone 3, the flow velocity profile is influenced by both the vegetation layer and the unobstructed flow over the canopy. Zone 4 is the unobstructed part of the profile, which present the common logarithmic distribution of velocities, due to the flow resistance exerted by the canopy top layer. In Figure 1.5b the flow velocity distribution is simplified in two main areas, one influenced by the canopy and one influenced by the shear stress at the canopy top layer. Note that the canopy height k is not constant with flow, as flexible meadows vegetation is bending according to intrinsic characteristics and flow velocity. For the use of the presented resistance model, the reference height of vegetation that should be used is the deflected plant height, which requires the additional knowledge of how the vegetation bends in presence of a determined flow condition (i.e Kouwen, 1988). In alternative, other authors proposed to determine directly the changes in terms of bed roughness, without taking into account changes in the shape of vegetation, but directly in terms of flow resistance (i.e. Whitehead, 1976). In the next paragraph a brief reference to this dynamic is exposed.

Darby (1999), realizing his Hydraulic Model for estimating the effect of riparian vegetation on flow resistance and flood potential pointed out how "Kouwen (1988) demonstrated that the significant stem properties are the stem density M and flexural rigidity in bending, given by J = EI, where E is the stem's modulus of elasticity, and I is the stem area's second moment of inertia. In laboratory experiments of flow over flexible plastic strips, where the values of M, E, and I are readily measurable, Kouwen and Li (1980) showed that the roughness height varies as a function of the amount of drag exerted by the flow

$$k = 0.14\, H \left(\frac{\left(\frac{MEI}{\tau}\right)^{0.25}}{H} \right)^{1.59} \qquad (1.22)$$

where H is the undeflected height of the strips (m); and τ is the local boundary shear stress (N/m2). For natural vegetation it is not so easy to measure M, E, and I, and just a few data is available, affected by noticeable heterogeneity. Instead, Kouwen and his coworkers viewed the combined effect of the product of M, E, and I as a single quantifiable parameter called MEI. According to Kouwen (1988), the combined term MEI indicates that an increase in the number of stems M per unit area has an effect similar to increasing the stiffness EI of individual elements. This compensating effect between stem density and stem stiffness was experimentally verified by Kouwen and Unny (1973), as well as by Temple (1982). The use of the single term MEI to reflect the overall resistance to deformation of vegetation as a result of a flow passing over it is, therefore, justified (Kouwen, 1988). The key aspect of successful application of eq. 1.22 appears to lie in the success of relating the combined parameter MEI to measurable characteristics of natural vegetation. This aspect has been researched by Temple (1987), who undertook laboratory experiments in which MEI was correlated with vegetation height H for a range of growing and dormant grass species

$$MEI = 319H^{2.3} \qquad (1.23a)$$

$$MEI = 25.4H^{2.26} \qquad (1.23b)$$

where (1.23a) is for green, growing grasses, and (1.23b) is for dormant or dead grass. In Temple's experiments, MEI was back-calculated on the basis of flow measurements. The strong dependency of MEI on the height of vegetation stems appears to be due to the way in which the deflection of the vegetative mat under shear occurs, namely through vertical compression of the stems as they bend (Kouwen 1988)."

A different description of the bending behavior of submerged meadows was presented by Whitehead (1976), in which the roughness coefficient of flexible submerged grass was measured for different conditions of flow, expressed by the parameter V*R, where V average velocity and R hydraulic radius. The author proposed five different laws for the same number of vegetation types (Figura 1.6), expressed in terms of qualitative density (Low or High) and average height (Table 1.3). Whitehead's approach omits the determination of the deflected height, since he propose to determine directly the corresponding roughness coefficients from laboratory experiments.

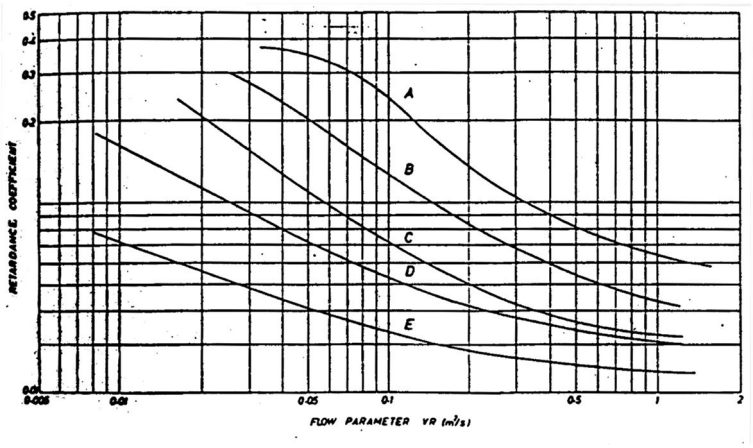

Figure 1.6. Whitehead (1976) proposal for roughness variation with flow.

Density	Average height (cm)	Category
High	>76	A
”	28-61	B
”	15-25	C
”	5-15	D
”	<5	E
Low	>76	B
”	28-61	C
”	15-25	D
”	5-15	D
”	<5	E

Table 1.3. Vegetation parameters for the use of the Whitehead (1976) curves.

Further studies on the same approach kept on describing the flexible behavior of grass bended by the water flow, i.e. Morgan & Rickson (1995). The authors presented how the equivalent Manning roughness is increasing with flow depth up to the submergence. When the water flow exceeds the plant height, thus in complete submergence conditions, the grass resistance falls down because of bending, and stabilizes again when the grass is fully deflected (Figure 1.7).

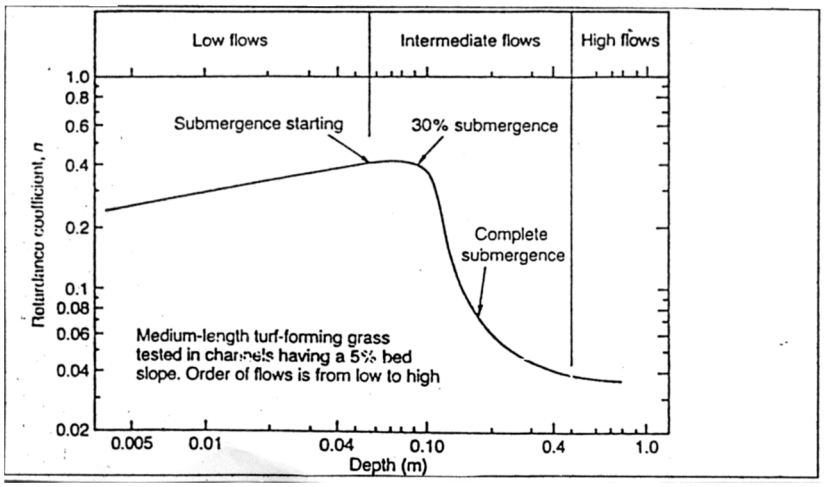

Figure 1.7. Flow depth-roughness relation for average-height grass (Morgan & Rickson, 1995).

1.3 Flow resistance at the reach scale

A different point of view was proposed recently by Luhar & Nepf (2013), introducing the reach scale approach based on the blockage factor. The base of this theory is the assumption that, in case of dense patches of vegetation distributed within the flow section, the flow velocity is influenced as follows. The flow velocity through a dense array of vegetal elements often results several orders of magnitude lower than the one in the unobstructed areas (Nepf, 2012). Therefore, the vegetated patches can be considered a sort of obstruction of cross section, in which the discharge contribution can be considered negligible, as completely blocked. This theory can be applied in those cases where the patches are not covering the most of the cross section. The model is valid both for completely submerged vegetation (where the blockage factor is a continuous patch at the bottom) both for distributed patches across the channel.

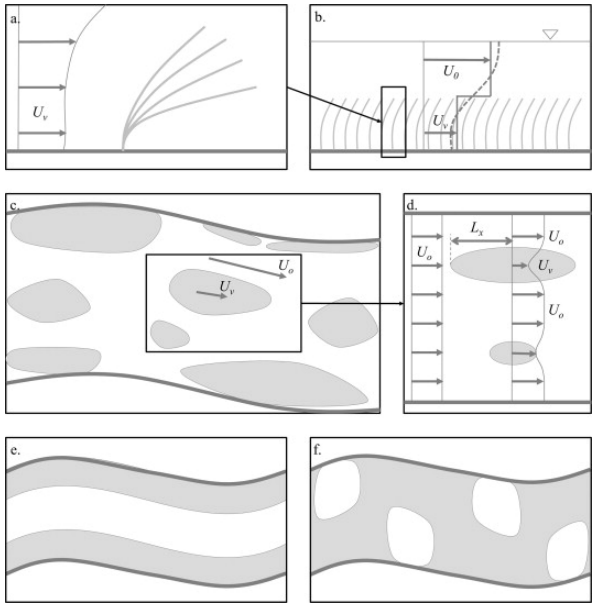

Figure 1.8. (From Luhar & Nepf, 2013). Different schematics of vegetated patches distribution along the channel. The grey parts represent vegetation in panels.

The portion of the channel blocked by vegetated patches is called Blockage factor, B_x. The average velocity is determined as follows:

$$u = \left(\frac{2}{C_*}\right)^{\frac{1}{2}} (1 - B_x)^{\frac{3}{2}} (gih)^{-\frac{1}{2}} \qquad (1.24)$$

A key parameter for this approach in the coefficient C_*, the Drag coefficient of the patch. In fact, considering the vegetated patches as blocked areas, it becomes fundamental to determine which are the drag forces occurring at the edge of the patches, as they are considered as bulked elements. $C_* = 0.05–0.13$, based on fits to field data (Luhar & Nepf 2013). The same authors showed how the flow resistance in a reach with a variable number of patches N but a constant B_x flow resistance was increased at most 20%, so that N=1 is a reasonable simplifying assumption.

Taking into account the Chezy formula, the Manning's n can be considered as:

$$n = \frac{h^{\frac{2}{3}} i^{\frac{1}{2}}}{u} \qquad (1.25)$$

Substituting 1 in 2 we obtain the Manning's n as a function of the Blockage factor:

$$n = \frac{h^{\frac{2}{3}} i^{\frac{1}{2}}}{\left(\frac{2}{C_*}\right)^{\frac{1}{2}} (1-B_x)^{\frac{3}{2}} (gh)^{-\frac{1}{2}}} \qquad (1.26)$$

Simplifying *i* and *h* we finally have:

$$n = \left(\frac{C_*}{2}\right)^{\frac{1}{2}} (1 - B_x)^{-\frac{3}{2}} \frac{h^{\frac{1}{6}}}{g^{\frac{1}{2}}} \qquad (1.27)$$

The blockage factor is obtained as the ratio between the patch frontal area and the whole cross section interested by the flow. The patch frontal area varies with velocity because of the reconfiguration of stems and leafs due to drag forces. The height of deflected vegetation is written as k. Assuming patches of total width w, and a channel of width W, the blockage factor can be determined as:

$$B_x = \frac{wk}{Wh} \qquad (1.28)$$

Where

W is the total width of the patches, k is the height of deflected vegetation, W the channel width, h the water depth. In the case the vegetation is covering the whole channel bottom, w=W and then:

$$B_x = \frac{k}{h} \qquad (1.29)$$

Substituting Eq. (1.29) in (1.27) we obtain that:

$$n = \left(\frac{C_*}{2}\right)^{\frac{1}{2}} \left(1 - \frac{k}{h}\right)^{-\frac{3}{2}} \frac{h^{\frac{1}{6}}}{g^{\frac{1}{2}}} \qquad (1.30)$$

Equation (1.30) allows to determine the Manning's n for channels where the whole wetted perimeter is covered by vegetation, where k<<h.

1.4 Composite roughness calculations

The Manning coefficients obtained from the equations presented above must be considered as the measure of the total flow resistance of the channel, despite the vegetation was not homogeneously distributed along the wetted perimeter. Thus, the obtained values must be considered as equivalent roughness coefficients, as they are not describing only the resistance of the vegetated parts, but an average among the vegetated and non-vegetated parts of the wetted perimeter. In other words, the channel total roughness is comparable to the composition of different roughness coefficients distributed along the wetted perimeter, splitting the cross section in subareas with homogeneous sediments and vegetation densities.

In literature there are a number of different models to compute the composite roughness of a channel with heterogeneous resistance elements within the channel, i.e. Lotter, Horton, Pavlovskii, Colebatch and so on (Kelly McAtee and Leed, 2012). Here a short presentation of the most common ones is provided.

Pavlovskii Method

The method was developed in 1930s by the Russian professor and engineer Pavlovskii. Its derivation was based on the assumption that the total channel resistance force to flow is equal to the sum of subarea resistance forces. The method may be used for both irregularly shaped open channels and irregularly shaped closed channels. The method calculates the composite Manning's roughness coefficient for a compound channel using the following formula.

$$n_c = \sqrt{\frac{\sum_1^N (P_N n_N^2)}{P}} \qquad (3.7)$$

Where:

n_c composite Manning's roughness coefficient;

P wetted perimeter

n sub-areal Manning's roughness coefficient

N total number of the subareas

Horton method

The Horton method was developed in the 1930s by the hydrologist Robert Horton. The Horton method derivation was based on the assumption that the total cross-sectional mean velocity is equal to each and every of the subarea cross-sectional mean velocities. Since the assumption that velocities in the main channel and fllodplains are equal would be very false, tis method should be used carefully.

$$n_c = \left(\frac{\sum_1^N (P_N n_N^{1.5})}{P}\right)^{\frac{2}{3}} \qquad (3.8)$$

Where:

n_c composite Manning's roughness coefficient;

P wetted perimeter

n sub-areal Manning's roughness coefficient

N total number of the subareas

Colebatch method

The Colebatch method was developed in 1940s by G.T. Colebatch. It is the same as the Horton method except the water cross-sectional area is used instead of wetted perimeter in the calculation of a composite manning's roughness coefficient. The method is normally used for irregularly shaped open channels such as natural floodplains.

$$n_c = \left(\frac{\sum_1^N (A_N n_N^{1.5})}{A}\right)^{\frac{2}{3}} \qquad (3.9)$$

Where:

n_c composite Manning's roughness coefficient;

A wetted perimeter

n sub-areal Manning's roughness coefficient

N total number of the subareas

Yen method

Professor Ben Chie Yen proposed a number of different methods in the early 1990s, part of which were based on the premise that total shear velocity should be equal to a weighted sum of subarea shear velocities. Different weighting factors were given to the same basic equation based on various assumptions, regarding relationships between velocities and hydraulic radii of the subdivided areas. This resulted in the hydraulic radii terms being raised to different powers. Only the equation with the hydraulic radii terms raised to the 1/6 power is presented here.

$$n_c = \frac{\sum_1^N \left(\frac{P_N n_N}{R_N^{1/6}} \right)}{\frac{P}{R^{1/6}}} \qquad (3.10)$$

Where:

n_c composite Manning's roughness coefficient;

P wetted perimeter

n sub-areal Manning's roughness coefficient

R hydraulic radius

N total number of the subareas

The methods that are available are various and based on different assumptions. However, we decided to use just the presented ones to estimate the roughness coefficient of the vegetated sub-areas, considering the experimental channel cross-section as a composite section with different roughness coefficients.

1.5 Summary

Reflecting the variety of different situations that are possible to be found along a natural or artificial stream, the academy produced models which can be also far from each other in terms of basic principles. The flow through vegetation can be divided into flow through submerged and emergent vegetation. Flow

resistance of submerged vegetation can be described by equations that are able to take into account the bending, the stem density as well as other vegetation physical parameters (i.e. Kouwen, 1988, Nepf, 2012, etc), or to choose the best roughness coefficients basing on flow parameters, as proposed by Whitehead, 1976 and other authors. An alternative can be represented by not considering at all the flow through the vegetation patch, but instead to determine the blockage factor according to the reach scale approach proposed by Luhar & Nepf, 2013). Focusing on emergent vegetation, different pathways are available if considering the plants as regular, rigid elements or, differently, as flexible elements. In the first case, in literature a number of studies about arrays of emergent cylinders are present (i.e. Petryk & Bosmaijan, 1975; Thompson & Robertson, 1976; Baptist et al., 2007), for which the required input parameters are represented by the frontal area, the drag coefficient, the stem density per unit area. These models are successful in describing flow resistance through leafless, branchless rigid stems, as floodplain forest of tall trees. When the plant characteristics are closer to the shrub form, or the water level reaches the tree crown, these models fails since the plants shape is not constant and not regular anymore. In this case, the most known proposal is represented by the Järvelä model (2004), recently validated by other authors on real-scale plants. This model requires the knowledge of physical parameters of plants which are not easy to determine, included the crown frontal area and flexibility coefficients. A strong innovation proposed by this model was also the use of the LAI for the determination of vegetation density. The Leaf Area Index offers the possibility to use remote sensing techniques, as well as spatialization techniques which enables to map the floodplain vegetation roughness also on wide areas (Forzieri et al. 2012).

Despite the large choice of possible modelling solutions, the application of the presented theories in practice is not yet established. Zahidi et al. (2014) pointed out that "*although there is a considerable collection of studies done on the subject of vegetation interaction with flow through a number of laboratory experiments, there is still a gap in applying the information in the industry*". As a matter of fact, the implementation of vegetation modules on the common hydraulic modelling is still affected by the lack of input data. The totality of the presented studies need to be applied a number of parameters regarding vegetation characteristics, as well as a detailed positioning within the stream sections. Collecting those kinds of data requires a) specific knowledge of both hydraulic engineering and botany, as well as forestry, geomorphology and so on; b) environmental data collection is characterized by large time consumption and data processing, therefore by high costs which are not always affordable. A possible development of environmental hydraulic modelling is nowadays represented by the fast improvement of environmental surveys with remote sensing techniques, such as LiDar, TLS, Photogrammetry, Satellite Image Processing, etc. An additional boost to these methods was given by the outcome of Unmanned Aerial Vehicles, which already showed a great potential also in the field of environmental sciences.

2. MATERIALS AND METHODS

2.1. Study area

The study area is located right outside of the Migliarino - San Rossore - Massaciuccoli Regional Park, a protected area that was established in 1979. It covers approximately 24’000 hectares situated along the coast between Viareggio (Lucca province) and Livorno province, on the north-west coast of Tuscany, Italy. Water plays an essential role in the Park, as the area covered with marshes, rivers, lakes and ponds is of about 3’000 hectares. Although it lies in the middle of a strongly urbanized area, this territory has maintained considerable natural features both for wetlands and coastal sites of relevant interest.

The Massaciuccoli area was in former times the ancient mouth of the Arno river. It was historically known as a marshland, part of which has been drained for cultivation and to contain the diffusion of malaria, the marsh fever. The lake and the drainage channels were, up to some decades ago, an important site for migratory bird species. Since the soil is composed by a layer of peat with a thickness of several meters, lying on a deep layer of sand, the first human impact was characterized by the extraction of peat and sand for the industry.

The main land use of the non-urbanized area is represented by crops as corn and wheat. An important high-value agricultural activity is represented by floriculture and horticulture, both of which need greenhouse structures. The drained soil composed by peat results to be very fertile, as the farmers often do not practice the traditional rotation with other species different than cereals. The forest areas are characterized by the presence of hygrophile species, adapted to a surface water table. A densely urbanized area (Viareggio city) is located along the coast nearby, so that the traditional management of the in-channel vegetation aims to minimize the risk of flood. Within the Versilian plain the presence of settlements and industrial areas is relevant. The flat territory, often below the sea level, crossed by channelized and rectified streams coming from the hills, represents a situation of high risk of flood. The agricultural drainage system, designed for cultivating purposes, has now also a role of flood prevention for the urbanized areas.

2.1.a. Location of the study area.

Figure 2.1.b Location of the study area, detail of the Masaciuccoli plain.

2.1.1 The drainage system

The drainage system was implemented in different periods, lastly at the beginning of the twentieth century, in order to maintain the water table at a level that allows the cultivation of cereals, and for peat extraction. A first reclamation system was realized in the XVth century, without completely solving the

problems of malaria and accessibility of this portion of territory. A dense network of channels drains the fields, which are in part located below the sea level. The high dunes, combined with the subsidence of the peat fields located backwards, are the main reason of the problem of ponding and flooding of the Versilian area.

The first reclamation works in medieval times aimed at cutting the dune system to open drainage channels connecting the fields to the sea. These works did not reach the target completely since the beginning of the last century, when mobile gates were installed at the mouths of the main emissary streams. In fact, the birth of the first official Reclamation Consortiums was during the Twenties, after the First World War.

The basal structure of the modern reclamation system of the area was the building of levees along the main streams coming from the hills, hydraulically separating the uphill waters from the waters of the flat, subsided areas. These territories were then drained by channels (one of which is the experimental site of this thesis) that are collecting rain and infiltration waters to lifting pumping stations, located at the dykes of the main streams. The drainage waters are thus lifted above the sea level and discharged within the diked streams to flow to the sea. In other works, were the ground level was not high enough to move the water to the sea, an artificial lifting system needed to be implemented to drain the fields.

2.1.2 Vegetation and fauna

The area is chracterized by the presence of typical marsh species, such as *Pragmithes australis, Nynphaea spp., Lemna minor, Ceratophyllum demersum, Lemna gibba, Osmunda regalis, Typha latipholia, Thypa angustifolia, Iris pseudoacorus.* The wetlands of the park are the wider extension of Cladium mariscus in Italy, while their value is even increased by the presence of wide area with Sphagnum spp. The environmental value of the Massaciuccoli area noticeably diminished because of water eutrophization, a problem not solved yet which caused the disappearance of a number of water bird for whose the area was famous, and a vegetation alteration.

Within the park and in the neighboring areas are present *Circus aeruginosus L., Ardea cynerea L., Ardea alba L., Bubulcus ibis L., Egretta garzetta L., Gallinago gallinago L., Fulica L., Anas platyrhynchos L, Cettia cetti T., Acrocephalus scirpaceus, Acrocephalus arundinaceus, Chlidonias leucopterus* (logo of the park) and many others. It is noticeable to point out that many of these species are connected at least for a part of their life to the presence of vegetation along the water reservoirs and channels. The presence of mallard, which is hunted at the borders of the Park, and other bird species reproducing in this area raised attention on the environmental and ecological impact of vegetation management.

The waters of the lake and the connected channels are populated both by autoctone and alloctone species. Here a list of the most common species: *Tinca tinca, Cyprinu carpio, Carassius carassius, Micropterus salmoides, Perca fluviatilis, Esox lucius, Anguilla anguilla, Gambusia holbrooki*, different species of *Mugilidae, Ictalurus melas* (an alloctone specie which at the moment results the prevalent in the Massaciuccoli lake), and others. In the 1990s, the introduction of Lousiana crawfish (Procambarus clarkii) impacted the balance of the fish communities, as well documented by the research of prof. Francesca Gherardi. Nowadays the specie seems to partially limited by the predating activity of a number of predatory birds.

2.1.3 The traditional vegetation management

The management of the drainage channels network has been practiced historically by the Reclamation Consortium, as it represents an issue of the whole community of farmers and landowners included in the area. From a rational point of view, the drainage network had to be designed in order to subtract the least land as possible to the agricultural activities. Moreover, since the construction of the drainage network was a cost, the traditional approach has been traditionally oriented to realizing the channels the narrowest possible for a given discharge capacity. As a consequence, the channel design was realized taking into account the bare soil as the bed surface, minimizing the flow resistance and so maximizing the discharge capacity for a given cross section. Therefore, the drainage network has been designed historically considering a Manning roughness coefficient of 0.02-0.03, assuming bare soil at the banks and the channel bottom. The result of this designing approach is that the growth of natural vegetation within the streams is seen as a problem to solve, as it modifies the hydraulic design conditions.

The most common practice for channels management is the removal of the entire vegetation canopy from the whole cross section. The cut is conducted at least twice per year on the banks: a first cut in June and a second in October, by means of an agricultural mulcher (see Fig.2.2). Every second year, according to the vegetation growth, the cut is executed also within the channel by an excavator equipped with a weed cutting bucket, able to cut the vegetation under the water surface (see Fig. 2.3). In particular, the intervention with this kind of device is oriented to the removal of the reed roots, that are growing within the mud at the channel bottom, while the plants growing on the banks are just cut at the ground level. The bucket cuts the reeds in the channel at the roots, and removes a part of the mud, restoring the original cross section. With this intervention, the growth of the reeds in the central part of the channel is usually very slow, so that the cut is not practiced with the same frequency of the banks. At the banks, the roots are not removed, since the cut is practiced at the ground level. The common practice, carried on twice per year along the whole drainage network, is to cut just the emergent part of the reeds growing from the banks, by means of mulchers carried by agricultural tractors. These machines are not able to cut under water, so

that the reeds that are growing from the submerged part of the bank are just cut above the water surface, while the submerged part of the stem stays untouched.

Figure 2.2. Mulching of the vegetation on the banks. The device is not able to work below the water surface.

Figure 2.3. Detail of the cutting bucket mounted on excavator. The device works also under water and is able to cut the roots within the mud.

As a matter of fact, the vegetation management resulted to be strongly impactful for the animal communities which are living part or the entire life cycle in the reed vegetation. Their habitat is destroyed periodically, in some cases even during the reproduction season. The justification of this practice is given by the need to maintain the design discharge capacity of the channels, to prevent flooding. In the next chapter the materials and methods of the research that we conducted to estimate at the real scale the effect of reed are presented.

2.1.4 The Bresciani channel

The survey location is a straight stretch of length 300 m, located at the end of the Bresciani drainage channel (Upstream border N 43.884181, E 10.286261; Downstream border N 43.886163, E 10.284005) in the Versilia-Massaciuccoli reclamation area, Bonifica di Ponente section. The Bresciani main channel has a total length of 2790 m, draining a catchment of 55.4 hectares, and is part of the Sinistra Sassaia drainage system. It starts draining the fields on the left bank of the Gora di Stiava stream, then it underpasses this stream , flowing straight for 900 m. Its mouth is located at the end of this straight stretch, within the Brentino Channel, which flows to the pumping station at the Sassaia stream. The cross section at the study site has a trapezoidal shape, with quasi-vertical banks, a bankfull width of 5.3 m and a depth of 1 m. The bed slope is approximately constant and equal to 0.0004. The bed material is composed by peat. The stretch was chosen because of its regular shape and slope, and for the regular distribution of the vegetation along the whole reach. In figure 2.2 (Casarosa et al, 2006) the whole Bresciani reach is presented. The experimental site is located downstream the bridge.

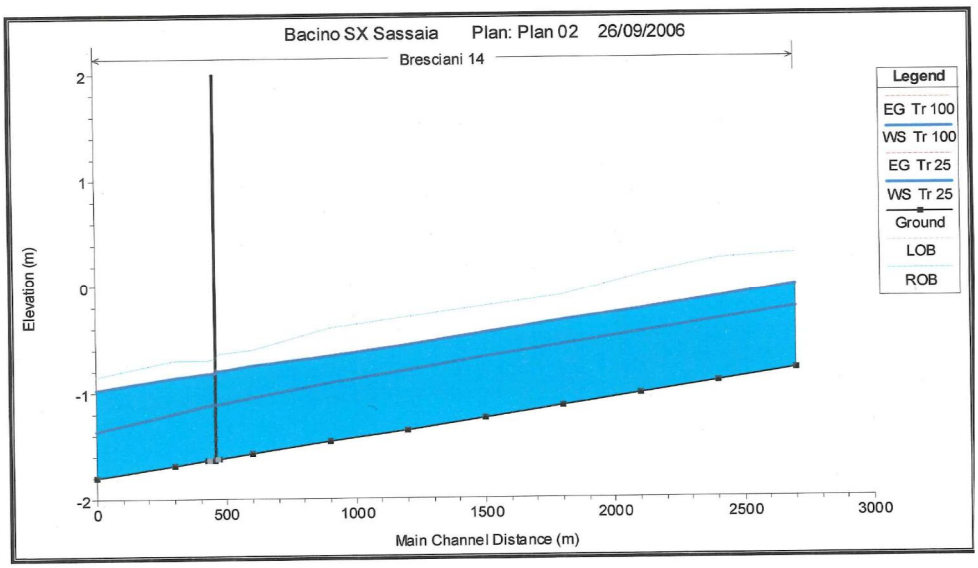

Figura 2.4 (Adapted from Casarosa et al, 2006). Bresciani channel with the 25 years return time discharge in design conditions. The bed slope resulted to be homogeneous, allowing the instauration uniform flow condition.

The Bresciani channel is located below the sea level, thus below the level of the streams that are flowing to the coast. Therefore, the water coming from this channel need to be lifted up to the stream connected to the sea to be taken away from the reclamation area. To do this, at the end of the drainage network, more precisely 1116 m downstream the experimental stretch, a water lifting station was built in the twenties. The lifting station is dimensioned to be able to pump the discharge of the connected drainage network in case of flood, and is composed by 3 pumps. To maintain the water table below the level that is necessary for cultivation, one of the pumps, with a discharge capacity of 0.6 m^3/s, automatically starts when the water exceeds a determined threshold. The additional pumps are manually activated in case of emergency.

The channel vegetation is mainly composed by common reed (Phragmites australis) with a slight presence of Iris pseudoacorus. Reeds are growing homogeneously both on the riverbanks and within the channel. The stem density is higher on the banks, because at the channel bottom the periodic reshaping of the cross section, which every second year needs an intervention with excavators to remove the peat that is falling from the banks within the main channel. The continuous income of ground within the channels was already pointed out during the last update of the reclamation system in 2006 by Casarosa et al. (2006). The authors pointed out that this phenomena is due to the intrinsic characteristics of the ground, which has scarce cohesion, but also to the impact of the agricultural machines which moves too close to the channel banks.

2.2 Field surveys

2.2.1 Topographic surveys

A detailed survey of the channel morphology was carried out to collect information about the regularity of the cross sections and of the channel slope. In collaboration with the topographer of the Toscana Nord Reclamation Office 10 cross section were surveyed from the mobile pumps inlet point and the water lifting station at the end of the whole Sinistra Sassaia drainage network. Survey were carried out using a Trimble topographic total station with integrated GNSS system (Fig. 3.1). The total station was georeferenced using fixed target points located in the surroundings, with a sub-centimetric precision rate.

Figure 2.5. Topographic survey be means of the Trimble total station.

Because of the constant presence of water within the stream and the absence of a consistent sediment at the bottom, the channel bed level was initially hard to determine. After various attempts, the best solution was found using an iron rectangular plate (30x30 cm) at the foot of the topographic target rod.

To have an additional confirmation of the validity of the surveys carried out with this methodology, the experimental stretch of 300 m was closed upstream and downstream by means of ground clogs, and totally dried before the survey. This operation was also functional to the measures aimed at characterizing the vegetation.

2.2.2 Vegetation surveys

The vegetation survey was fundamental to describe the characteristics of the roughness elements within the channel. The measurements were conducted at the three cross sections previously surveyed with the total station and gauged with the staff gages, the day before the hydraulic measures. Moreover, the measures were conducted three times during the growth season on six control plots, at a distance of 20 days one from the other. The 1x1 plots were signed with iron pickets in order to return exactly at the same point. The aim of these last surveys, conducted during the 2015 vegetative season, was to describe the evolution of the vegetative parameters during the growing season, to check if such a monitoring could bring useful information in determining the optimal cutting season.

The aim of the survey was to collect the data that were found to be related with the flow resistance of vegetation (see the State of the Art chapter), in particular the average diameter of the stems, the number of stems/m^2, the average height, the maximum height of the plants. The diameter of the stems was

measured by means of a high precision iron caliper, while the plant height by mean of a metric rod. The number of stems in each plot was manually counted.

Figure 2.6. Vegetation survey in plots 1x1 m.

Figure 2.7 Example of plot along the experimental reach.

At each surveyed cross section, starting from one bank, the aforementioned parameters were measured within a square of 1 m^2, that was moved from one bank to the other, without overlays or gaps. Thus, a continuous strip of width 1 m, oriented in parallel to each cross section and split in sections of 1x1m was surveyed to describe the horizontal distribution of the vegetation along each cross section. To correctly position the surveyed strip with the section, the squares located at the banks were georeferenced and

reported in planimetry with the channel. In this way, the vegetation distribution was georeferenced and positioned correctly within each cross section.

A detailed species classification was not conducted, as the dominant specie was the common reed, *Phragmites australis*, which basically formed a mono-specific canopy along the whole channel. An exception was represented by sparse groups of *Iris pseudacorus*, which are considered negligible compared to the *Phragmites* at the reach scale.

2.2.3 Airborne data acquisition

An interesting opportunity in environmental research is emerging in the last years from the use of UAV - Unmanned Aerial Vehicles. The availability of compact high-resolution digital cameras mounted on a drone allowed to capture detailed images of the survey area. Aerial Imagery was collected along the whole experimental reach using two different digital camera: RGB Sony WX 18.3 MP and Near Infrared Camera Canon S110 NIR 12 MP attached to the Fixed-Wing UAV eBee Ag SenseFly. (Figure 2.8). Twelve Ground control points (GCPs) were positioned the site before image acquisition. GCPs were surveyed using a total station and were important for the subsequent georeferencing of the imagery.

Figure 2.8. eBee drone used for the flights.

The flights were conducted before and after the cut of vegetation covering the enire experimental reach. The elaboration of RGB imagery allowed the production of high-definition ortophotos. By means of the SFM (Structure From Motion) procedure, the point clouds before and after the removal of vegetation were realized. The elaboration of the point clouds allowed the creation of the Digital Surface Model (the surface

of vegetation) and the Digital Terrain Model (the bare ground morphology). Subtracting the DTM from DSM it was possible to determine the volume of vegetation along the reach, with a pixel of 5x5 cm at the ground.

The NIR imagery allowed to capture the NDVI index distribution along the channel. This parameter was found to be related to a number of vegetation density indexes, one of which is the LAI – Leaf Area Index. The LAI was used by Jarvela (i.e. 2002a) as the most important input parameter in determining the flow resistance in vegetated floodplains. Future developments of this work will regard the extraction of a LAI map for the experimental channel, and the application of such models to the case study.

2.2.4 The experimental setup

The main question for the Reclamation managers was the estimation of the effects of the natural vegetation at its maximum growth rate. As a matter of fact, the managers still do not know the quantitative effect of channel vegetation in terms of roughness, thus they apply a conservative approach removing from the channel every possible resistance element. Therefore, the hydraulic measures aimed at determining the quantitative differences between a channel in condition of full vegetation development, and the same channel after an ordinary management cut. For instance, the cut that is traditionally practiced along the drainage channels aims at removing the entire vegetation. Thus, the two scenarios were established in the two cases: first and after the cut of the entire channel. However, we found these two scenarios as the extremes of a situation that could be solved with an intermediate proposal. Thus, we proposed to test an alternative, less impactful management technique, aimed at satisfying both environmental and hydraulic requirements. In detail, we proposed to cut the vegetation on one bank and along the whole channel bottom, saving a buffer of undisturbed canopy covering the entire other bank. This solution was unknown by the managers, as its efficacy in terms of discharge capacity and flow resistance were never tested before. We found of interest to test this alternative solution as it could represent a positive innovation for the whole area.

The first hydraulic survey was conducted on vegetation at its maximum development. Then, the first partial cut was conducted by means of an agricultural mulcher and an excavator equipped with a cutting bucket. The mulcher removed the entire emergent canopy from the left bank along the entire experimental segment. Then, the excavator refined the work, removing the submerged stems from the left bank and from the channel bottom. The canopy along the right bank, from the emergent top to the submerged toe, was left untouched, as the aim of this approach was to leave a buffer for animal refuge and nesting.

Figure 2.9. Full vegetated scenario.

Figure 2.10. Half vegetated scenario.

Figure 2.11. Non-vegetated scenario.

Then, the hydraulic measures were carried out for the half vegetated scenario. The last hydraulic measure focused on the totally cleared scenario. Thus, the vegetation on the right bank was removed with the same equipment mentioned for the partial cut. Last, the velocity and water level measures were carried out for the cleared scenario, as reference situation for the determination of the bed roughness.

2.2.4.1 The pumping system for artificial discharges

To describe the effect of vegetation on flow the measures for just one discharge were not sufficient. According to what already presented in the state of the art, the flow interaction of flexible vegetation is not constant for different hydraulic conditions, as the plants reconfiguration brings variation in the flow resistance due to the plants drag forces. As a matter of fact, the description of the effect of channel vegetation on flood risk required to measure the hydraulic parameters of the flow during a condition of high discharge. Therefore, we decided to implement a system able to pump into the experimental channel different discharges, up the bankfull condition. Thus, to analyze the behavior of the plants for different hydraulic conditions, we decided to trace the flow-rate curves for different vegetated scenarios. For each scenario, four discharges were pumped gradually increasing up to reach the bankfull condition.

The water was taken from the Gora di Stiava channel, an embanked stream coming from the hills and flowing directly to the sea (Fig.. 2.12). This stream is flowing about 1 m above the ground level, contained by dikes made of earth. The drainage system, part of which is represented by the Bresciani channel, is therefore about 2 m below. At one point of its course (Coordinates 43.880134 N, 10.291507 E), 440 m upstream the experimental stretch, the Bresciani channel is flowing under the Gora di Stiava, through a culvert made of concrete. This point was chosen as the best site to take the water from the Gora di Stiava, to pump it into the Bresciani channel. Despite the water was located higher than its destination, pumps were needed to lift the water over the levee.

The pumping station was composed of four mobile lifting pumps carried by agricultural four-wheel tractors (60 to 85 hp). The pumps were located at the top of the levee of the Gora di Stiava. Attached to each pump outlet, a rubber pipe of length 5 m was carrying the water down to the Bresciani channel. The lifting pumps were powered by the tractor engines. It was not possible to directly measure the discharge at the pump outlet, as the discharges were too high to be estimated by common water meters. More precisely, every pump had a maximum discharge capacity of 0.3-0.4 m^3/s. A constant rpm regime for each machine was set, while the four tractors were started one after the other, thus pumping four different increasing discharges.

The choice of not measuring the water discharges at the pumps outlet was also motivated by the high distance between the inlet of the artificial discharge and the experimental stretch, and the possible

consequent water losses. In fact, the 440 m long channel segment located between the pumps and the experimental site was characterized by permeable banks, moreover interrupted several times by secondary drainage canals, along which a part of the discharge could be lost.

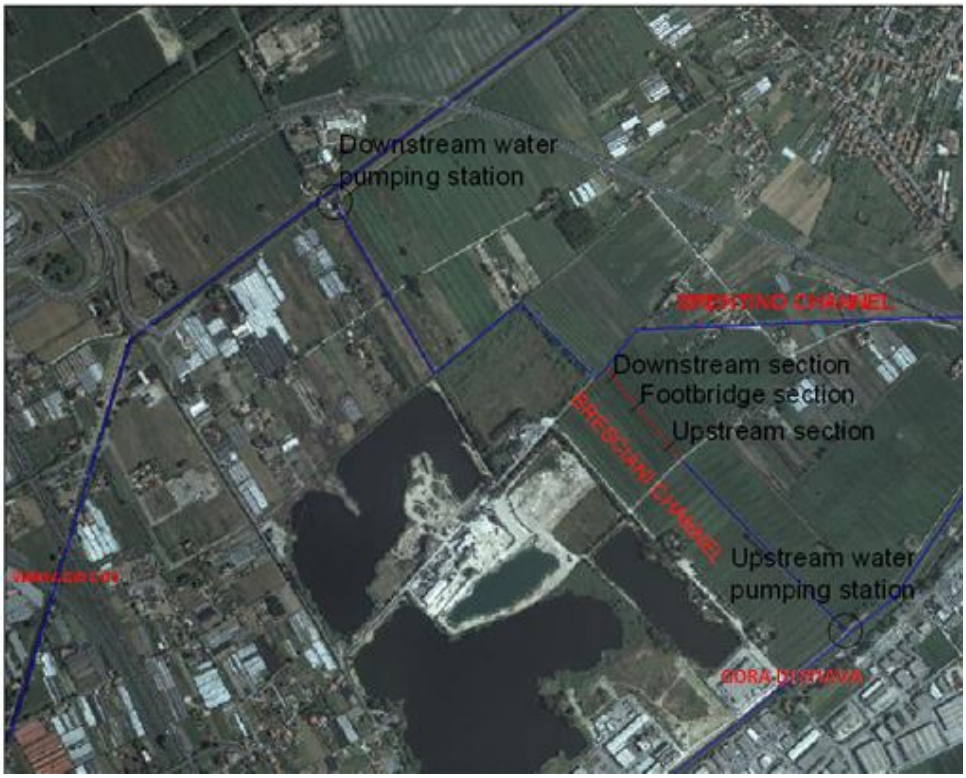

Figure 2.12. Aerial view of the study area. The upstream and downstream pumping station are located in correspondence of the confluence with the two higher channels delimiting the reclamation area. The experimental reach is colored in red.

By means of a mobile iron floodgate, the Bresciani channel was clogged at the outlet of the culvert through which it passes below the Gora di Stiava. The floodgate was necessary to hydraulically isolate the upstream part, located at the left side of the Gora di Stiava stream, from the downstream part, at the right of the same stream. With this layout, a rise in the water level in the downstream part have not lost water flowing backwards in the upstream part. As a matter of fact, given the low slope gradients in the Bresciani channel, this problem could have occurred. Moreover, isolating the upstream part, the only discharge getting to the experimental stretch was composed by pumped water, without perturbations from upstream. It has to be noticed that the closing time of the Bresciani channel was limited by the necessity to drain the water coming from upstream. Therefore, it was possible to keep the floodgate closed just for 7-8 hours per day. Anyway, this time was sufficient for tracing a rating curve of four discharges. The installation and the fixing of the floodgate was made by an excavator. The same excavator was left in position in order to keep the floodgate blocked against the culvert. The four rubber pipes coming from the pumps were pointed at the bucket of the excavator, to dissipate a part of the water energy. In this way, the water coming out from the pipes was not eroding the channel bottom.

Figure 2.13. Mobile pumping devices were taking water from a higher channel to be pumped in the experimental reach.

Figure 2.14. Introducing artificial discharges upstream the monitored reach. The bucket was placed to avoid the bottom erosion and to fix in position the floodgate closing the culvert, connected with an upstream part of the same channel.

2.2.4.2 Velocity measures

To describe in detail the velocity distribution along the channel cross section a grid of survey points distributed along the whole flow section was set-up. An iron footbridge was positioned at the middle cross section by means of an excavator, taking care of not to modify the cross section shape of the channel and not to occupy the water flow section. The velocity measures were carried out at the middle cross section of the experimental reach, by means of a USGS Type AA Current meter. The data was received and displayed by an AquaCount 5100 reader, and then manually transcribed on paper blocks. In the appendix attached to this chapter a detailed technical information of the used tools is provided. The velocity was measured at seven verticals, each 15 cm of depth. Three centimeters below the water surface and 10 cm from the bottom two additional points were measured for each vertical. With this approach, the grid was not regular, but it was better describing the whole flow field. Each velocity measure took 30 seconds of registration time, as the recorded value was an average value on 30 s of measuring. Given a not regular depth of the cross section, for each vertical 2-8 measure point were recorded. Therefore, according to the water depth, and the necessary number of survey points, the velocity survey took about 20-30 minutes for each measure. The verticals were monitored starting from the right bank. For each vertical, a measure just below the water surface was taken, moving then deeper of 15 cm each step. Once at the bottom, a measure 10 cm from the bottom was taken. The current meter position was determined as a reference to the staff gage head, which has been leveled during the topographic surveys. The velocity measures were hampered by the high turbidity of the water, that was hiding the current meter already at 15 cm of depth. In Appendix 2.b the distributions of the velocity measures for each discharge are presented.

Figure 2.14. Flow velocity measures by means of the USGS Type AA current meter.

In order to monitor the stability of the hydraulic conditions during the time of survey, the water level was measured continuously at three sections. The aim of the water level monitoring was to assess the

stability of the flow conditions and to monitor the flow variation between one discharge condition and the following one. Three staff gages were positioned at three cross sections previously recognized during the topographic survey. The elevation of each staff head was recorded, in order to rebuild the water surface profile for each discharge and each scenario. The staff gages were located 145 m upstream, at the velocity measuring station and 85 m downstream. The water levels were monitored by three people, each of one was recording the level each 3 minutes. The velocity measures were starting after 10 minutes of stability observed at the three gages. The time required to stabilize the water level between one discharge and the following was not constant, and varied for the same discharges for the different vegetation scenarios. Given 3 vegetated scenarios, and four discharges per each, a total number of 12 discharges were surveyed.

Figure 2.15. Staff gage positioned at one of the monitoring sections along the experimental channel.

3. RESULTS

In this chapter the results of the July 2016 survey are reported. The chapter is organized in 4 sections: vegetation parameters, velocity distributions, discharge estimations, , and roughness estimation.

3.1 Vegetation parameters

The vegetation surveys took place in two different vegetative seasons, aiming at different scopes. The first field campaign was conducted in late spring of 2015, with the aim of describing the vegetation development over the course of a vegetative season. The second survey, carried out a few days before the hydraulic measures in 2016, was more detailed and focused on the distribution of the vegetation parameters along the channel and across the cross sections.

As usual, the reed vegetation has been cut in October 2014, that corresponded to the second intervention of that year. Therefore, at the beginning of the dormant season the channel resulted totally cleared. The reed get through the winter naturally losing the whole aerial parts (stems and leaves), which naturally die and rot. The subterranean part, composed by rhizomes and roots, survives and produces new sprouts after the coldest season. In the Massaciuccoli area, the new vegetation starts to grow in march, and continue developing up to the summer, when the flowering states the end of the growing season. The first cut of the year is practiced in June-July, when the development is supposed to be at the maximum.

3.1.1 Monitoring the vegetation evolution

The survey conducted in 2015 aimed at measuring the growth rate during the season, focusing on the parameters related to vegetation resistance. Three surveys were conducted at the same six plots, homogeneously distributed along the experimental channel. More precisely, the plots were positioned in front of each other, at three cross sections, at the emergent part of the bank. Each plot was delimited by a wooden rectangle of size 0.7x1 m, fixed at the ground by means of iron pickets, in order to delimit a precise plot within which to repeat the measures after time.

The first survey was carried out in late April, when the reed already started to grow, while the third at the end of June, right before that the management cut was practiced, as usual every year. The last survey was conducted at the beginning of June, when the plants were still in the growth phase, but the cut was scheduled.

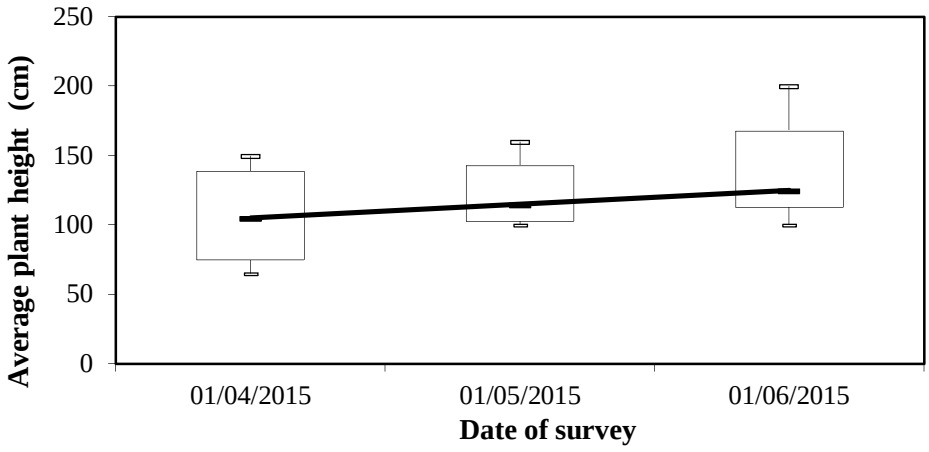

Figure 3.1. Average height evolution during the 2015 vegetative season.

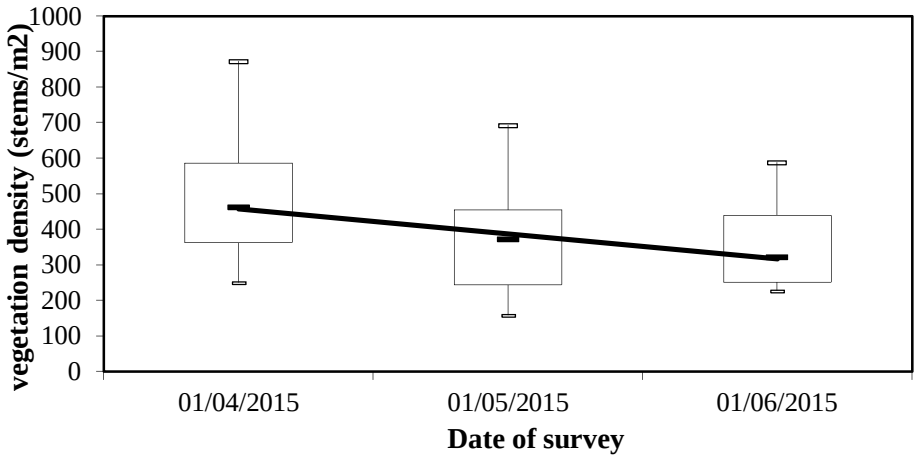

Figure 3.2. Average stem density during the 2015 vegetative season.

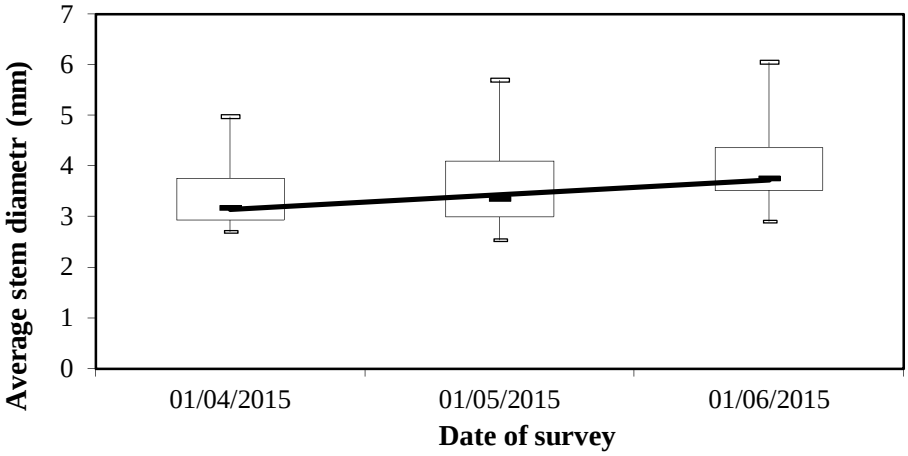

Figure 3.3. Average stem diameter during the 2015 vegetative season.

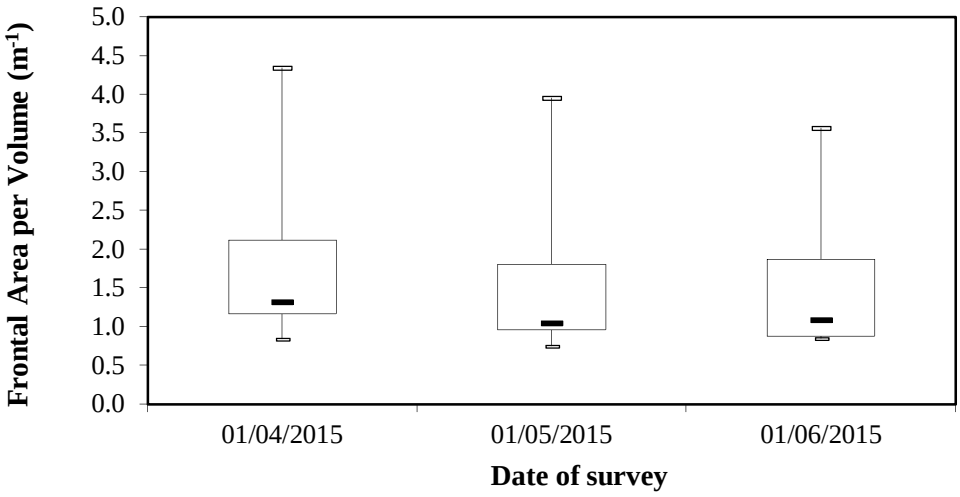

Figure 3.4. Average frontal area per volume (Nepf, 2012) during the 2015 vegetative season.

Results showed that the reed vegetation constantly increased in diameter and height, while the stem density trend decreased towards the full development season. In other words, the reed tended to select the best stems, while the smaller were succumbing because of competition for light. In terms of flow resistance, the parameter "frontal area per volume" initially decreased because of the reduction of the stem density, but changed in trend when the stem diameter increase more than balanced the loss of stems due to competition. Therefore, it is reasonable to assess that the increasing trend would have continued until the flowering season, when the plant growth normally stops.

3.1.2 Describing the vegetation distribution

The survey conducted in 2016 aimed at describe the vegetation distribution along the channel and the monitoring cross-sections. More precisely, the collection of the most important parameters influencing the flow resistance was carried out, in order to obtain the input data for the latest models of vegetation resistance. Each cross section was split in six subareas of width equal to 1 m. For each plot the parameters "number of stems", "maximum height", "average height", "average diameter" were collected. Results are presented in Tables 3.1 - 3.4.

Tab. 3.1 - Upstream section						
Sub-area [1m^2]	**1**	**2**	**3**	**4**	**5**	**6**
plants/m^2	130	70	0	0	28	71
max height [m]	2.1	2.0	0	0	1.6	1.8
average height [m]	1.9	1.8	0	0	1.4	1.7
average diameter [mm]	5.8	5.8	0	0	4.0	3.5

Tab. 3.2 - Middle section						
Sub-area	**1**	**2**	**3**	**4**	**5**	**6**
plants	105	25	3	45	129	40
max height [m]	1.6	1.5	2.3	2.3	1.9	2
average height [m]	1.3	1.3	2	2	1.4	1.4
average diameter [mm]	3.3	6.3	5.0	6.7	3.2	3.3

Tab. 3.3 - Footbridge section						
Sub-area	**1**	**2**	**3**	**4**	**5**	**6**
plants	150	120	18	47	40	40
max height [m]	1.3	1.9	2.2	2.3	2.5	1.3
average height [m]	1.1	1.7	1.9	2	2.1	1
average diameter [mm]	2.5	2.0	6.7	3.7	5.4	3.0

Tab. 3.4 - Downstream section						
Sub-area	**1**	**2**	**3**	**4**	**5**	**6**
plants/m2	90	105	52	17	25	52
max height [m]	1.5	2.0	2.0	2.2	2.3	1.8
average height [m]	1.0	1.9	1.9	2.0	2.0	1.5
average diameter [mm]	3.9	5.4	4.5	4.0	6.0	5.3

Table 3.1-3.4. Distribution of the vegetation parameters in the four sampling sections.

These data were used to calculate an average distribution for each subsection of the channel. In other words, the surveys at the four section were averaged to obtain an average distribution of the vegetation parameters along the experimental reach. As a matter of fact, the roughness values obtained with the hydraulic measures must be compared with the average of the ones calculated for each cross section. A synthesis of the observed data is presented in the Tables 3.5-3.6:

Tab 3.5 - Average stem density [stems/m^2]						
sect/subsect	**1**	**2**	**3**	**4**	**5**	**6**
Upstream	130	70	0	0	28	71
Middle	105	25	3	45	129	40
Footbridge	150	120	18	47	40	40
Downstream	90	105	52	17	25	52
Average	119	80	18	27		56

Tab 3.6 - Average diameter [mm]						
sect/subsect	**1**	**2**	**3**	**4**	**5**	**6**
Upstream	5.8	5.8	0.0	0.0	4.0	3.5
Middle	3.25	6.30	5.00	6.67	3.15	3.25
Footbridge	2.5	2.0	6.7	3.7	5.4	3.0
Downstream	3.9	5.4	4.5	4.0	6.0	5.3
Average	3.9	4.9	4.0	3.6	4.6	3.8

Tables 3.5-3.6. Average values for stem density and stem diameter.

3.1.3 Aerial Imagery data extraction

Structure-from-Motion Photogrammetry Imagery was processed using SfM software package PhotoScan Pro v.1.2.5 (Agisoft LLP), which works by matching conjugate points from multiple, overlapping images and estimating camera positions to reconstruct a 3D point cloud of the scene geometry. GCPs were used to optimize the image alignment and georeference the dataset. Outputs included an orthophoto and a digital surface model (DSM) for each flight– Figure NUMERO. The Four DSM and orthomosaic were coregisterd. The difference between DSM with vegetation (19.07.2016) and without vegetation (25.07.2016) were calculated to estimate the vegetation volumes.

N. Flight	**Date**	**Camera**	**Time of flight**	**Altitude**	**Overlap - Sidelap**	**N image**	**Ground Resolution**
1	19.07.2016	Sony WX 18.3 MP	10‘	60 m	85%-75%	98	2 cm
2	19.07.2016	Canon S110 NIR 12 MP	10’	53 m	85%-75%	69	2 cm
3	25.07.2016	Sony WX 18.3 MP	10’	60 m	85%-75%	98	2 cm
4	25.07.2016	Canon S110 NIR 12 MP	10’	53 m	85%-75%	69	2 cm

Table 3.7. Description of the drone flights.

DSM were produced from Aerial Photogrammetry, and the height of vegetation was mapped as the Z difference between the two surface models.

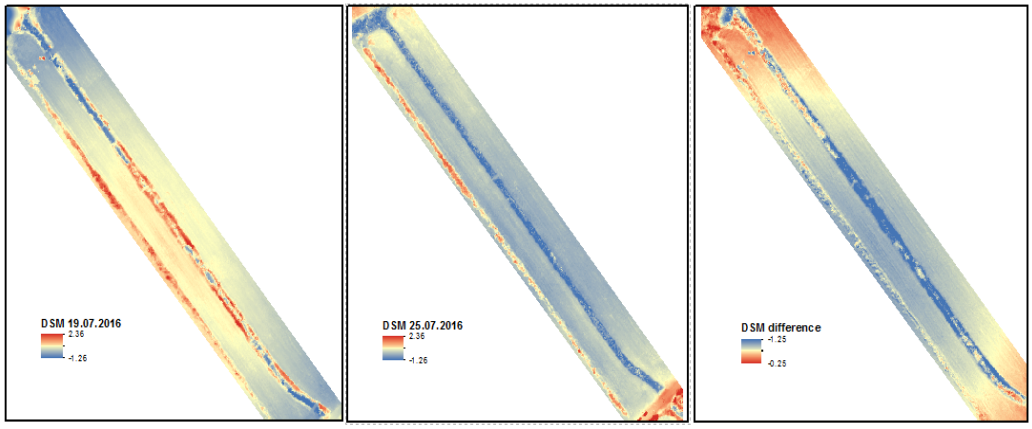

Fig 3.5. DSM before and after vegetation removal. The difference gives a value of average height of the plants for each pixel.

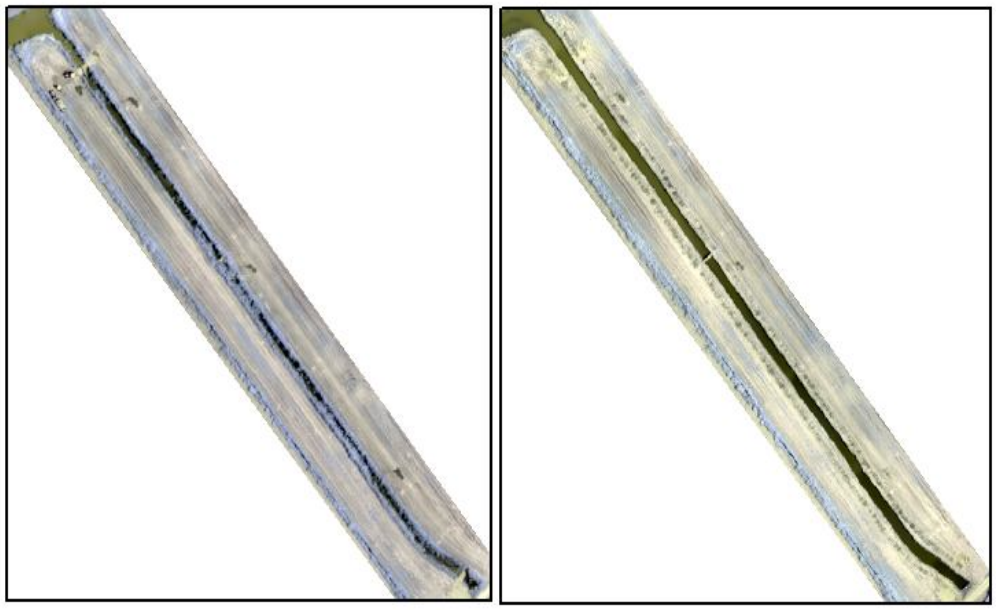

Figure 3.6. NIR imagery before and after vegetation removal. The data is consistent with vegetation density. NIR data will provide information about the canopy LAI (work in progress).

3.2 Flow analysis

The discharges were estimated by interpolating current meter measurements. The velocity measures were taken along a quasi-regular grid composed by 7 verticals. The results of these measurements were organized in tables of coordinates XYZ, in which the X axis represents the distance from the left bank, the Y axis represents the height above the sea level, while the Z represents the observed point flow velocity. Coordinates of the point measurements and the corresponding measured velocities are presented in Appendix 2.b.

The discharges at the middle cross section of the experimental channel were determined by means of two different interpolation methods: the polygonation and the triangular interpolation. The input data for both the estimations was represented by the dense grid of point flow velocity measurements that were conducted for each discharge and each vegetation scenario. This estimation was fundamental to trace the rating curves for the three vegetation scenarios, in order to quantify the increase of the water level due to increasing vegetation resistance. Estimated discharges were also used to determine the equivalent roughness coefficients through the Manning formula.

3.2.1 Polygonation Discharge Estimations

The surveyed cross section was represented in CAD environment (DraftSight). For each discharge and each vegetated scenario, the grid of velocity measurements was represented on the cross section. Basing on the measures at the staff gage, the water level during each velocity survey was assessed by the measurements at the staff gage.

The polygons were traced by combining the lines crossing the middle points between each velocity measurement. Given the irregular shape of the channel, the polygons were not always exactly rectangular but irregular instead. Moreover, the presence of a dense reed canopy at the borders hindered the velocity measurements close to the banks. It has to be noticed that the two external verticals, Vertical 1 and Vertical 7, were positioned as close as possible to the banks canopy.

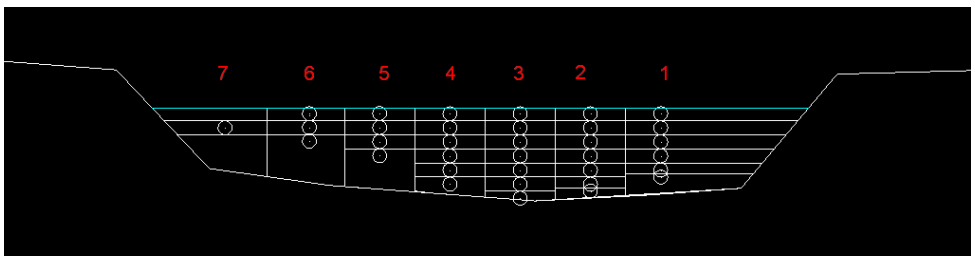

Figure 3.7. Example of polygonation based on the distribution of flow velocity measure points. The numbers refer to the Vertical IDs.

The area of each polygon was measured and reported in Excel. Multiplying each reference area with the corresponding velocity allowed to determine the discharge for each polygon. The sum of all the discharges gave the total discharge in the cross section. Results are shown in table 4.8.

Scenario	Code	Polygonation (m^3/s)
Full vegetation	1.1	0.31
Full vegetation	1.2	0.53
Full vegetation	1.3	0.75
Full vegetation	1.4	0.9
Half vegetation	2.1	0.31
Half vegetation	2.2	0.67
Half vegetation	2.3	0.93
Half vegetation	2.4	1.13
No vegetation	3.1	0.43
No vegetation	3.2	0.72
No vegetation	3.3	1.02
No vegetation	3.4	1.22

Table 3.8. Estimated discharges from polygonation method.

It has to be noticed that the four discharges were not exactly repeated for the three scenarios. Despite the four pumps were actioned in the same conditions for each trial, the discharge measured at the experimental section resulted increasing from the 1.n to the 3.n. Our hypothesis is that these differences were caused by water losses in the first part of the Bresciani channel, located between the pumping station and the study reach. This part was excluded from the experimental measures right because of the presence of several lateral ditches connected to it. In fact, the fields facing this segment of the channel are drained by numerous ditches, perpendicular to the Bresciani channel and tributaries of it. It is possible that part of the pumped water, especially the first day, was lost to fill up this additional ditch network and to saturate their bottom. We hypothesize that from the first day to the third day there was an accumulation of water in these ditches, which were every day less able to receive more water. These considerations could explain the increase of the discharges from the first day to the third day. However, since the roughness estimation was conducted in the downstream part, not connected to any lateral ditch, we can assume that there were no water losses along the experimental reach, so not influencing our measurements.

3.2.2 Discharge estimation by flow velocities triangular linear interpolation

A further processing of the velocity measurements was carried out by software Surfer, specifically developed for spatial interpolation of punctual data. The dataset was organized as a list of coordinates

where X= horizontal distance from the left riverbank, Y=water level, and Z=point flow velocity. To delimit the cross section perimeter and the water surface, the original grid of survey points was integrated with an additional list of nodes, according to the following criteria. The wetted perimeter was described by a list of nodes located along the riverbanks and at the foot of each survey vertical. At these nodes, the velocity was set equal to zero. The water surface was traced by means of a horizontal row of nodes. Two nodes were located at the riverbanks, with velocity equal to zero. Seven nodes were positioned at the top of each vertical, with a velocity equal to the value of the highest survey point at that vertical (located 1-5 cm below the water surface). In appendix 2.b the input grids for the twelve scenarios are presented.

By means of the Triangular linear interpolation method, the interpolation of the surveyed points was obtained as a convex surface, with a flat base on the plan XY and an elevation Z. The discharge (m3/s) was estimated as the volume delimited between the interpolated surface and the plan Z=0. Results are presented in table 3.9.

Scenario	Code	Discharge [m^3/s]
Full vegetation	1.1	0.25
Full vegetation	1.2	0.42
Full vegetation	1.3	0.60
Full vegetation	1.4	0.69
Half vegetation	2.1	0.27
Half vegetation	2.2	0.57
Half vegetation	2.3	0.78
Half vegetation	2.4	0.95
No vegetation	3.1	0.34
No vegetation	3.2	0.56
No vegetation	3.3	0.81
No vegetation	3.4	0.97

Table 3.9. Estimated discharges from the TIN interpolation.

The TIN interpolation was not necessarily the best solution method for this study case. Therefore, the same dataset was interpolated using other methods, as the kriging or the nearest neighbor. Results showed how the differences in term of discharge were substantially negligible (less than 5%), and therefore are not presented in this thesis. Conversely, a remarkable difference was found between the triangulation and the polygonation method. As a matter of fact, the discharges estimated by polygonation were substantially higher than the one obtained with the TIN. A comparison is presented in table 3.10.

Scenario	Code	Polygonation (m^3/s)	TIN (m^3/s)	Deviation (%)
Full vegetation	1.1	0.31	0.25	20
Full vegetation	1.2	0.53	0.42	20
Full vegetation	1.3	0.75	0.60	20
Full vegetation	1.4	0.9	0.69	23
Half vegetation	2.1	0.31	0.27	13
Half vegetation	2.2	0.67	0.57	15
Half vegetation	2.3	0.93	0.78	16
Half vegetation	2.4	1.13	0.95	16
No vegetation	3.1	0.43	0.34	21
No vegetation	3.2	0.72	0.56	22
No vegetation	3.3	1.02	0.81	20
No vegetation	3.4	1.22	0.97	21

Table 3.10. Comparison between the discharges obtained with polygonation and TIN methods.

Results presented in table 3.10 show how the TIN estimation is constantly lower than the polygonation method of about 20%. This deviation was found to be connected to the linear interpolation used by the software in determining the velocity distribution in proximity of the wetted perimeter. As a matter of fact, since the wetted perimeter was supposed to have Z=0, the linear interpolation drawn almost a straight line to link the channel perimeter to the flow velocity measures located within the flow area. On the other

hand, the polygonation did not take into account the effect of the boundaries, as the flow velocity along the wetted perimeter was supposed to be equal to the observed velocity at the center of each polygon.

A further analysis we carried out to better understand the difference between the two approaches was conducted modifying the polygon distribution as follows. At the foot of each vertical, a node with velocity set equal to zero was positioned. In tracing the polygons, this additional nodes implied the tracing of a buffer of the wetted perimeter with zero velocity. Even if the method appears to be coarser, the computation of the discharges perfectly coincided with the results obtained by linear interpolation.

As stated by the traditional hydraulic studies, the velocity profile at the bottom is well described by a logarithmic law, that is somehow in the middle between the polygonation method and the linear triangulation. Moreover, according to the latest studies concerning flow through vegetated canopies (i.e Nepf, 2012 or Baptist et al, 2007), the vertical flow velocity distribution is quasi homogeneous along the water depth, as it is influenced more by the presence of stems and leafs than from the bottom. Therefore, we assumed that the discharges estimated with the classic polygonation method were more reliable than those obtained with the other methods.

3.2.3 Tracing the velocity contour lines

Another interesting elaboration carried out with the software Surfer was to map the cross-section flow velocity field by spatial contours. Using the Triangulation with linear interpolation, assuming zero velocity at the boundary of the cross section, the flow velocity distribution was represented by contour lines (Figures 4.8-4.10). As it emerges from all the presented diagrams, there is a lack of data at the two verticals closer to the left bank. In fact, for these verticals, the flow velocity was measured just at two points close to the water surface. For reasons that were unknown because of the turbidity of the water, the current meter was not able to register velocity along the verticals at deeper points, despite the meter was not in contact with the channel bottom. Therefore, the zero velocity that was set at the boundary of the cross section at the foot of those verticals heavily influenced the velocity interpolation in that area, as it is evident in all the plots, vegetated or not vegetated. This, together with the uncertainty regarding the velocity profiles close to the channel bottom, was the reason why the two methods (polygonation and interpolation) gave different results in terms of discharge. However, the triangular linear interpolation was anyway useful to describe the flow velocity distribution across the channel section.

3.2.3.1 Velocity distribution in full-vegetated conditions

Analyzing the images of the full vegetated scenario (Figure 4.8), the flow results strongly concentrated in a small portion, that was found to be the less vegetated part of the cross section. The flow velocity

reached the highest peak at the fourth discharge (Code 1.4), estimated equal to 0.9 m^3/s, though it was the smaller discharge of the all fourth discharges pumped for the other two scenarios (2.4 and 3.4).

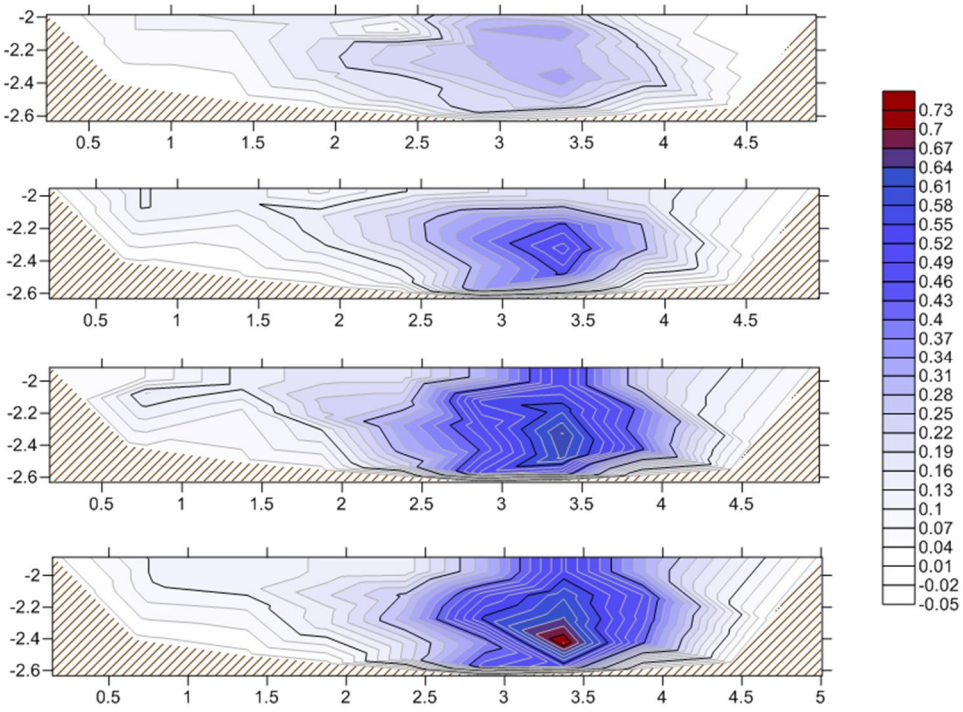

Figure 3.8. Interpolated flow velocity distribution for the full vegetated scenario. The four discharges are increasing from up to down.

3.2.3.2 Velocity distribution in half-vegetated conditions

The half vegetated scenario was obtained by removing all vegetation on the left riverbank and at the channel bottom. The vegetation was untouched on the right bank, from the channel bottom to the bankfull level. Analyzing the velocity distribution, it is evident how the main flow moved from the left side to the right side of the cross section. The influence of the vegetation is higher at the water surface, as the contours presents an area of zero velocity, which is not present going deeper towards the bottom, where velocity slightly increases. This can be explained by the fact that the flow resistance was higher at the surface because of the leaves. In fact, as already mentioned before, the Phragmites presented a leafless stem in the lower part, while the upper part was more leafed. Moreover, the area affected by the plants reduces with increasing discharges (from up to down in the figure). This can be explained by a partial reconfiguration of the leaves, which were observed to bend for increasing velocities.

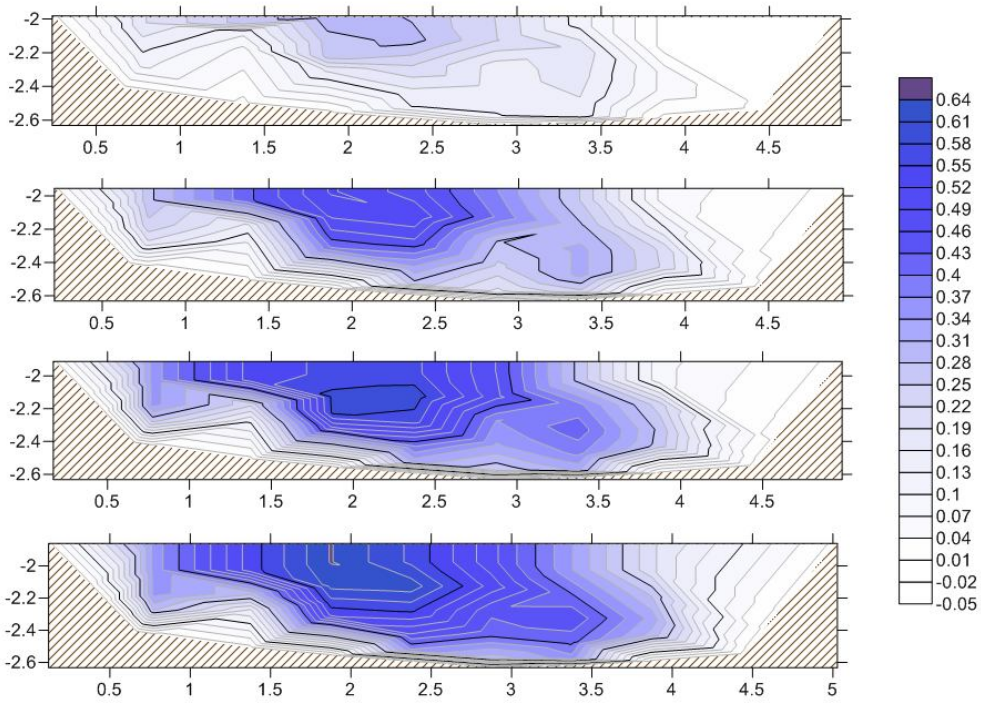

Figure 3.9. Interpolated flow velocity distribution for the half vegetated scenario. The four discharges are increasing from up to down.

3.2.3.3 Velocity distribution in non vegetated conditions

As expected, the non vegetated scenario presented a more homogeneous velocity distribution. The contours are regularly expanding from the center to the two banks. The only incongruence was found at the left bank, where the lack of data on the two left verticals (Vertical 6 and 7) caused an higher influence of the zero values set at the bottom.

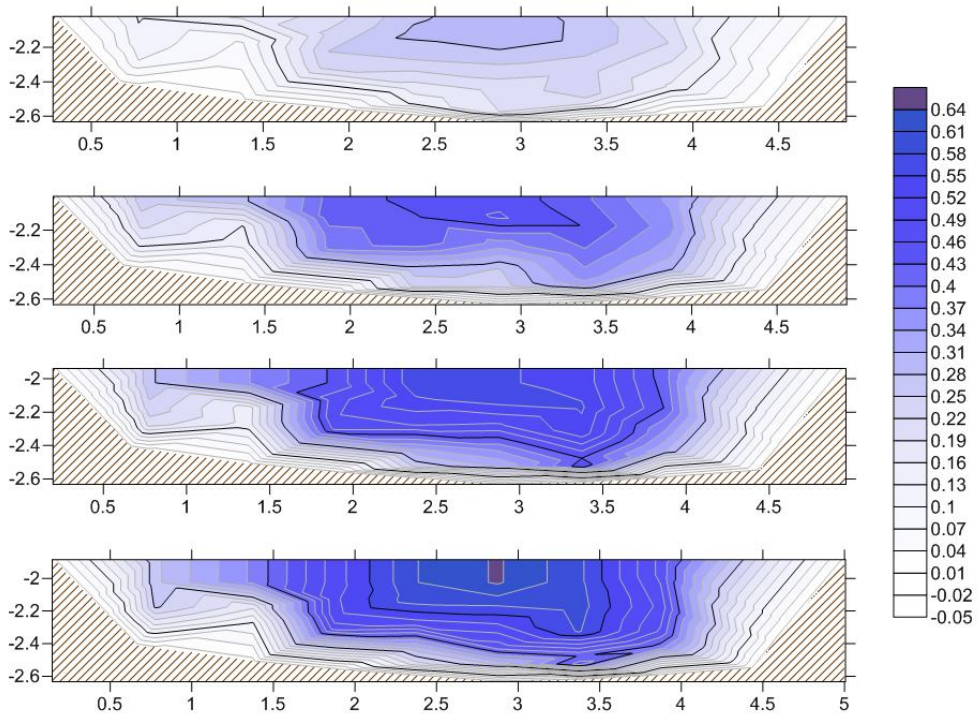

Figure 3.10. Interpolated flow velocity distribution for the non vegetated scenario. The four discharges are increasing from up to down.

3.2.4 Flow conditions

The water surface levels were monitored for each scenario and each discharge at the staff gages that were preliminarily positioned within the channel. These measurements were fundamental to detect the conditions of steady flow for each discharge, and to describe the flow conditions. In fact, for each discharge the velocity measurements were started when the water levels were found stable for 15 minutes. Observed water surface profiles are presented in Figures 3.11a,b and c.

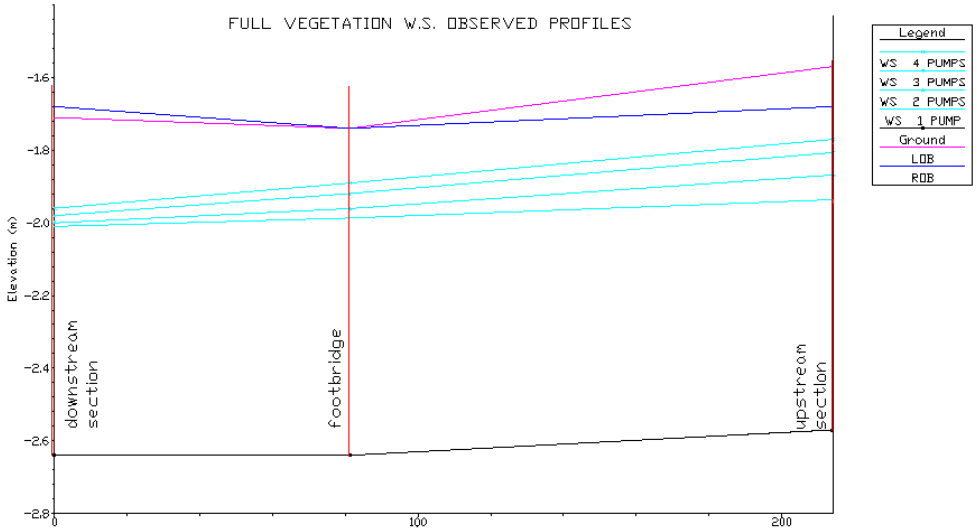

Figure 3.11 a. Observed water profile for the full vegetated scenario.

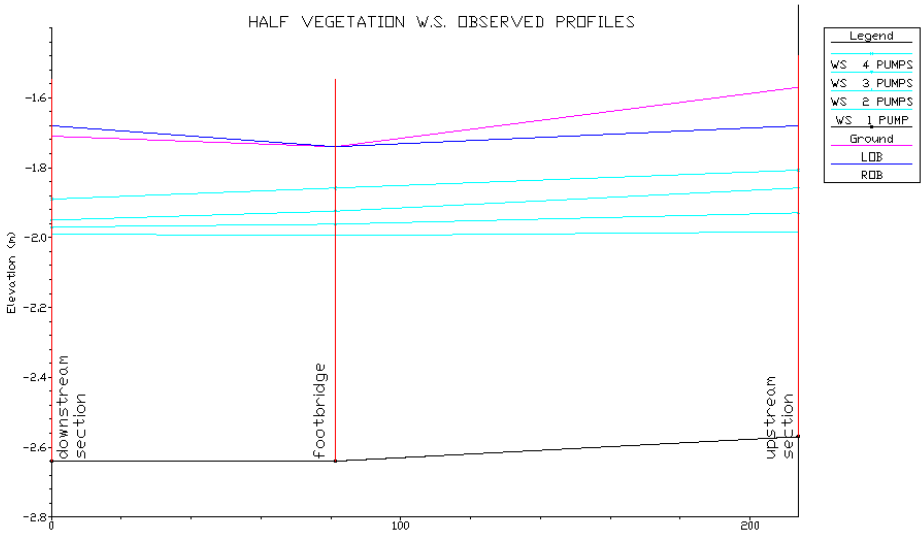

Figure 3.11 b. Observed water profile for the half vegetated scenario.

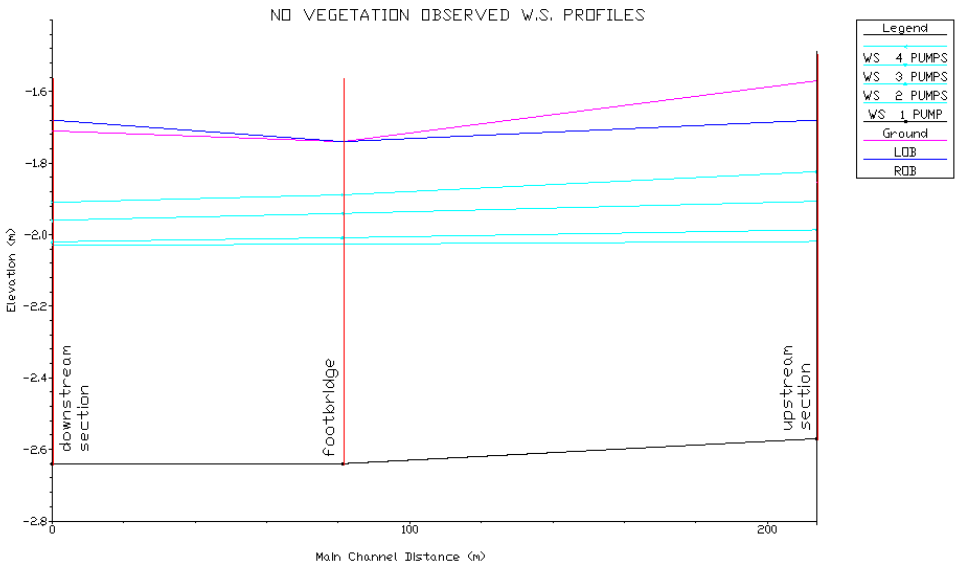

Figures 3.11 c. Observed water profiles for the non vegetated scenario.

As it emerges from the figures above, the uniform flow conditions were not found for any discharge of the examined vegetation scenarios. In fact, the water surface gradient resulted to be stable in time, but not equal tp the bottom slope. Moreover, water surface gradients vary for the different discharges with the same vegetation scenario. Analyzing the drainage network structure we realized that the water surface gradient was strongly influenced by the downstream boundary conditions, as the slopes are considerably low and the flow conditions are always subcritical. As a matter of fact, the water level of the downstream channel (Brentino) was influencing the water levels of the entire experimental segment.

The part of Bresciani that was used for this survey was chosen because of its straightness and because it was one of the few portions of the network that did not present tributaries for an acceptable length. On the contrary, the downstream main channel of which Bresciani is a tributary resulted to be too close to the experimental cross sections. Therefore, despite a good uniformity of cross section and vegetation distribution, the expected conditions of uniform flow were not reached. However, the variations were smooth along the channel, as the vegetation distribution was homogeneous, the bed slope was constant and the channel morphology was regular. Thus, we can assess with a good grade of approximation that the experiment was carried out in gradually varied steady flow conditions.

3.2.4.1 Tracing the stage- discharge rating curves

Once the discharges were determined, it was possible to trace the stage-discharge relation. The water depth that is graphed corresponds to the average between the upstream and the middle section, as the flow was in steady-gradually varied flow conditions. Results are presented in Figure 3.12.

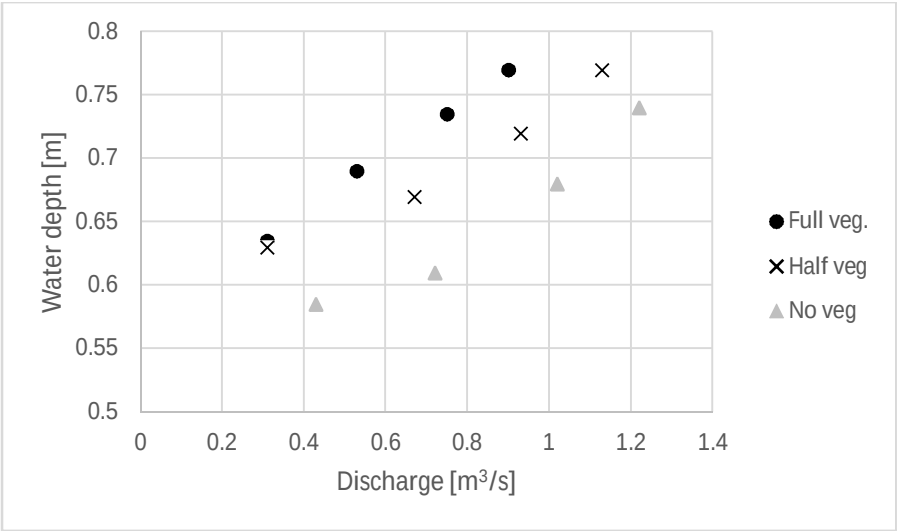

Figure 3.12. Measured stage-discharge relations for the three vegetated scenario for the upstream portion of the experimental channel.

The black dots represent the results for the full vegetated scenario. As it is easily appreciable, the full vegetation curve is located higher than the other two, pointing out that the full vegetated scenario is influenced by the presence of vegetation. Thus, in case of flood, hence in condition of high discharge rates, the vegetation plays a key role in rising the probability (or hazard) of overflow. However, encouraging results were obtained with the so-called half vegetated scenario, represented by black crosses. This vegetation management technique was proposed by the research team as a possible solution to reduce the impact on the channel ecosystem, maintaining an acceptable level of discharge capacity, comparable to the cleared situation. As expected, the half vegetated scenario resulted to be in between the two extreme solutions. Apparently, to keep an untouched reed canopy on one of the banks (from the emergent top to the submerged foot) could be a practicable solution in terms of flood hazard. The third curve, represented by grey triangles, constitutes the reference situation of maximum discharge capacity, or rather the design condition, for the experimental channel.

3.3 Roughness coefficients estimation

3.3.1 Extracting total roughness coefficients for the three scenarios

The discharge was estimated by the interpolating the point velocity measurements of the surveyed flow cross-section. Although the flow was not in uniform conditions, the determination of average flow velocities and discharges for each pumping layout can be considered reliable. The problem that emerged during computations was referred to the estimation of roughness coefficients by means of the Manning formula. If the flow was in uniform conditions, the Manning n could be obtained as:

$$n = \frac{R^{\frac{2}{3}} i^{\frac{1}{2}}}{V} \qquad (3.1)$$

Where R and V are respectively the hydraulic radius and the average velocity at a cross section (assuming that at all the section the conditions are constant), and i is the gradient slope, intended as the slope of the channel bottom, equal to the slope of the water surface.

Since we found that the flow conditions were not uniform, but steady gradually varied instead, this law was not effective anymore. In fact, in such conditions the head loss was not related just to channel energy losses J, but also to the loss of elevation I, given by the channel slope. To use the Manning formula in steady gradually varied flow conditions, in literature it is considered acceptable to use not the parameters of one section, but the average of two sections, located upstream and downstream the study reach.

Therefore, we decided to estimate the roughness coefficients taking into account not just the data observed at the middle station (named “footbridge”), but also those data at the upstream one (named “upstream section”). In other words, we applied the principle of conservation of energy for the upstream half of the experimental segment. The choice was motivated by the fact that the upstream part of the experimental channel presented a channel slope more similar to the the whole Bresciani ditch, so more representative of the entire channel. Moreover, the downstream part was more influenced by the downstream boundary conditions, as the last cross section was positioned in proximity of the confluence with the main collector, the Brentino channel. The determination of the average Manning coefficients for the upstream part was conducted as follows.

First, the profiles of the two cross section were traced during the topographic surveys. Then, the water levels were registered for each discharge at two staff gages. It was reasonable to assume that the discharge was not varying between the two sections, as the experimental segment did not present lateral ditches. Then, the discharge was estimated at the footbridge section from the velocity measurements (see

chapter on discharges estimations). Last, the average flow velocities at the two cross sections were determined as:

$$V = \frac{Q}{\Omega} \qquad (3.2)$$

Where V is the average flow velocity, Q is the estimated discharge, Ω is the flow area, determined in CAD environment based on the surveyed cross section profiles and the observed water levels. By applying the energy equation for gradually varied steady flow between the upstream (2) and footbridge (1) sections, we obtain:

$$z_2 + h_2 + \frac{V_2^2}{2g} - z_1 - h_1 - \frac{V_1^2}{2g} = L \frac{V_m^2}{C_m^2 R_m} \qquad (3.3)$$

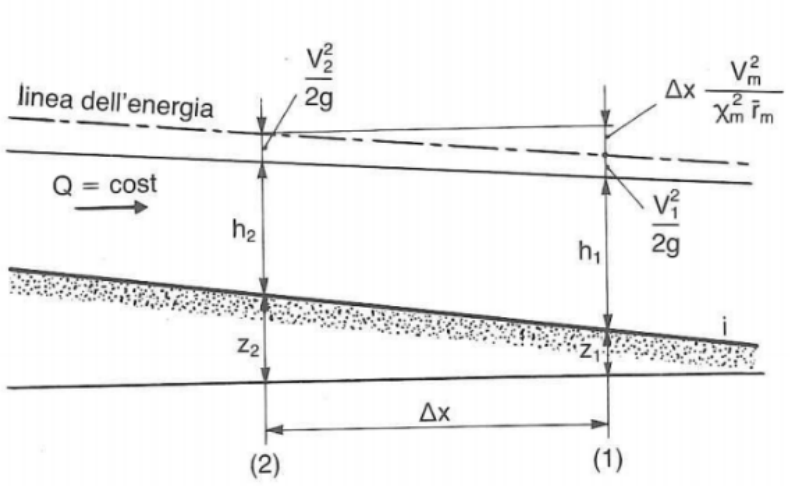

Figure 3.13. Energy components in steady flow conditions (adapted from Benini, 1990).

Where V_m is the average flow velocity between the two sections, R_m is the average hydraulic radius, L is the channel length, and C is the Chezy coefficient, which according to the Manning formula can be expressed as:

$$C = \frac{1}{n} R^{\frac{1}{6}} \qquad (3.4)$$

Replacing Eq. 3.4 in Eq. 3.3, we obtain:

$$z_2 + h_2 + \frac{V_2^2}{2g} - z_1 - h_1 - \frac{V_1^2}{2g} = L \frac{V_m^2}{\left(\frac{1}{n} R_m^{\frac{1}{6}}\right)^2 R_m} \qquad (3.5)$$

Where the Manning's n is the only value that is unknown, since all the other parameters were measured on field. Finally it was possible to determine the equivalent Manning coefficient for the experimental segment, according to the following relation:

$$n = \sqrt{\frac{z_2 + h_2 + \frac{V_2^2}{2g} - z_1 - h_1 - \frac{V_1^2}{2g}}{L}} \cdot \frac{R_m^{\frac{2}{3}}}{V_m} = \frac{J^{\frac{1}{2}} \cdot R_m^{\frac{2}{3}}}{V_m} \quad (3.6)$$

Where J is the slope of the total energy line. Results are presented in Table 3.11.

Scenario	Discharge [m^3/s]	Equivalent Manning's n
Full Vegetation	0.31	0.074
Full Vegetation	0.53	0.069
Full Vegetation	0.75	0.067
Full Vegetation	0.9	0.063
Half Vegetation	0.31	0.030
Half Vegetation	0.67	0.032
Half Vegetation	0.93	0.036
Half Vegetation	1.13	0.034
No Vegetation	0.43	0.019
No Vegetation	0.72	0.013
No Vegetation	1.02	0.022
No Vegetation	1.22	0.021

Table 3.11 Estimated total roughness coefficients and discharges for the three scenarios.

As expected, the estimated roughness coefficients in the three vegetation scenarios are very different. The full vegetated scenario presented the highest Manning's n, confirming that the vegetation influenced the flow along the experimental segment. The flow resistance showed a decreasing trend for increasing discharges, probably due to a partial reconfiguration of the vegetation elements caused by the flow drag. The half vegetated scenario presented lower resistances, as most part of the channel cross section was cleared by a partial cut. Moreover, the roughness varied without a precise trend, presenting small variation between different discharges. The totally cleared scenario presented the lowest Manning coefficients for all the discharges. The values are comparable with those proposed by literature for regular channels with natural bed. In the chapter "Discussion", a more detailed analysis of these results is provided.

As already observed in other works, (i.e. Gwinn & Ree, 1980; Rhee et al, 2008), a good parameter that was found to be used to express the variations of vegetation roughness is the parameter V*R, where V is the average flow velocity and R is the hydraulic radius. The obtained total Manning's n are plotted over this parameter in 3.14. The presence of vegetation raised the roughness coefficients, and presented a decreasing resistance for increasing VR. This behavior was probably related to the reconfiguration of the

flexible parts of the plant, as already observed by other authors for the Phragmites and other flexible species. In the Discussion section this argument is examined more in depth.

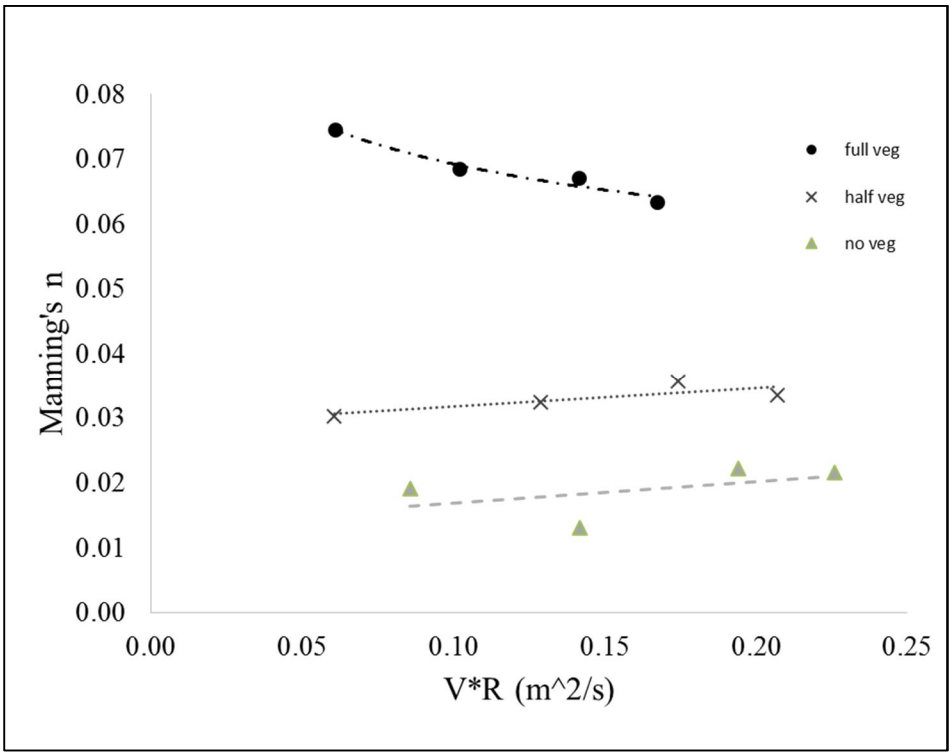

Figure 3.14. Manning's n –VR retardance curves for the three vegetated scenarios.

3.3.2 Extracting the roughness from vegetated subareas

Basing on the vegetation surveys in full-vegetated conditions, that were conducted splitting the cross section in six sub areas of width equal to 1 m each, we built up a simplified model to schematize the composite section. More in detail, we simplified the vegetation distribution as follows: the main channel was represented by a central sub-area of width 2 m, while the rest of the cross section was supposed to be covered by a homogeneous distribution of reeds.

To apply the various methods, the hydraulic parameter of each sub-area (i.e. P_N, R_N, A_N) had to be measured for each one of the four discharges that were pumped for the full-vegetated scenario. The bed roughness was assumed to be equal to the average of the four values observed for the cleared scenario, thus equal to 0.02. results are presented in Table 3.12.

	Horton	**Pavlovskii**	**Colebatch**	**Yen**	**AVG**
1.1	0.100	0.0879	0.1139	0.102	0.101
1.2	0.090	0.0805	0.1032	0.092	0.091
1.3	0.088	0.0786	0.1003	0.089	0.089
1.4	0.082	0.0740	0.0936	0.082	0.083

Table 3.12. Manning's n of the vegetated part of the section obtained by means of four different averaging methods, for each discharge in full-vegetated conditions.

This scheme must be considered a simplification, as the vegetation surveys showed how there was a sort of variability in terms of stem diameter and density between the different vegetated sections. However, this approach allowed to estimate the role of vegetation more precisely than the bulked roughness coefficients that were estimated directly from field observations. Moreover, the obtained values could be used in other situation where, for example, the channel width is different but the vegetation characteristics are comparable to the ones of this case study.

The Manning's n values presented in Table 3.12 represent the total resistance of the vegetated part of the channel. However, as proposed by Cowan (1956), the total resistance can be split in sub-components, as it is affected by different factors. Given an absent meandering effect (m=1), and a negligible effect of the small cross section shape variations (n_2=0), the total resistance of the vegetated channel is represented by the sum of:

$$n = n_1 + n_3 + n_4 \tag{3.11}$$

Where:

n_1 is the bed resistance

n_2 is the obstruction resistance

n_3 is the vegetation resistance

To determine the resistance due to vegetation, we subtracted the bed roughness n_1 from the total roughness of the vegetated patch. The resulting coefficients are taking into account the effect of vegetation due to flow resistance and channel obstruction. The average Manning's n values become therefore:

Discharge	**n vegetation**
1.1	0.0797
1.2	0.0704
1.3	0.0678
1.4	0.0619

Table 3.13. Manning's n for the vegetated patches, once subtracted the bed roughness.

The values are comparable with the ones that are suggested by Cowan for densely vegetated channels with low obstruction. As suggested by Rhee et al. (2008), the reed must be considered both for its effect of obstruction (due to the frontal area occupied by stems) and for flow resistance due to friction.

3.4 Comparing results to hydrologic studies

3.4.1 Hydrology of the Bresciani catchment

The reclamation drainage system design was updated in 2006 after a study conducted by Casarosa et al.. The designers started from the determination of the critical rainfall for different return times. Then they estimated the water losses of the basins by means of the Curve Number method, and last, the discharges for the return times of 25 and 100 years for each channel of the network. The rainfall distribution analysis was conducted on the series of the maximum rainfalls for different durations at the Viareggio rain gauge, located 1 km far from the reclamation area. The DDF were traced and validated using the Gumbel distribution method, for the return times of 10-25-50-100-200 years. Formulas are reported below.

10 years: $h = 56.7 \cdot t^{0.266}$ (3.12)

25 years: $h = 67.7 \cdot t^{0.27}$ (3.13)

50 years: $h = 75.9 \cdot t^{0.27}$ (3.14)

100 years: $h = 84 \cdot t^{0.27}$ (3.15)

200 years: $h = 92 \cdot t^{0.274}$ (3.16)

The DDFs can be summarized by the following equation, taking into account the variation of the *a* coefficient related to the return time, and assuming *n* as a constant equal to the average of the five presented values:

$$h = 39.79 \cdot Tr^{0.161} \cdot t^{0.27} \quad (3.17)$$

Where Tr is the return time expressed in years, and t is the event duration time. The formula NUMERO allows the estimation of the total rainfall height for a determined return time and a determined rainfall duration, for the Viareggio area.

The direct runoff was estimated according to the Curve Number method, through the determination of all the parameters influencing permeability (land use, soil characteristics, lithology). The curve number for the Bresciani catchment was estimated equal to 71. The runoff coefficient, for a return time of 25 years, was estimated equal to 0.4.

The discharges of assigned return time were then determined, assuming as critical rainfall the event of duration equal to the catchment concentration time. In table 3.14 the discharges calculated for the Bresciani channel, closed at the end of the experimental segment, are presented.

Tr [years]	Q [m^3/s]
25	0.91
100	1.70
200	2.16

Table 3.14. Discharges of assigned Return time at the downstream section of the experimental reach.

Based on the data obtained by means of the reservoir method, the return time-discharge relation is the following:

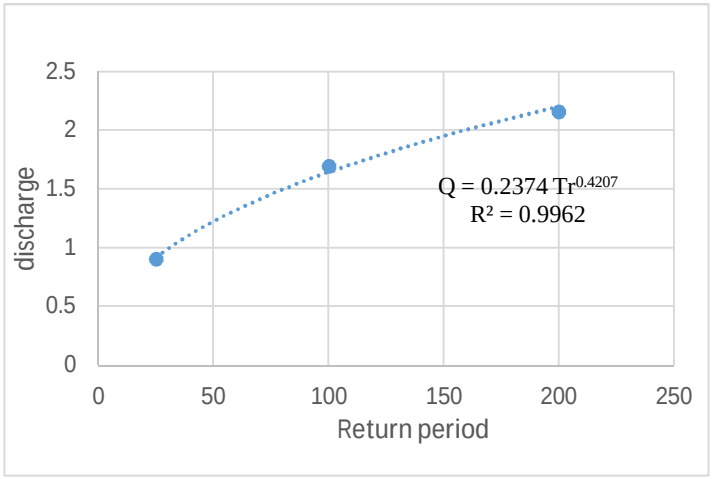

Figure 3.15. Peak flow discharges graphed over the return time.

Last, the design of the cross section was carried out assuming a bank slope equal to 1, and a maximum velocity of 0.6 m/s. The design roughness was expressed by the parameter γ, which is included in the Bazin formula for the determination of the Chezy resistance coefficient:

$$\chi = \frac{87}{1+\frac{\gamma}{\sqrt{R}}} \qquad (3.18)$$

Taking into account a ditch in bad conditions of maintenance, assuming as the worst situation "the period that is farther from the last management operation", the designers adopted the value of $\gamma = 1.75$ which is comparable to a Manning's n equal to 0.029. The maximum sustainable flow velocity was estimated equal to 0.6 m/s, according to the characteristics of the substrate. A comment of this design choice will be provided in the Discussion section.

3.4.2 Hydraulic design and experimental discharges

The pumped discharge were obtained increasing the number of working pumps from one to four. The discharge estimation was carried out by means of the flow velocity measurements and the subsequent interpolation of the point velocity data. Given the relation between the return period and the peak flow discharge, we estimated the return period of each pumped discharge, in order to make considerations about the effects of vegetation on the potential flood frequency. Results are presented in table NUMERO.

Discharge	Scenario	Discharge (m^3/s)	Return time (Yrs)	water depth (m)
1.1	Full veg	0.31	2	0.65
1.2	Full veg	0.53	7	0.69
1.3	Full veg	0.75	15	0.72
1.4	Full veg	0.9	24	0.75
2.1	Half veg	0.31	2	0.66
2.2	Half veg	0.67	12	0.69
2.3	Half veg	0.93	26	0.73
2.4	Half veg	1.13	41	0.78
3.1	No veg	0.43	4	0.62
3.2	No veg	0.72	14	0.64
3.3	No veg	1.02	32	0.7
3.4	No veg	1.22	49	0.76

Table 3.15. Return times of the experimental discharges.

In Table 3.15 the experimental discharges obtained by means of the polygonation, their return period and the related water depth are presented. While the discharge-return time relation is independent from the channel conditions, the water level is obviously influenced. Therefore, it is interesting to remark the differences between the different scenarios, to express the effect of vegetation in terms of return time.

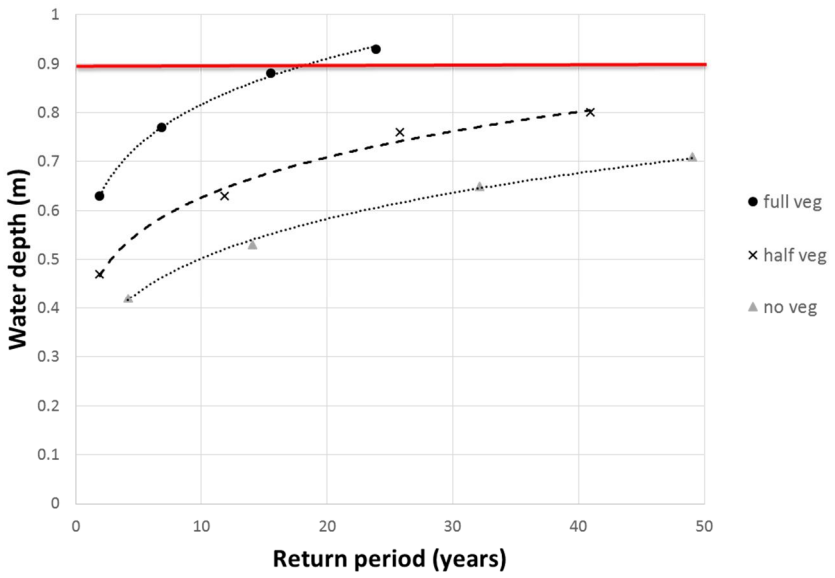

Figure 3.16. water level over return time for the three experimental scenarios.

In Figure 3.16 the return time-water depth relation is presented. An important remark is that, in bankfull conditions, for the representative Bresciani cross section the maximum water depth is equal to 0.93 m. For the full-vegetated scenario, this depth is reached with a return time of 25 years, while for the same discharge, in condition of half vegetation there is a tolerance of more than 20 cm, while in the totally cleared condition more than 25 cm.

From another point of view, fixing a maximum water level of 0.73 m (assuming a tolerance of 0.2 m), the return period varies from less than five years in full vegetated condition from 50 years in non vegetated conditions. The half vegetated conditions are in the middle, with a return time of approximately 25 years.

3.5 Modeling the vegetation resistance

As presented in the State of the Art, in the last years the academy proposed several different models to predict vegetation resistance . Nonetheless, these models were divided in “families”, of which the main distinction was the submergence level of plants. More precisely, all the models make a precise distinction between resistance of totally submerged plants and emergent-just submerged plants. For totally submerged meadows or patches, the flow resistance is comparable to the effect of a boundary layer roughness, as the effect of plants modifies the vertical profile of the water flow. On the other hand, the just-submerged-emergent conditions imply that the whole vertical profile of the flow is somehow influenced by the presence of vegetal elements, subjected to drag forces.

Most of theories about submerged meadows take into account the progressive bending of plants, which reduce their height and therefore their flow resistance for increasing V*R rates. On the other hand, plants in emergent conditions present a flow resistance that is increasing with flow depth, as the flow disturbance are increasing because of turbulences. An intermediate behavior was observed and modelled by Jarvela (2002a, 2002b) for flexible shrubs and branches. The author proposed a model based on various parameters of the vegetation, describing the density with the LAI – Leaf Area Index. Another fundamental factor that needed to be estimated for each specie was the χ, a coefficient that expresses for each specie the capacity to modify the frontal area due to the flow drag force. These values are not available in literature for the Phragmites australis. Moreover, we have not yet surveyed them on field. Therefore, the applicability of this third approach is not yet possible. In the next paragraphs the modelling of vegetation based on various approaches is presented.

At a first glance, the observed “n” trend for increasing Q seems to assume a “submerged vegetation” behavior for the full vegetated condition and “emergent vegetation” behavior for half vegetated condition (Pasquino V., personal communication). Bearing in mind that our vegetation arrangement was emergent for all the eight discharges (1.1-2.4) the observed decreasing trend can be due to the combined effect of stems and leaves. While the rigid stems increased the flow resistance with increasing discharges, the submerged leaves presented a flexible behavior. Since the total plant resistance was a combination of those two opposite effects, it is reasonable to assume that the leaves had an important role in terms of drag.

We decided to test three models developed for emergent vegetation, in order to assess which is better fitting with the field observations: Nepf (2012), James et al. (2004) and Yang & Choi (2010). The three models are presented in the State of the Art of this thesis. Different modelling approaches were adopted for the full vegetated scenario and the half vegetated scenario.

Hereafter, in order to evaluate which model presents the best performance considering our n measured we choose the average of EF statistical factor (ERROR FACTOR):

$$EF\% = \frac{n_{model} - n_{observed}}{n_{observed}} \quad (3.19)$$

3.5.1 Modeling the full vegetated scenario

The modeling of the full vegetated scenario was conducted with two different approaches. The first approach was the use of an average value of the vegetation parameters for the total cross section, assuming a homogeneous distribution of the plants along the wetted perimeter. More in detail, the average number of stems/m^2, the average stem diameter and the average hydraulic radius were used as input in the models. The second approach was the subdivision of the cross section in subareas, corresponding to the survey plots that were delimited to measure the vegetation parameters. Thus, the cross section was divided in six sub areas of width 1 m (from A to F). For each subarea, the vegetation parameters were averaged from the values of the four surveyed cross section. Then, the models were run for each subarea, considering the hydraulic radius of each. After, the sub-area Manning's n were averaged according to the composite section roughness calculation, by means of the four different methods already used for the determination of the experimental roughness of the vegetated patch.

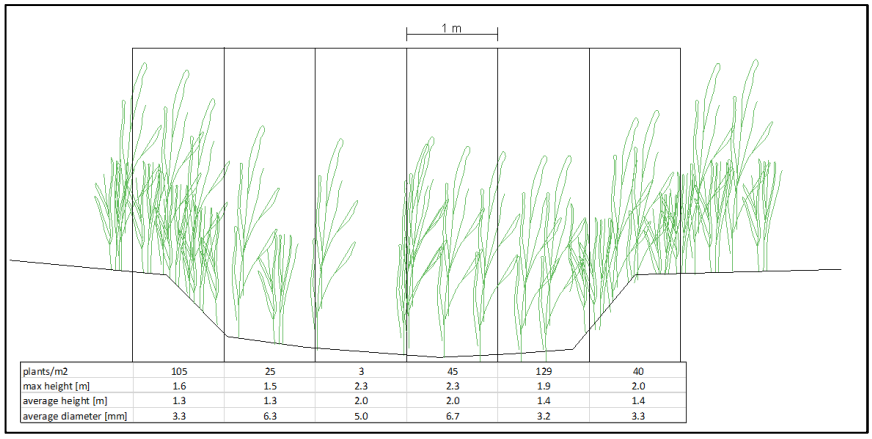

Figure 3.17. Surveyed distribution of the vegetation parameters across the section.

3.5.1.1 First approach: averaged vegetation parameters

A simplified method to assess vegetation resistance by means of resistance models could be represented by the survey of vegetation along one or more channel cross sections, to determine an average value of stem density (stems/m^2) and an average stem diameter for the whole reach. Basing on the vegetation surveys conducted just before the hydraulic measurements, we calculated these two parameters for the experimental channel and we run the three resistance models mentioned above. Note that modeling results are giving a resistance value that must be considered comprehensive of the bed resistance, as the models are neglecting the bed shear stress from the computation, considering it negligible. A comparison between the experimental total n values and the computation results of the three models is presented in Table 3.16.

n measured	n Nepf	%error	N James	%error	N Yang	%error
0.0740	0.0772	4%	0.0856	16%	0.0820	11%
0.0690	0.0816	18%	0.0905	31%	0.0867	26%
0.0670	0.0850	27%	0.0944	41%	0.0904	35%
0.0630	0.0876	39%	0.0972	54%	0.0931	48%
avg EF%		**22%**		**36%**		**30%**

Table 3.16. Error factors for the predicted manning's n assuming homegenously distributed vegetation.

As evident in Table 3.16, the use of the average parameters for the entire cross section resulted in a noticeable EF%. The best values was obtained by the use of the Nepf model, which anyway still presents a 22% of Error compared to the observed data. To increase the correspondence between reality and model scenario, the cross section was divided in sub areas with different vegetation distribution, as observed during the field surveys.

3.5.1.2 Second approach: composite Manning's n

The section was divided in six sub areas, in which the vegetation parameters were averaged among the four sections. The same resistance models were run for each sub-areas, obtaining a different Manning's n for each sub-area and each discharge. The following Tables show the predicted sub-section Manning's n for the four discharges in full vegetated scenario.

Nepf Manning's n	A	B	C	D	E	F
1.1	0.040	0.085	0.043	0.052	0.073	0.023
1.2	0.043	0.089	0.045	0.054	0.076	0.025
1.3	0.045	0.093	0.046	0.056	0.079	0.026
1.4	0.047	0.096	0.048	0.057	0.081	0.027

Yang Manning's n	A	B	C	D	E	F
1.1	0.057	0.085	0.043	0.052	0.073	0.033
1.2	0.061	0.089	0.045	0.054	0.076	0.035
1.3	0.063	0.093	0.046	0.056	0.079	0.037
1.4	0.066	0.096	0.048	0.057	0.081	0.039

James Manning's n	A	B	C	D	E	F
1.1	0.063	0.094	0.048	0.058	0.081	0.036
1.2	0.067	0.099	0.050	0.060	0.085	0.039
1.3	0.070	0.103	0.052	0.062	0.088	0.041
1.4	0.074	0.107	0.053	0.063	0.090	0.043

Tables 3.17a,b and c. Predicted Manning's n for each sub-area of the cross section in full vegetate dconditions.

Then, the determination of the equivalent roughness coefficient for the whole section four different models were used to average the values: Pavlovskii, Lotter, Horton, Yen and Colebatch. Results are shown in Tables 3.18-3.20.

Table 3.18. Nepf composite roughness estimation for the full vegetated scenario.

Discharge	n Lotter	EF%	n Pavlovskii	EF%	n Horton	EF%	n Yen	EF%	n Colebatch	EF%
1.1	0.052	-28.7%	0.061	-17.2%	0.059	-19.4%	0.058	-21%	0.0615	-16.2%
1.2	0.053	-20.2%	0.063	-5.1%	0.062	-7.7%	0.060	-10%	0.0644	-3.5%
1.3	0.057	-15.1%	0.065	-2.3%	0.063	-5.0%	0.062	-7%	0.0665	-0.4%
1.4	0.058	-6.9%	0.067	7.0%	0.065	4.0%	0.064	2%	0.0686	9.3%
	Average EF	-17.7%		-4.4%		-7.0%		-9%		-2.7%

Table 3.19. Yang composite roughness estimation for the full vegetated scenario.

Discharge	n Lotter	EF%	n Pavlovskii	EF%	n Horton	EF%	n Yen	EF%	nColebatch	EF%
1.1	0.056	-23.2%	0.066	-9.5%	0.065	-11.2%	0.065	-11%	0.0660	-10.1%
1.2	0.057	-13.9%	0.070	4.2%	0.068	2.2%	0.068	2%	0.0692	3.7%
1.3	0.061	-8.2%	0.072	7.5%	0.070	5.5%	0.071	6%	0.0716	7.2%
1.4	0.063	0.8%	0.074	18.1%	0.073	15.8%	0.073	16%	0.0739	17.8%
	Average EF	**-11.1%**		**5.1%**		**3.1%**		**3%**		**4.6%**

Table 3.20. James composite roughness estimation for the full vegetated scenario.

Discharge	n Lotter	EF%	n Pavlovskii	EF%	n Horton	EF%	n Yen	EF%	n Colebatch	EF%
1.1	0.059	-21.3%	0.069	-6.9%	0.068	-8.6%	0.068	-9%	0.0689	-7.5%
1.2	0.060	-12.7%	0.073	6.0%	0.071	3.9%	0.071	4%	0.0723	5.5%
1.3	0.064	-4.9%	0.075	11.8%	0.074	9.6%	0.074	10%	0.0747	11.4%
1.4	0.066	3.8%	0.077	22.2%	0.076	19.8%	0.076	20%	0.0772	21.9%
	Average EF	**-8.8%**		**8.3%**		**6.2%**		**6%**		**7.8%**

In Tables 3.18-3.20 the error factor is for each discharge of the full vegetated scenario is presented. Analyzing the data, it is evident how the average errors (obtained as the average of the error calculated for the four discharges) are reduced by the division of the cross section in sub-areas and the composition of the Manning's n. All the three models predicted values with an average error of below ±10%, which is an excellent result considering the uncertainties that could affect as the vegetation surveys, the ability of the model in predicting the resistance, as the averaging assumption of each composition approach. It has to be noticed that the Nepf and the James models showed an excellent ability in predicting the Manning's n for the highest discharges, while the Yang method was more accurate for the lower discharges. Since in most cases the hydraulic design concerns the peak discharges for flood risk assessment and reduction, we can assess that Nepf and James should be preferred for the estimation of roughness in high flow conditions. The best prediction was obtained by the use of the Nepf model, averaged by means of the Colebatch method, with an average error of 2.7%.

3.5.2 Modelling the half vegetated scenario

3.5.2.1 The blockage factor B_x

For the case of vegetation that does not cover the whole channel width, Luhar and Nepf (2012) and in particular Nepf (2012), proposed a formula based on the Blockage factor B_x, which can be obtained as the ratio between the patch frontal area on the total flow area. The model is based on the assumption that the flow velocity through the patch is some orders of magnitude lower than the undisturbed flow. In these conditions, the portion of the cross section that is occupied by the patch can be considered obstructed, or in other words, blocked.

For $B_x < 1$: $$n = \left(\frac{C_*}{2g}\right)^{\frac{1}{2}} (1 - B_x)^{-\frac{3}{2}} R^{\frac{1}{6}} \qquad (3.20)$$

In which C_+(0.05-0.13 from experimental tests) represents the drag coefficient related at the external surface of the vegetated patch.

In our study, the experimental half vegetated scenario represented a case that could be well described by this model, as the channel was cleared by vegetation on the bottom and on one of the banks, and almost blocked by a dense canopy on a small, lateral portion of the section. The Nepf model was run considering as blocked the sub-section E, as presented in Figure 3.18. The best results were obtained with the minimum value of the C_* variation range, C_*=0.05. Results are presented in Table 3.21.

Discharge	n measured	n Nepf HV	EF%
2.1	0.0297	0.0444	49.2%
2.2	0.0323	0.0448	39.0%
2.3	0.0363	0.0455	25.3%
2.4	0.0336	0.0459	36.7%
		avg %	**37.5%**

Table 3.21. Predicted Manning's coefficients for the half vegetated scenario by means of the Blockage factor formula (Luhar & Nepf, 2012).

As shown in Table 3.21, the blockage factor model resulted overestimating the roughness coefficients. In fact, the average Error Factor % was equal to 37.5%. It is probable that the assumption that the velocity through the patch was some orders of magnitude lower than the undisturbed flow was not correct for this study case. Moreover, the sensitivity to the drag coefficient C_* suggests that further studies are required to improve the use of this approach. However, the current meter used in this research was not able to measure the flow velocity within the dense patches of reed, thus we do not have experimental confirmation of this theory.

3.5.2.2 Composite section roughness

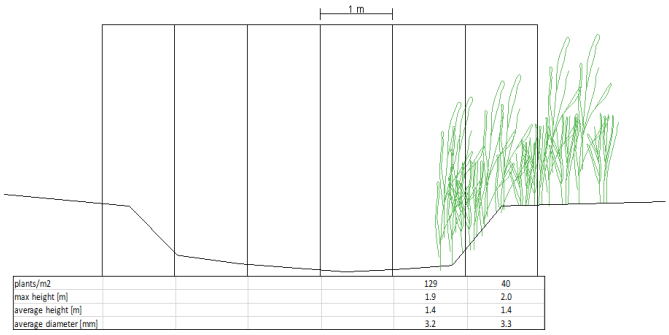

Figure 3.18. Vegetation distribution in the half-vegetated scenario.

As already presented for the full vegetated scenario, the composite section analysis was carried out to estimate the composite roughness coefficients. The Manning's n experimentally determined for the cleared scenario was assigned to the subsections A-B-C-D, while for E-F the Manning's n was predicted by means of the three models presented before.

Nepf – half veg	**1**	**2**	**3**	**4**	**5**	**6**
2.1	0.021	0.021	0.021	0.021	0.0730	0.0230
2.2	0.021	0.021	0.021	0.021	0.0764	0.0248
2.3	0.021	0.021	0.021	0.021	0.0789	0.0260
2.4	0.021	0.021	0.021	0.021	0.0814	0.0272

Yang - half veg	**1**	**2**	**3**	**4**	**5**	**6**
2.1	0.021	0.021	0.021	0.021	0.0776	0.0346
2.2	0.021	0.021	0.021	0.021	0.0812	0.0372
2.3	0.021	0.021	0.021	0.021	0.0839	0.0391
2.4	0.021	0.021	0.021	0.021	0.0866	0.0410

James - half veg	**1**	**2**	**3**	**4**	**5**	**6**
2.1	0.021	0.021	0.021	0.021	0.0810	0.0362
2.2	0.021	0.021	0.021	0.021	0.0848	0.0389
2.3	0.021	0.021	0.021	0.021	0.0876	0.0408
2.4	0.021	0.021	0.021	0.021	0.0904	0.0428

Tables 3.22a, b and c. Predicted Manning's n for the half vegetated scenario.

The average experimental n of the bed was assumed to be constant for the non-vegetated sub-areas.Then, the averaging aimed at determining the global Manning's n for the cross section was determined by the five models of roughness composition. Results are presented in tables 3.23-3.25.

Table 3.23. Nepf composite roughness estimation for the half vegetated scenario.

Discharge	n Lotter	EF%	n Pavlovskii	EF%	n Horton	EF%	n Yen	EF%	n Colebatch	EF%
1.1	0.024	20.8%	0.039	30.2%	0.035	19.1%	0.033	11%	0.0365	22.7%
1.2	0.023	28.7%	0.040	23.7%	0.036	12.6%	0.033	4%	0.0376	16.4%
1.3	0.024	34.3%	0.041	12.4%	0.037	2.0%	0.034	-6%	0.0384	5.7%
1.4	0.024	28.9%	0.042	24.1%	0.038	12.3%	0.035	3%	0.0391	16.6%
	Average EF	**28.2%**		**22.6%**		**11.5%**		**3%**		**15.4%**

Table 3.24. James composite roughness estimation for the halfl vegetated scenario.

Discharge	n Lotter	EF%	n Pavlovskii	EF%	n Horton	EF%	n Yen	EF%	n Colebatch	EF%
1.1	0.024	20.0%	0.043	44.0%	0.039	30.9%	0.036	21%	0.0394	32.6%
1.2	0.023	27.9%	0.044	37.3%	0.040	24.4%	0.037	14%	0.0407	26.1%
1.3	0.024	33.6%	0.045	25.2%	0.041	13.1%	0.038	4%	0.0416	14.7%
1.4	0.024	28.1%	0.047	38.7%	0.042	25.0%	0.039	15%	0.0426	26.8%
	Average EF	**27.4%**		**36.3%**		**23.4%**		**14%**		**25.1%**

Table 3.25. Yang composite roughness estimation for the half vegetated scenario.

Discharge	n Lotter	EF%	n Pavlovskii	EF%	n Horton	EF%	n Yen	EF%	n Colebatch	EF%
1.1	0.024	-20.2%	0.041	38.9%	0.038	26.9%	0.035	18%	0.0382	28.6%
1.2	0.023	-28.1%	0.043	32.5%	0.039	20.5%	0.036	12%	0.0395	22.3%
1.3	0.024	-33.8%	0.044	20.7%	0.040	9.6%	0.037	1%	0.0404	11.2%
1.4	0.024	-28.3%	0.045	33.7%	0.041	21.0%	0.038	12%	0.0412	22.8%
	Average EF	**-27.6%**		**31.4%**		**19.5%**		**11%**		**21.2%**

The average Manning's roughness coefficients of the composite section estimation resulted significantly more effective than the blockage factor method in predicting the experimental values. However, the prediction was not as precise as happened for the full vegetated scenario, as the Error Factors resulted higher for all the methods. Again, the best result was obtained by the use of the Nepf model, this time averaged by the Yen method, with an EF% equal to 3%. Nevertheless using James-Yen and Yang-Yen the predicted error was very low, meaning that Yen model of roughness composition better perform for quasi boundary layer model

4. DISCUSSION

Comparing the experimental conditions of the previous studies with the present (i.e. the papers cited by Vargas-Luna et al, 2015), it has to be noticed how just a few works were realized at the real scale. In fact, this type of experiments are hindered by the difficulties of finding appropriate locations with the availability of high amounts of water in well controlled conditions. The majority of the studies about vegetation resistance were realized in flumes or in laboratory, with a reduced scale and a number differences compared to a real channel. Moreover, the discharges that were used in this study were significantly higher than what found in literature. In this chapter the discussion of the most relevant results is provided.

4.1 Flow conditions

As already presented in the results, the experimental flow conditions were not comparable to the uniform flow. Despite the bed slope, as well as the channel cross-section, were approximately constant, the water surface gradient was not constant for varying discharges and not equal to the bed slope. This condition was found to be influenced by the downstream boundary condition, that was represented by the water level of the main channel of which the experimental reach was a tributary. However, the conditions of steady flow were fulfilled thanks to the absence of discharge variations along the measurement reach. Moreover, given the regularity of the channel and the good homogeneity of the vegetation distribution along the reach, computation were conducted considering steady gradually varied flow conditions.

The design of the reclamation ditches has been traditionally referred to the uniform flow conditions. Thus, the boundary conditions are not taken into account. This assumption is considered acceptable, as the average flow conditions in such channels can be reasonably close to uniform flow. Moreover, it has to be considered that, with high probability, the uniform flow conditions were reached in another part of the channel, most probably located upstream the experimental reach. Therefore, from an engineering point of view, the rating curves observed in experimental conditions are not useful for the channel design, as they are not referred to the average condition that can be found in this kind of projects.

This observation raised by modelling the water surface profile with HEC RAS, to validate the accuracy of the steady flow simulation in reproducing the measured data. The channel geometry was defined according to the topographic survey, and extended up to the upstream end of the Bresciani channel,

where the pumping station was positioned. A cross section was appositely surveyed also there, in order to have a real measure of the bed slope also 400 m upstream the measurement reach, delimited by the red staff gages (Figure 4.1).

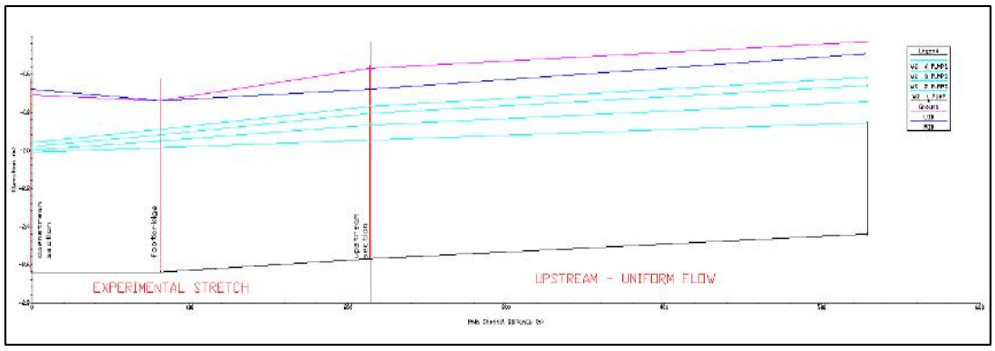

Figure 4.1. Predicted water profiles for the experimental reach and upstream. The flow conditions tend to the uniform flow conditions.

The roughness coefficients were set equal to the values calculated over the experimental measures. The simulation was conducted using the measured discharges, varying the roughness coefficients with the discharge, as observed in field. Since the flow conditions were subcritical, we needed to set the downstream boundary conditions, located at the downstream end of the experimental reach. The DBC were set equal to the water levels that were observed during the hydraulic measurements.

The model predicted with excellent accuracy the water profiles along the experimental reach, with deviations lower than 1 cm from the observed stages at each staff gage. This result can be considered as an additional confirmation that the field measurements and the roughness coefficients estimation were consistent with reality.

An additional useful result of the steady flow modelling was represented by the tracing of the stage-discharge rating curve for the upstream part of the channel, upstream the experimental stretch, in which the flow conditions were basically uniform (Figure 4.2). This simulation aimed at describing the effects of the experimental roughness values in condition of uniform flow, as a support for the hydraulic design, which is conducted in this condition. Despite the experimental stretch was not in uniform flow conditions, it is probable that in the upper part of the Bresciani channel, as well as in longer stretches of the other channel of the drainage network.

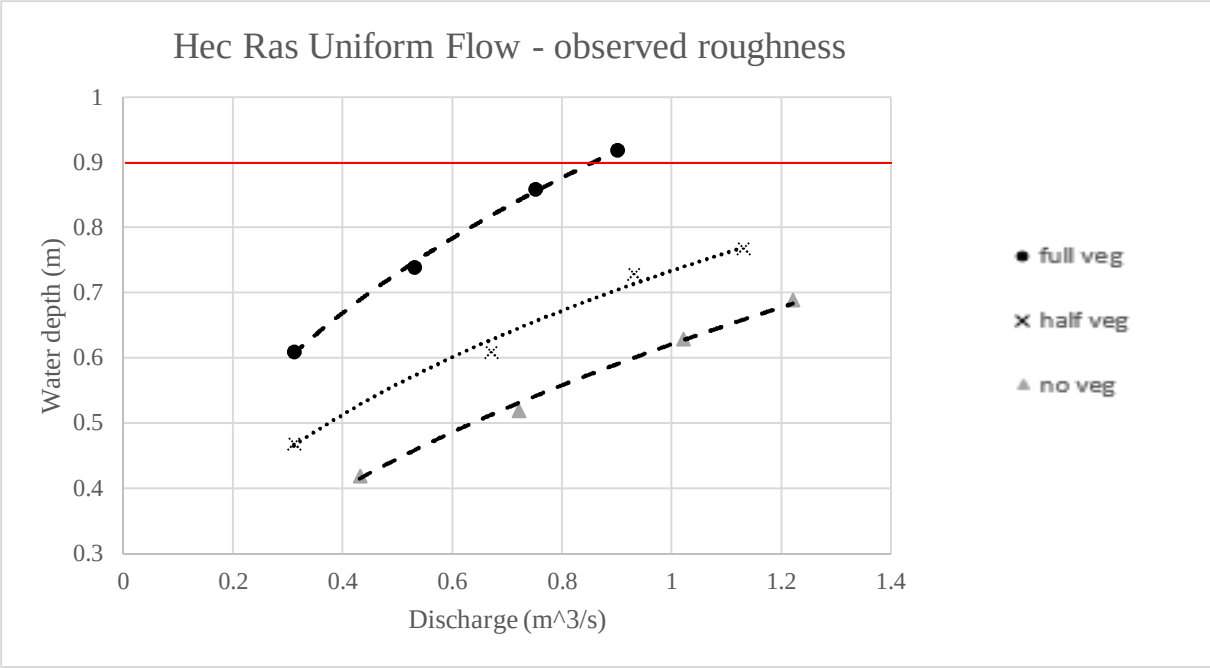

Figure 4.2. The stage-discharge curve obtained in the upper part of the channel can be considered representative of uniform flow conditions.

It has to be noticed that the rating curve computed in uniform flow conditions is significantly different from the experimental one. In fact, the difference between full vegetated and non-vegetated scenarios is considerably higher, reaching the bankfull level (0.95 m) with a discharge equal to 0.9 m^3/s. On the other hand, the half vegetated scenario resulted almost equal to the non-vegetated one, suggesting that its use should be taken in consideration as a possible improved management technique.

Looking at the project realized in 2006 for the design of the drainage network in which the Bresciani channel is included, we see that the designers chose the uniform flow as design condition. The choice was motivated by the regularity of the channel and the unknown variability of the downstream boundary conditions, represented by the water level of the Brentino channel. Therefore, the stage-discharge curves that must be taken into account in the design of channel colonized by Phragmites australis with the observed characteristic are probably the uniform flow curves. Moreover, it has to be noticed that the non-vegetated and half vegetated scenarios are well defined in terms of resistance distribution. Higher uncertainties can concern the full-vegetated scenario, which can be influenced by the presence of different species, or simply by different characteristics of the Phragmites canopy. Indeed, even without defining a precise full-vegetated scenario, the half-vegetated scenario resulted to be comparable to the non-vegetated scenario from an hydraulic point of view, but it presented a great advantage in terms of environmental quality, as an important component of the habitat is partially preserved.

4.2 Observed roughness coefficients

The present study aimed at evaluating the roughness coefficients of three different scenarios of possible vegetation management. As already commented before, the experimental values referred at an average value that was representative of the average resistance of the cross section, without dividing the wetted perimeter in sub-section with homogeneous characteristics. This approach is partially in contrast with all the previous experimental studies about vegetation resistance. In fact, peculiarity of all the studies conducted in flumes or channels were analyzing artificially-designed vegetation layouts, in which the variables such as stem density, diameter, height etc.were regularly distributed along the wetted perimeter, with smooth, vertical banks and flat bottom (i.e. Rhee et al., 2008; Nepf and Vivoni, 2000; Baptist et al, 2007; Järvelä 2012a, 2012b; etc.). In such conditions, the assumption that R=h (hydraulic radius equal to water depth) was often proposed.

In the present study case, the channel characteristics were significantly different. Considering the full-vegetated conditions, it was evident how the vegetation was not homogeneously distributed along the wetted perimeter of each section. Moreover, there were slight differences between the surveyed sections, as the vegetated patches were not perfectly regular in the flow direction. The Manning's n that were obtained for this scenario must be considered an "equivalent" roughness coefficient, representative of the global resistance of the study reach. These findings represent the answer to the question that animated the present study, as the reclamation authority was interested in estimating exactly this situation, that was representative of the unmown scenario for the local drainage network.

Anyhow, the collected data were also analyzed to extract information extendable to other case studies. The reverse composite section analysis that was conducted with different methods to estimate the average resistance of the lateral vegetated patches was part of these. The simplified vegetation layout allowed to estimate the roughness of the lateral patches, considering them as patches of vegetation with a regular distribution of resistance between left and right bank. Results showed that, as was observed for the equivalent roughness coefficients, the full-vegetated scenario presented a Manning's n decreasing with increasing discharges.

The observed trend was in contrast with the classic models of emergent vegetation, and with the study of Rhee et al. (2008) regarding the Phragmites communis, a species with similar characteristic to the P. australis. In fact, the flow resistance of emergent vegetation was expected to increase with the water level. Typically, the vegetative drag force increases with the water level up to the full submergence conditions, which corresponds to the point of maximum resistance. For further increases in water level, the resistance assumes a decreasing trend, well described by a number of studies (i.e. Whitehead, 1976;

Kouwen, 1988; Morgan&Rickson, 1995; Nepf, 2012). A comparison between the observed data (subtracted of the bed resistance n_b, as proposed by Cowan,1959) and the findings of Whitehead (1988) is proposed in figure 4.3.

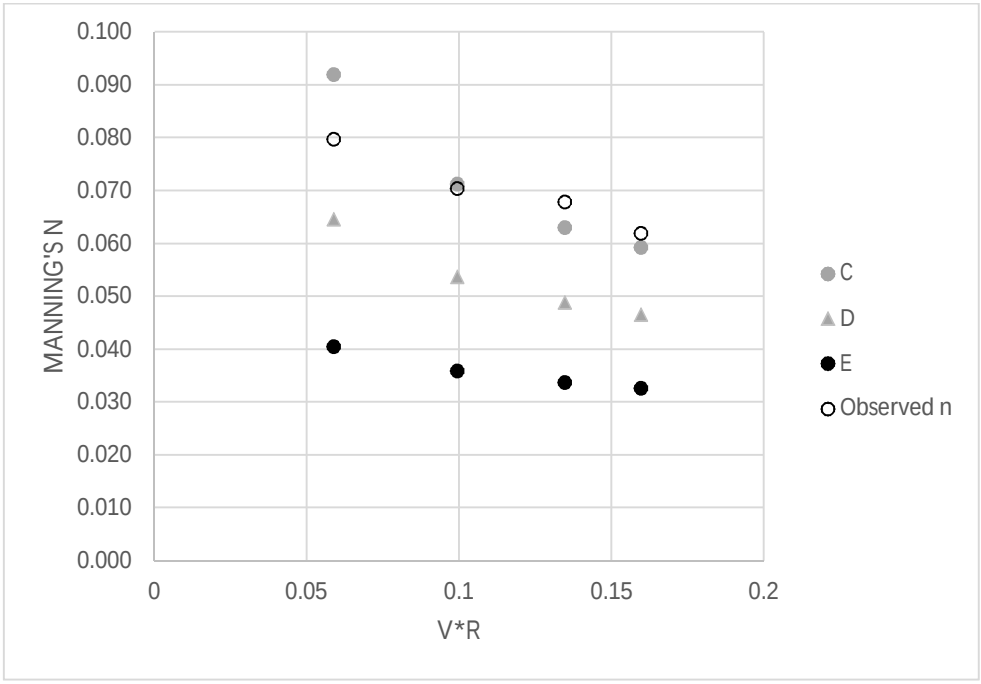

Figure 4.3. Comparison between the estimated roughness coefficients for the studied vegetated patches and the Whitehead models. C, D and E are three of the five grass stiffness cathegories proposed by the authors.

Our experimental values presented a lower decreasing trend compared to the curves found by Whitehead for grasses of different stiffness and densities (C medium stiffness, E low stiffness). However, Whitehead models were developed for submerged meadows of grass, while our case was constituted by emergent reed. Our hypothesis about this difference is that a combined effect of stems and leaves occurred for raising water levels. In other words, it is possible that the increase in flow resistance of the most rigid, emergent stems somehow compensated the reduction of frontal area due to the leaves reconfiguration and bending of the smaller plants. A further discussion is proposed below.

Rhee et al. (2008) described the roughness variation of three different species, one of which was the Phragmites communis, both in emergent and submerged, in steady gradually-varied flow conditions. The most relevant result to be compared to this work regards the Manning's n-VR retardance curve, that was developed both for green and dormant reed.

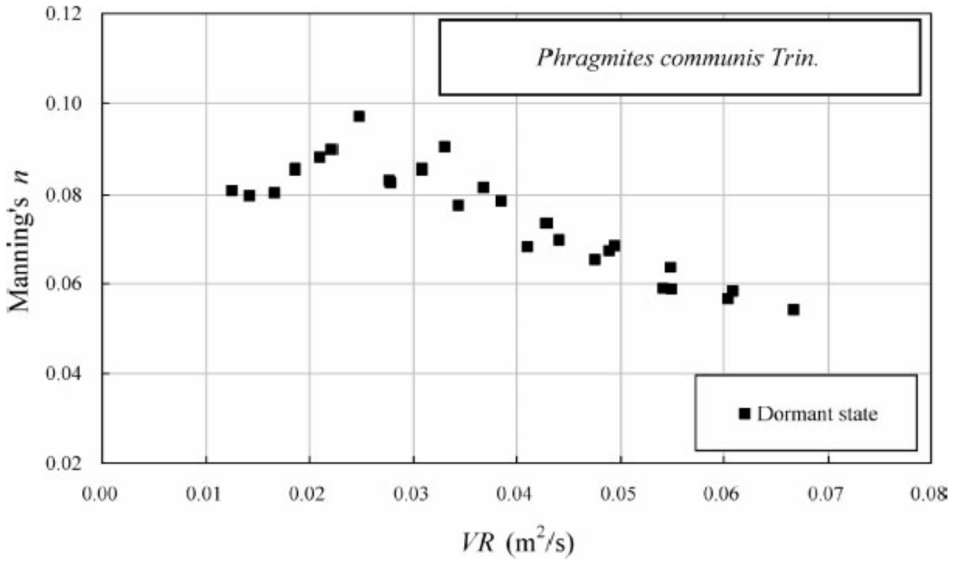

Figure 4.4. Adapted from Rhee et al. (2008). Manning's n for Phragmites communis in dormant state.

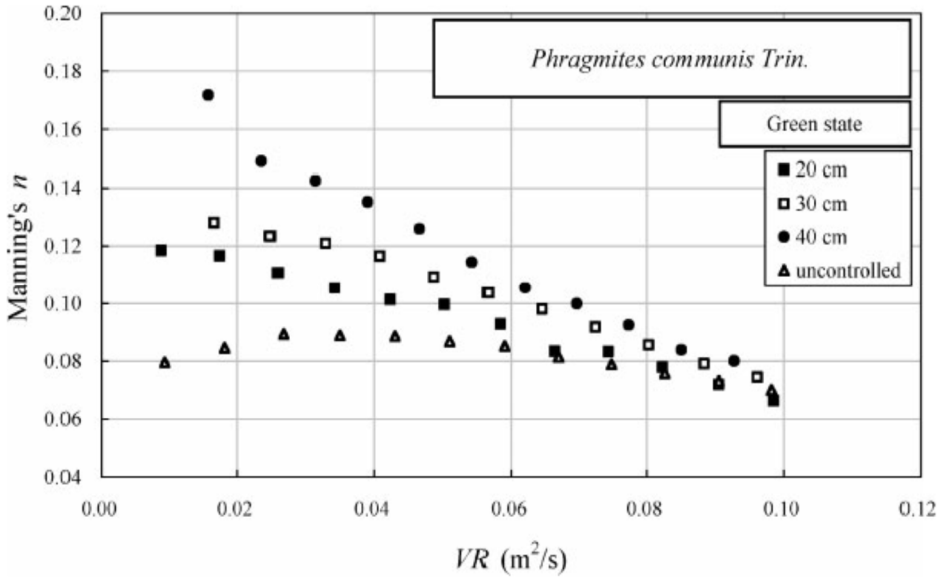

Figure 4.5. Adapted from Rhee et al. (2008). Manning's n for Phragmites communis in Green state for different water stages.

Starting from the presented experimental data, the authors subtracted from the observed Manning's n values the roughness factors not related to vegetation, according to the Cowan (1956) approach. The resulting roughness coefficients were related just to the vegetation resistance, as they were obtained subtracting from the total Manning's n the n_b. The curves that were obtained are different in dormant and green condition:

Dormant: $n = 0.0013/VR + 0.005$ (4.1)

Green: $n = 0.0025/VR + 0.013$ (4.2)

The equation that was better describing the retardance law total n-V*R for the full-vegetated scenario in our study case, subtracting from the total Manning's n the average n observed for the non-vegetated scenario ($n_b = 0.021$), the retardance curve was:

$$n = 0.0015/VR + 0.055 \quad (4.3)$$

It is interesting to see how the observed retardance coefficient lies in the middle of the ones proposed by Rhee et al. (2008). The authors presented two different retardance curves for the "green" state and the "dormant" state. Citing the authors, "'Green' state means that the tested grasses are fully green and in active growth state. 'Dormant' state means that the tested grasses are inactive and starting to be wilted or dead." Our study case resulted somehow in the middle between of these two scenarios. In fact, looking at the plant height and stem densities used by Rhee et al., the green state appears a younger stage of growth compared to ours. On the other hand, our vegetation was not yet in dormant season, as the surveys were conducted at the maximum development before flowering. Considering the retardance coefficient as a measure of the reconfiguration of flexible elements, our findings are coherent with the ones obtained by Rhee et al. for the same species.

A more evident difference concerns the value of the horizontal asymptote, which is markedly higher in our study case (0.055) than in the two scenarios presented by Rhee et al. This parameter represents the minimum roughness coefficient that is related to the canopy when this is forced by a flow with high V*R. For submerged meadows, this number tends to decrease until the maximum bending is reached. For emerged plants, this value stabilizes at the minimum frontal area that can be assumed by the submerged portion of the plant. In the Korean experiment, the plants presented a maximum height of 0.7-0.8 m and were flooded by a maximum depth of 0.4 m., while in our case the same specie was 1.3-1.9 meters high, and were flooded up to 0.9 m. It is probable that the stem diameters were higher in our case, and that the flexible parts were representing just a part of the total resistance. Indeed, for low velocities the resistance was represented by a combined effect of the plant components. For the higher discharges, or at high V*R rates, the resistance was mainly represented by the rigid stems, as the leaves started to bend, contributing to decrease flow resistance. In presence of rigid stems, it is coherent to have higher resistances also in case of high velocities and water depths, as the emergent stems are not modifying their shapes, how probably happened in the study case of Rhee et al.

Comparing the observed results with modeling, we can assess that the observed resistance exerted by reed is in the middle between the flexible behavior of a rigid cylinder (represented by the emergent stems) and a bending grass (represented by the leaves). Therefore, the reed resistance should be

described as the one of a shrub. Moreover, the leaves distribution along the stem is varying with the season, as the higher the plants the less leaves will survive at the lower part of the stem. Thus, as already observed by Rhee et al.(2008), it is correct to assess that the reed presents a seasonality that varies the flow resistance within the year.

An interesting aspect that should be further studied is the bed resistance in vegetated channels. In fact, it is possible that the bed resistance that is measured in absence of vegetation would not be equal to the bed resistance in a vegetated channel, as the vegetation itself strongly modifies the flow-bed interaction. According to this theory, it is even more correct to compare directly the two global coefficients than to extrapolate a vegetative roughness that could be affected by other kinds of errors, i.e. the estimation of a bed resistance that could be not correct. Additionally, the loamy soil that was used in the research of Rhee et al. (2008) probably did not have a great difference in terms of bed resistance. The variation range of the V*R parameter were comparable, with the one of our study slightly higher (0.06-0.16 for the full vegetated scenario).

4.3 Modelling

The vegetation parameters obtained by the field surveys were used to test the prediction capacity of different models available in literature. In particular, the full vegetated scenario and the half vegetated scenario were modeled by the use of the Nepf formula, the James formula and the Yang formula.

The section was first modeled considering an homogeneous distribution of plants along wetted perimeter, and then decomposing the cross section in six sub-areas, according to the vegetation surveys carried out before the hydraulic measures. While the prediction was not excellent with the first approach (40-50% of Error), the composite section model was more accurate, in some cases with an error lower than 10%. The best results were obtained by the combined use of the Nepf model, averaged along the wetted perimeter by the Colebatch method for the full vegetated scenario, and by the Yen method for the half-vegetated scenario. Thus, our results pointed out that well conducted vegetation surveys, aimed at estimating the distribution of resistance elements along the wetted perimeter, could represent a valid solution in estimating the roughness coefficients for vegetated channels.

Three resistance models were developed for the estimation of roughness of emergent vegetation. The used models assumed the stems as rigid cylinders. As a consequence, the modeled Manning's n resulted increasing with the flow depth. This trend was found to be in contrast with our findings, as the plants in our study case were leafed. The effect of leaves was probably the reason of the decreasing trend. The results of the full vegetated scenario showed that the predicted values were often underestimated for the

lower discharges, and overestimated for the higher discharges. For the half vegetated scenario, most of predictions resulted overestimated for all the discharges. However, the reed stems resulted to be correctly comparable to rigid cylinders, given their regular shape and stiffness, at least when submerged for a small part of their height. The modelling predictions confirmed this supposition, as the average errors within the experimental interval were very low, despite the trends over discharges were not the same. Finally, we can consider that an opportune sharing of channel section, combined with different models can predict very well the flow resistance of the channel. Moreover, the general overestimation of roughness coefficients represents a precautionary approach which can just raise the safety in case of flood risk reduction projects.

Future research have to deepen this aspect considering additional recent models that include flexure rigidity and LAI of the vegetation, and probably an averaged value of drag force along the channel. This aspect can be considered as fundamental to obtain better formula at the reach scale and to reduce the error of total roughness height in vegetated channels.

5. SUMMARY AND CONCLUSIONS

An experimental study was realized aimed at estimating the roughness coefficients of a vegetated reclamation channel at the real scale. The vegetation was represented by common reed (*Phragmites australis* (Cav.) Trin ex. Steudel). Hydraulic measures were conducted in unmown conditions, after a partial cut, and after the complete removal from the whole channel section. Four increasing artificial discharges were pumped for each scenario within the channel to measure the total resistance for different water depths up to the bankfull condition. The velocity distribution at the middle cross section was measured by means of a current meter for the discharge estimation. Additionally, the vegetation was accurately surveyed to collect information about the distribution of parameters such as the stem diameter, plant height and stem density throughout the experimental reach. Three resistance models were tested to assess their prediction accuracy as compared with the observed values.

The roughness coefficients were calculated by analyzing the hydraulic variables observed during the field experiments under the assumption of steady-gradually varied flow. The full vegetated scenario resulted in the highest Manning's *n*, with values varying between 0.074-0.063, presenting a decreasing trend for increasing discharges. The half-vegetated scenario was evaluated as possible management strategy of the channel vegetation which could reconcile the need to ensure an efficient hydraulic conveyance with the environmental protection needs. The vegetation was left untouched on one of the banks, while totally removed from the main channel and the other bank. The experimental total Manning's n varied in the range 0.030-0.036, without showing a precise trend with increasing discharges. The cleared scenario was obtained removing the vegetation also from the other bank, and it was representative of the maximum conveyance of the channel. Manning's n varied between the values 0.013-0.022, without a trend with the discharges. The values of the cleared scenario were assumed as the bed resistance of the experimental reach.

The vegetation density was not homogeneously distributed along the wetted perimeter, but reed was significantly denser at the sides than in the central channel. Schematizing the cross section as a central channel of width 2 m without vegetation, and two lateral patches of homogeneous vegetation at the sides, the values of total resistance for the full vegetated scenario were processed to extract the Manning's n due to the only vegetation. By means of four different composite roughness estimation methods, we obtained the corresponding Manning's n for the vegetated subareas, given the roughness of the bed and the total roughness. Then, the obtained values were subtracted of the bed resistance to calculate the value to be attributed only to the vegetation resistance. The vegetation Manning's n varied

between 0.080 and 0.062. The retardance law Manning's n-V*R was produced for these values, and compared to other studies about vegetation resistance.

The vegetation surveys aimed at collecting the input parameters for three different resistance models: Nepf, James et al. and Yang & Choi. The resistance models were run with different rates of approximation. Averaging the vegetation parameters along the wetted perimeter, the models resulted affected by significant errors, but the use of the composite channel section raised up the prediction capacity of the three models to an excellent level, showing errors lower than 10% compared to the observed values. In any case, the best prediction were obtained by the use of the Nepf (2012) model for emergent vegetation. However, a discrepancy between observed and predicted values was found in the trend of Manning's coefficients with discharges. In fact, all the models developed for emergent vegetation do not take into account the plant reconfiguration, resulting in increasing Manning's n for increasing discharges. This was not observed in reality, since the measured n resulted slightly decreasing for increasing V*R values, while the models were slightly increasing. However, the predicted values can be considered acceptable as the discrepancies for a given discharge were not high. Moreover, the prediction error resulted to be lower for the higher discharges, which are the most relevant to be taken into account for flood risk management.

The present study was funded by the Toscana Nord reclamation consortium with the precise scope to assess the rise in terms of flood risk related to vegetation. The analysis of the variation in terms of return time demonstrated how the presence of dense vegetation increases the flood risk, as the frequency of the bankfull condition increases significantly because of the rise of the water level due to the higher flow resistance. However, the results obtained for the so-called half vegetated scenario demonstrated how it could represent an innovative solution able to combine multiple advantages both in terms of environmental protection, cost efficiency and flood risk reduction.

The results of the present research demonstrated also how a good level of prediction is feasible also by the use of existing models, which were found to have a good prediction capacity. From this perspective, the limitation could come from the high costs related to the field surveys on vegetation, that are complex and time consuming. A possible solution could be represented by the fast development of remote sensing techniques, as the UAV that was tested I this study. Future developments will include the estimation of vegetation parameters from aerial imagery, aimed at realizing roughness maps for management planning.

As a matter of fact, the management of natural streams and drainage networks has to deal with the reduction of flood risk and the protection of the riverine-aquatic ecosystems. Since the reclamation system were realized by humans to allow the cultivation of wetlands, the management of natural aquatic

and riparian vegetation along the drainage channels has been historically practiced without taking into account the environmental protection. Indeed, channel and ditches were realized with the only aim to drain the fields and protect crops and human infrastructures from ponding and flooding.

The progressive reduction of the environmental quality of aquatic habitats such as rivers, channels, lakes and wetlands led in the last years to a growing attention for these ecosystems. Therefore, environmentalist associations and the scientific community started to remark the high impact of management practices on the aquatic and riparian vegetation. This phenomena called for the better comprehension of the effective role of vegetation on flood risk, aimed at optimizing the management strategies to reduce the environmental impact of an indispensable practice as it is flood protection.

From this perspective, the present study contributed to the essential knowledge of the real effect of vegetation on flood risk. Results will contribute to plan management strategies oriented to a reduction of the impact on the environment.

6. REFERENCES

Arcement G.J., Schneider V.R. (1989), “Guide for selecting Manning's roughness Coefficients for natural channels and flood plains”, United States Geological Survey Water-Supply in cooperation with the United States Department of Transportation, Federal Highway Administration, paper 2339;

Armanini, A., Righetti, M., Grisenti, P. (2005). Direct measurement of vegetation resistance in prototype scale. J. Hydraulic Res. 43(5), 481–487.

Baptist M.J., Babovic V., Rodriguez Uthurburu J., Keijzer M., Uittenbogaard R.E., Mynett A., Verwey A. (2007), “On inducing equations for vegetation resistance”, Journal of Hydraulic Research 45(4), pp. 435 – 450;

Benini G. (1990) Sistemazioni idraulico forestali. Utet edizioni.

Casarosa M., Milano V., Viti C. (2006). Adeguamento idraulico della zona orientale del bacino di Ponente del Comprensorio di Bonifica della Versilia. Master degree thesis, University of Pisa, Faculty of Engineering.

Chen, L., Stone, M.C., Acharya, K., Steinhaus, K.A. (2011). Mechanical analysis for emergent vegetation in flowing fluids. J. Hydraulic Res. 49(6), 766–774.

Dittrich, A., Aberle, J., Schoneboom, T. (2012). Drag forces and flow resistance of flexible riparian vegetation. In Environmental fluid mechanics: Memorial colloquium on environmental fluid mechanics in honour of Professor Gerhard H. Jirka, 195–215, W. Rodi, M. Uhlmann, eds. CRC Press, London.

Fathi-Moghadam, M. (1996). Momentum absorption in non-rigid, non-submerged, tall vegetation along rivers. University of Waterloo, Canada. (Doctoral thesis.)

Fathi-Moghadam, M. and Kouwen, N. (1997). “Nonrigid, nonsubmerged, vegetative roughness on floodplains”, J. Hydr. Engrg., 123(1), 51–57.

Florineth, F., Meixner, H., Rauch, H.P., Vollsinger, S.(2003). Coppice at River Banks - Properties, hydraulic action and behavior. Landnutzung und Landentwicklung, 44 (1), pp. 19-25.

Folkard, A.M. (2011). Vegetated flows in their environmental context: A review. Eng. Comp. Mech. 164(EM1), 3–24.

Forzieri G., Castelli F. & Preti F. (2012): Advances in remote sensing of hydraulic roughness, International Journal of Remote Sensing, 33:2, 630-654

Ghisalberti, M., Nepf, H.M. (2004). The limited growth of vegetated shear layers. Water Resour. Res. 40(W07502), doi:10.1029/2003WR002776.

Gwinn, W.R. and W.O. Ree. 1980. Maintenance effects on the hydraulic properties of a vegetation lined channel. ASAE Trans. 23:636-42.

Huthoff, F. (2012). Theory for flow resistance caused by submerged roughness elements. J. Hydraulic Res. 50(1), 10–17.

Huthoff, F., Augustijn, D.C.M., Hulscher, S.J.M.H. (2007). Analytical solution of the depth-averaged flow velocity in case of submerged rigid cylindrical vegetation. Water Resour. Res. 43 (W06413), doi:10.1029/2006WR005625.

Jalonen J., Järvelä J., Aberle J. (2013), "Leaf Area Index as vegetation density measure for hydraulic analyses", Journal of Hydraulic Engeneering 139, pp. 461 – 469;

Jalonen, J., Järvelä, J., Aberle, J. (2012). Vegetated flows: Drag force and velocity profiles for foliated plant stands. Proc. Int. Conf. River Flow 2012, San José, Costa Rica, 233–239, R.E. Murillo Munoz, ed. Taylor & Francis, London, UK.

Jalonen, J., Järvelä, J., Aberle, J. (2013). Leaf area index as a vegetation density measure for hydraulic analyses. J. Hydraulic Eng.

James, C.S., Goldbeck, U.K., Patini, A., Jordanova, A.A. (2008). Influence of foliage on flow resistance of emergent vegetation. J. Hydraulic Res. 46(4), 536–542.

James, C.S., Birkhead, A.L., Jordanova, A.A., O'Sullivan, J.J. (2004). Flow resistance of emergent vegetation. J. Hydraul.Res. 42(4), 390–398.

Järvelä, J. (2002a). "Flow resistance of flexible and stiff vegetation: a flume study with natural plants", J. Hydrol., 269(1–2), 44–54.

Järvelä, J. (2002b). Determination of flow resistance of vegetated channel banks and floodplains. In River Flow 2002 (Eds. Bousmar, D. and Zech,Y.), Swets & Zeitlinger, Lisse, pp. 311–318.

Järvelä, J. (2004). Determination of flow resistance caused by non-submerged woody vegetation. Int. J. River Basin Manag. 2(1), 61–70.

Kelly McAtee P.E., Leed A.P. (2012); Introduction to compound channel flow analysis for floodplains. SunCam continuing education course.

Klaassen, G.J. and Zwaard, J.J. (1974). “Roughness coefficients of vegetated floodplains”, J. Hydr. Res., 12(1), 43–63.

Konings, A.G., Katul, G.G., Thompson, S.E. (2012). A phenomenological model for the flow resistance over submerged vegetation. Water Resour. Res. 48, W02522, doi:10.1029/2011WR011000.

Kouwen N. (1992), “Modern approach to design of grassed channels”, Journal of Irrigation and Drainage Engeneering 118(5), pp. 733 – 743;

Kouwen, N. (1988). ‘‘Field estimation of the biomechanical properties of grass.’’ J. Hydr. Res., Delft, The Netherlands, 26(5), 559–568.

Kouwen, N., Fathi-Moghadam, M. (2000). Friction factors for coniferous trees along rivers. J. Hydraulic Eng. 126(10), 732–740.

Kouwen, N., Li, R.M. (1980). Biomechanics of vegetative channel linings. J. Hydraulic Div. 106(6), 1085–1103.

Kouwen, N., Unny, T.E. (1973). Flexible roughness in open channels. J. Hydraulic Div. 99(5), 713–728.

Kubrak, E., Kubrak, J., Rowiñski, P. (2012). Influence of a method of evaluation of the curvature of flexible vegetation elements on vertical distributions of flow velocities. Acta Geophys. 60(4), 1098–1119.

de Langre, E. (2008). Effects of wind on plants. Ann. Rev. Fluid Mech. 40, 141–168.

Lightbody AF, Nepf HM. Prediction of velocity profiles and longitudinal dispersion in emergent salt marsh vegetation. Limnol Oceanogr 2006;51(1):218–28.

Luhar M, Rominger J, Nepf H.M. Interaction between flow, transport and vegetation spatial structure. Environ Fluid Mech 2008;8(5–6):423–39.

Luhar M., Nepf H.M. (2013), “From the blade scale to the reach scale: a characterization of aquatic vegetative drag”, Advances in Water Resources 51, pp. 305 – 316;

Luhar, M., Rominger, J., Nepf, H. (2008). Interaction between flow, transport and vegetation spatial structure. Environ. Fluid Mech. 8(5–6), 423–439.

Morgan RCP and Rickson R.J., (1995) Slope stabilization and erosion control. A bioengineering approach, Spon, London

Nepf, H.M. (2012a). Flow and transport in regions with aquatic vegetation. Ann. Rev. Fluid Mech. 44, 123–142.

Nepf, H.M. (2012b). Hydrodynamics of vegetated channels. J. Hydraulic Res. 50(3), 262–279.

Nepf, H.M. (1999). Drag, turbulence, and diffusion in flow through emergent vegetation. Water Resour. Res. 35(2), 479–489.

Nepf, H.M.,Vivoni, E.R. (2000). Flow structure in depth-limited, vegetated flow. J. Geophys. Res. 105(C12), 28457–28557.

Nikora, V. (2010). Hydrodynamics of aquatic ecosystems: An interface between ecology, biomechanics and environmental fluid mechanics. River Res. Applic. 26(4), 367–384.

Pasche, E., Rouvé, G. (1985). Overbank flow with vegetatively roughened flood plains. J. Hydraulic Eng. 111(9), 1262–1278.

Petryk, S., Bosmajian, G. (1975). Analysis of flow through vegetation. J. Hydraulic Div. 101(7), 871–884.

Raupach, M.R. (1992). Drag and drag partition on rough surfaces. Boundary-Layer Meteorol. 60(4), 375–395.

Ree, W.O. (1949). Hydraulic characteristics of vegetation for vegetated waterways. Agric. Eng. 30, 184–189.

Rhee D.S., Woo H., Kwon A. B., Ahn H.K. (2008) “Hydraulic resistance of some selected vegetation in open channel flows”; River Res. Applic. 24: 673-687

Ricardo, A.M., Franca, M.J., Ferreira, R.M.L.(2016). Turbulent flows within random arrays of rigid and emergent cylinders with varying distribution. Journal of Hydraulic Engineering, 142 (9), DOI: 10.1061/(ASCE)HY.1943-7900.0001151

Righetti, M. (2008). Flow analysis in a channel with flexible vegetation using double-averaging method. Acta Geophys. 56(3), 801–823.

Shucksmith, J.D., Boxall, J.B., Guymer, I. (2011). Bulk flow resistance in vegetated channels: Analysis of momentum balance approaches based on data obtained in aging live vegetation. J. Hydraulic Eng. 137(12), 1624–1635.

Stone, M.C., Chen, L., McKay, S.K., Goreham, J., Acharya, K., Fischenich, C., Stone, A.B. (2011). Bending of submerged woody riparian vegetation as a function of hydraulic flow conditions. River Res. Appl.

Sukhodolov, A., Sukhodolova, T. (2010). Case study: Effect of submerged aquatic plants on turbulence structure in a lowland river. J. Hydraulic Eng. 136(7), 434–446.

Vargas-Luna A., Crosato A., Uijttewaal W.S.J. (2015) Effects of vegetation on flow and sediment transport: comparative analyses and validation of predicting models. Earth Surf. Process. Landforms 40, 157–176. DOI: 10.1002/esp.3633

Västilä, K., Järvelä, J. (2012). Foliage and stem drag: Comparison between four riparian species. Proc. 2nd IAHR Europe Congress, Munich.

Vogel, S. (1994). Life in moving fluids: The physical biology of flow. 2nd ed. Princeton University Press, Princeton.

Whitehead E. (1976), "A guide to the use of grass in hydraulic engineering practice", Construction Industry Research and Information Association.

Wilson, C.A.M.E., Hoyt, J., Schnauder, I. (2008). Impact of foliage on the drag force of vegetation in aquatic flows. J. Hydraulic Eng. 134(7), 885–891.

Wilson, C.A.M.E., Xavier, P., Schoneboom, T., Aberle, J., Rauch, H. P., Lammeranner, W., Weissteiner, C., Thomas, H. (2010). The hydrodynamic drag of full scale trees. Proc. Int. Conf. River Flow 2010, Vol. 1, Braunschweig, 453–459, A. Dittrich, K. Koll, J. Aberle, P. Geisenhainer, eds. Bundesanstalt für Wasserbau, Karlsruhe, DE.

Yang, W., Choi, S.-U. (2010). A two-layer approach for depthlimited open-channel flows with submerged vegetation. J. Hydraulic Res. 48(4), 466–475.

Yang,W., Choi, S.-U. (2009). Impact of stem flexibility on mean flow and turbulence structure in depth-limited open channel flows with submerged vegetation. J. Hydraulic Res. 47(4),445–454.

Yen, B.C. (2002). Open channel flow resistance. J. Hydraulic Eng. 128(1), 20–39.

2.a Appendix

The current meter

This current meter, commonly known as the Price-type current meter, is suspended in the water using a cable with sounding weight or wading rod (taking the tail section off) and will accurately measure streamflow velocities from 0.1 to 25 feet per second (0.025 to 7.6 meters per second). The main features of this meter are the uniquely designed bucket wheel shaft bearings and the two post contact chamber. The bucket wheel has six conical shaped cups, is five inches (12.7 cm) in diameter and rotates on a vertical axis inside the yoke. The tungsten carbide bearings for the bucket wheel shaft are located in deeply recessed inverted cups. When the meter is in use, these cups become air chambers and the entrapped air effectively excludes water and silt from the bearing surfaces giving extremely low starting velocities and minimal friction in the bearings.

Figure 2.16. USGS Type AA current meter. The meter was suspended at various depth by means of a wading rod.

The contact chamber houses a penta gear and two binding posts, each having a fine platinum alloy contact wire. One wire makes contact with the bucket wheel shaft once during every revolution; the other is used when fast velocities are encountered, and makes contact with the penta gear once during every five revolutions of the bucket wheel.

Each current meter is provided with a U.S. Geological Survey approved standard rating table to convert bucket revolutions to stream velocity in either English units (feet per second) or metric units (meters per second), spare parts, instrument oil, cleaning cloth, screwdriver and an instrument case with a water tight o-ring seal that floats if dropped in the water and provides proper protection of the meter during transportation and storage.

The meter is made from brass and stainless steel and all exposed surfaces are chrome plated for corrosion-free service. The standard Type AA was designed for use with all of the counters as well as the AquaCalc 5000 Digital Flow Computer. No conversion kits or replacement contact chambers are necessary to use the latest digital technology with this meter.

The Aquacount

The data measured by the meter was receveid by a AquaCount - Model 5100 Price-Type Current Meter Digitizer. The AquaCount provides a digital readout for Price-type AA and Pygmy current meters. It eliminates use of the headphone and stopwatch while it is a simplified version of the AquaCalc 5000 flow computer. The AquaCount not only counts the revolutions, calculates and displays velocity in feet per second or meters per second, but time, revolutions and velocity are all simultaneously displayed on the LCD display. The AquaCount can be used with no modification or retro-fit of a standard Price-type current meter. Just plug it into the same connector you have for your headphone and immediately start reading velocity, revolutions and time. The AquaCount can be used with wading rods or cable suspended systems. It uses the same advanced CMOS circuitry as the AquaCalc 5000 which has proven itself in the USGS to be the accepted standard.

Figure 2.17. Aquacount digitizer. It was used to read the measurements of the current meter.

Features:

Directly compatible with any existing Price-type current meter. No retrofit or modification required.

Advanced CMOS circuitry with crystal based timing for accu- rate and reliable measurements.

Display simultaneously shows velocity, revolutions and time. No need to wait until the end of a measurement cycle.

Easy to read 32 character LCD display reading 4 significant figures.

Uses a single 9 V battery with power conserving standby circuitry for long battery life.

Sealed membrane buttons and water resistant sealed circuitry.

Physical Characteristics:

Size:7" x 4" x 1" (18 cm x 10 cm x 3 cm)

Weight:1 lb. (.4 kg)

Velocity Range: 0 to 25 ft/sec. (0 to 7.6 m/sec.)

Temperature Range:- 20 degrees C to + 70 degrees C

Display Resolution: 0.001

2.b Appendix

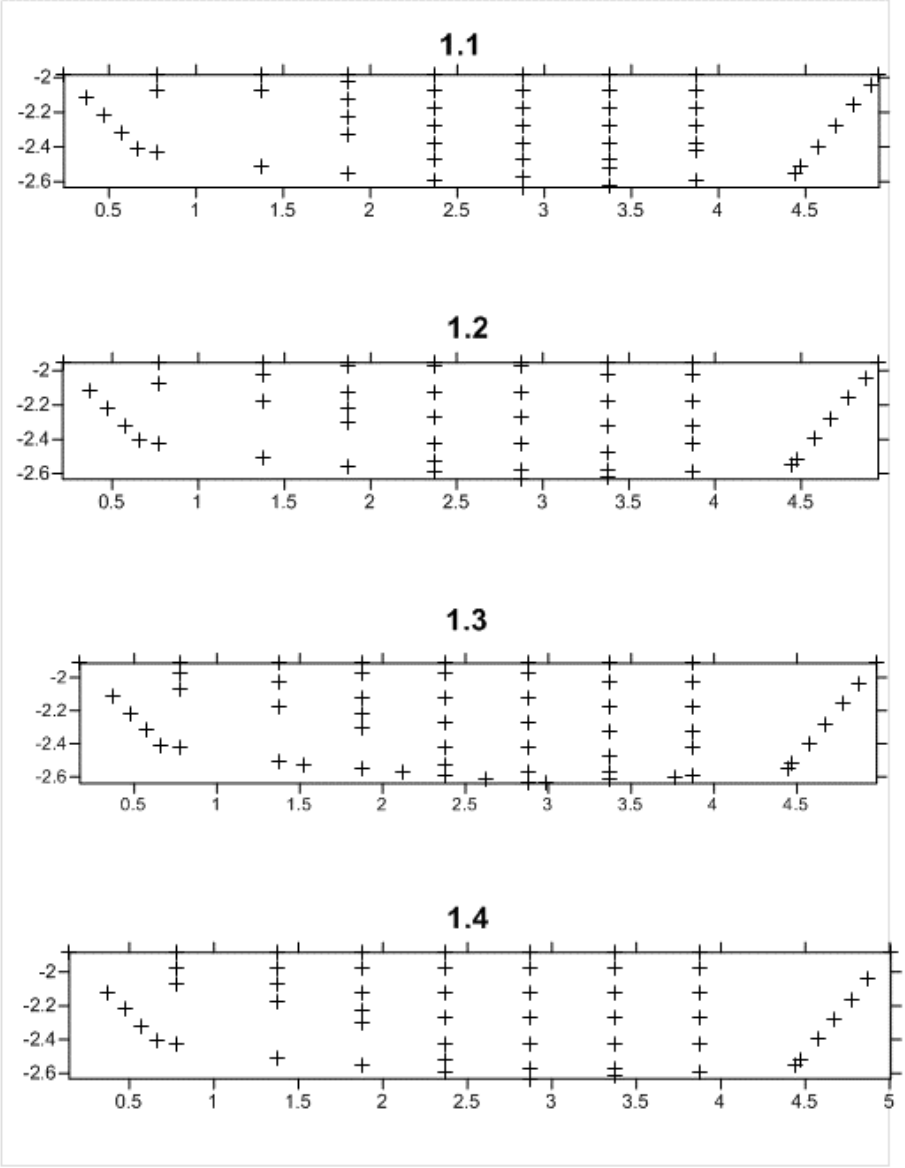

Figure A.1. Flow measures distribution for the full vegetated scenario. The Y axis is expressed in m a.s.l.

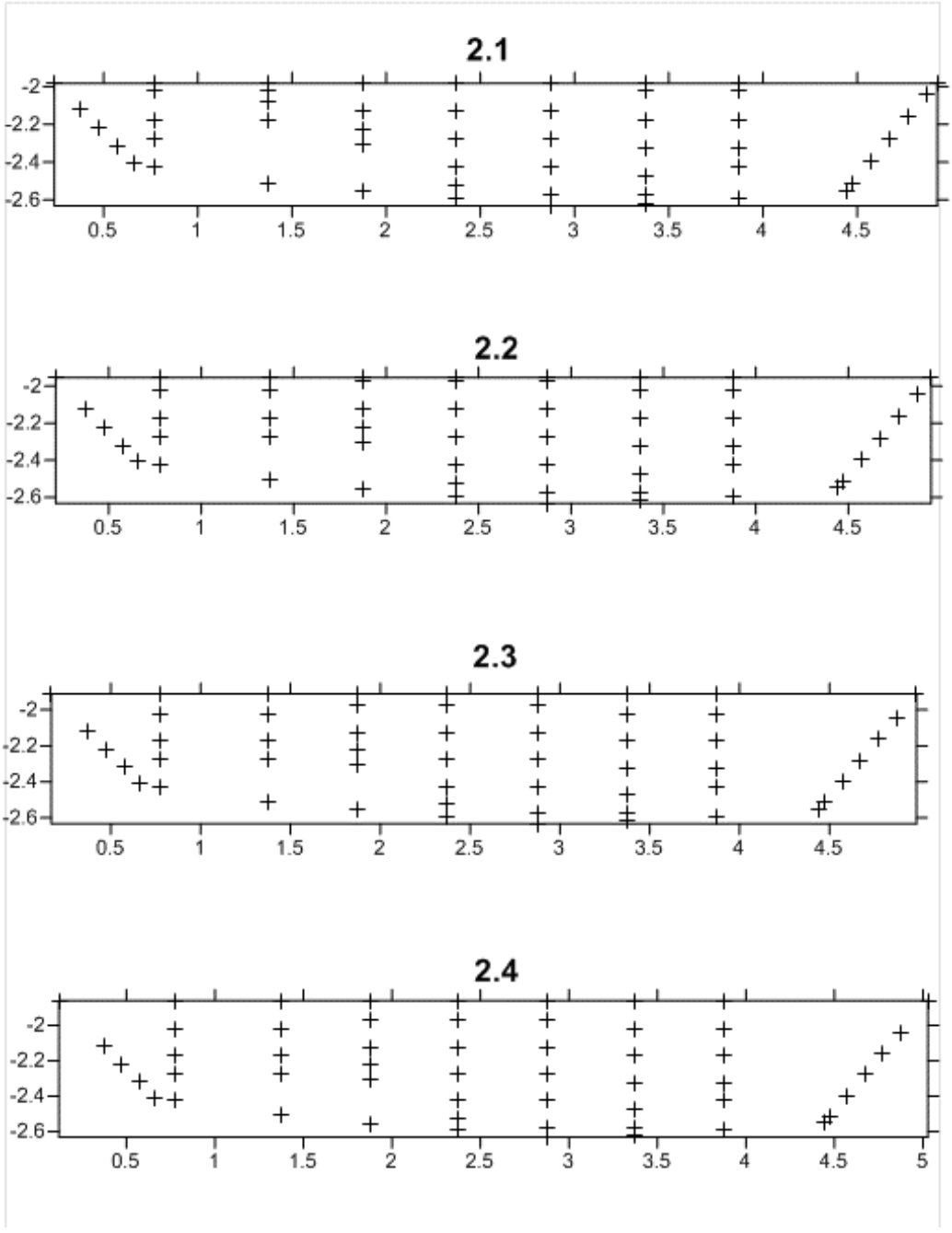

Figure A.2. Flow measures distribution for the half vegetated scenario. The Y axis is expressed in m a.s.l.

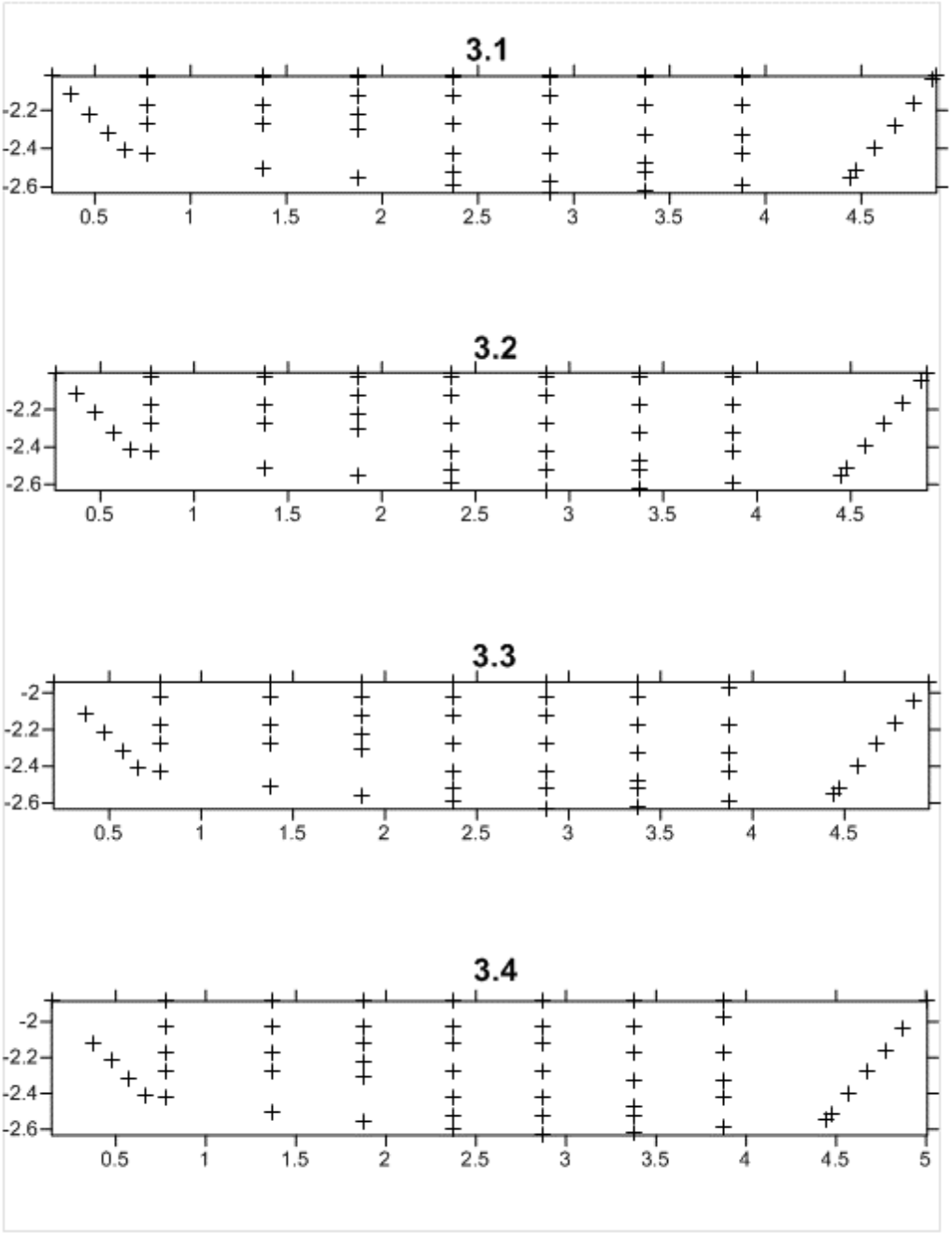

Figure A.3. Flow measures distribution for the non vegetated scenario. The Y axis is expressed in m a.s.l.

List of symbols

a Frontal area per volume

Ac Frontal area

b Vogel exponent

B_x Blockage factor

C_* Vegetational patch drag coefficient

C_D Vegetal drag coefficient

C_b Bottom drag coefficient

C Chezy coefficient

C Wetted perimeter

$Cd\chi$ = drag coefficient of a leafy bush or tree

D Stem diameter

F_D Drag force

f Darcy-Weisbach Friction factor

f' Bed friction factor

f'' Vegetation friction factor

g Gravitational acceleration h water depth

H Plant height

i water surface gradient

LAI Leaf Area Index

m Number of stems per m^2

MEI Vegetational stiffness parameter

Ω Flow area

R Hydraulic radius

S Bed slope

τ Total shear stress

τ_b Bed shear stress

τ_v Vegetation shear stress

u Flow velocity

$U\chi$ = lowest velocity used in determining χ

wk Patch width

Wh Channel width

ρ_0 Water unit weight

χ Species-specific vegetation parameter

Acknowledgments

This thesis is the result of an intense field activity and data analysis, which involved a huge amount of time and energy. Fortunately, I had the luck to be helped by great people who strongly contributed to the success of this research, and I want to warmly thank them. I want to thank Roberta Muoio and Melanie Maxwald, two brilliant students who participated to the research works during their degree thesis. Thanks also to Ing. Francesco Orlandi, who took part to the experiments with great interest. I want to thank prof. Luca Solari for the helpful early suggestions and for borrowing instruments that were employed for the measurements. A special thank goes also to Ing. Vittorio Pasquino, who gave a significant contribution to the data interpretation and modeling. Hopefully this will be the first of a long series of collaborations. Last but not least, thanks also to the Tutor of my doctorate, Prof. Ing. Federico Preti, for proposing me this topic and contributing to the whole three years of studies.

It is important for me to thank the two reviewers of this thesis, prof. Giovanni Battista Chirico and doct. Johannes Peter Rauch, who provided a detailed review of the work, proposing helpful improvements. The attention you payed was really appreciated.

The entire experimental setup realized thank to the great contribution of the Consorzio di Bonifica Toscana Nord, which funded this research and provided personnel and machines for the experiments. A special thank goes therefore to Ing. Leonardo Giannecchini and his staff for the support.

Alessandro Errico